Measurement of dijet azimuthal decorrelations in pp collisions at $\sqrt{s} = 8$ TeV with the ATLAS detector and determination of the strong coupling

M. Aaboud *et al.*[*]
(ATLAS Collaboration)

(Received 15 May 2018; published 7 November 2018)

A measurement of the rapidity and transverse momentum dependence of dijet azimuthal decorrelations is presented, using the quantity $R_{\Delta\phi}$. The quantity $R_{\Delta\phi}$ specifies the fraction of the inclusive dijet events in which the azimuthal opening angle of the two jets with the highest transverse momenta is less than a given value of the parameter $\Delta\phi_{\max}$. The quantity $R_{\Delta\phi}$ is measured in proton-proton collisions at $\sqrt{s} = 8$ TeV as a function of the dijet rapidity interval, the event total scalar transverse momentum, and $\Delta\phi_{\max}$. The measurement uses an event sample corresponding to an integrated luminosity of 20.2 fb^{-1} collected with the ATLAS detector at the CERN Large Hadron Collider. Predictions of a perturbative QCD calculation at next-to-leading order in the strong coupling with corrections for nonperturbative effects are compared to the data. The theoretical predictions describe the data in the whole kinematic region. The data are used to determine the strong coupling α_S and to study its running for momentum transfers from 260 GeV to above 1.6 TeV. Analysis that combines data at all momentum transfers results in $\alpha_S(m_Z) = 0.1127^{+0.0063}_{-0.0027}$.

DOI: 10.1103/PhysRevD.98.092004

I. INTRODUCTION

In high-energy particle collisions, measurements of the production rates of hadronic jets with large transverse momentum p_T relative to the beam direction can be employed to test the predictions of perturbative quantum chromodynamics (pQCD). The results can also be used to determine the strong coupling α_S, and to test the pQCD predictions for the dependence of α_S on the momentum transfer Q (the "running" of α_S) by the renormalization group equation (RGE) [1,2]. Previous tests of the RGE through α_S determinations in hadronic final states have been performed using data taken in ep collisions ($5 < Q < 60$ GeV) [3–5], in e^+e^- annihilation ($10 < Q < 210$ GeV) [6,7], in $p\bar{p}$ collisions ($50 < Q < 400$ GeV) [8–10], and in pp collisions ($130 < Q < 1400$ GeV) [11–15]. The world average value is currently $\alpha_S(m_Z) = 0.1181 \pm 0.0011$ [16].

Recent α_S results from hadron collisions are limited by theoretical uncertainties related to the scale dependence of the fixed-order pQCD calculations. The most precise $\alpha_S(m_Z)$ result from hadron collision data is $\alpha_S(m_Z) = 0.1161^{+0.0041}_{-0.0048}$ [9], obtained from inclusive jet cross-section data, using pQCD predictions beyond the next-to-leading order (NLO). However, when the cross-section data are used in α_S determinations, the extracted α_S results are directly affected by our knowledge of the parton distribution functions (PDFs) of the proton, and their Q dependence. The PDF parametrizations depend on assumptions about α_S and the RGE in the global data analyses in which they are determined. Therefore, in determinations of α_S and its Q dependence from cross-section data the RGE is already assumed in the inputs. Such a conceptual limitation when using cross-section data can largely be avoided by using ratios of multijet cross sections in which PDFs cancel to some extent. So far, the multijet cross-section ratios $R_{\Delta R}$ [10] and $R_{3/2}$ [11] have been used for α_S determinations at hadron colliders. In this article, α_S is determined from dijet azimuthal decorrelations, based on the multijet cross-section ratio $R_{\Delta\phi}$ [17]. The RGE predictions are tested up to $Q = 1.675$ TeV.

The decorrelation of dijets in the azimuthal plane has been the subject of a number of measurements at the Fermilab Tevatron Collider [18] and the CERN Large Hadron Collider (LHC) [19,20]. The variable $\Delta\phi_{\text{dijet}}$ investigated in these analyses is defined from the angles in the azimuthal plane (the plane perpendicular to the beam direction) $\phi_{1,2}$ of the two highest-p_T jets in the event as $\Delta\phi_{\text{dijet}} = |\phi_1 - \phi_2|$. In exclusive high-$p_T$ dijet final states, the two jets are correlated in the azimuthal plane with $\Delta\phi_{\text{dijet}} = \pi$. Deviations from this ($\Delta\phi_{\text{dijet}} < \pi$) are due to additional activity in the final state, as described in pQCD by processes of higher order in α_S. Due to kinematic constraints, the phase space in $2 \to 3$ processes is restricted to $\Delta\phi_{\text{dijet}} > 2\pi/3$ [21] and lower $\Delta\phi_{\text{dijet}}$ values are only accessible in $2 \to 4$ processes. Measurements of dijet production with $2\pi/3 < \Delta\phi_{\text{dijet}} < \pi$ ($\Delta\phi_{\text{dijet}} < 2\pi/3$)

[*]Full author list given at the end of the article.

therefore test the pQCD matrix elements for three-jet (four-jet) production.

The quantity $R_{\Delta\phi}$ is defined as the fraction of all inclusive dijet events in which $\Delta\phi_{\rm dijet}$ is less than a specified value $\Delta\phi_{\rm max}$. This quantity can be exploited to extend the scope of the previous analyses towards studies of the rapidity dependence of dijet azimuthal decorrelations. Since $R_{\Delta\phi}$ is defined as a ratio of multijet cross sections for which the PDFs cancel to a large extent, it is well suited for determinations of $\alpha_{\rm S}$ and for studies of its running.

The quantity $R_{\Delta\phi}$ has so far been measured in $p\bar{p}$ collisions at a center-of-mass energy of $\sqrt{s} = 1.96$ TeV at the Fermilab Tevatron Collider [22]. This article presents the first measurement of $R_{\Delta\phi}$ in pp collisions, based on data at $\sqrt{s} = 8$ TeV taken with the ATLAS detector during 2012 at the LHC, corresponding to an integrated luminosity of 20.2 ± 0.4 fb^{-1} [23]. The data are corrected to “particle level” [24], and are used to extract $\alpha_{\rm S}$ and to study its running over a range of momentum transfers of $262 < Q < 1675$ GeV.

II. DEFINITION OF $R_{\Delta\phi}$ AND THE ANALYSIS PHASE SPACE

The definitions of the quantity $R_{\Delta\phi}$ and the choices of the variables that define the analysis phase space are taken from the proposal in Ref. [17]. Jets are defined by the anti-k_t jet algorithm as implemented in FastJet [25,26]. The anti-k_t jet algorithm is a successive recombination algorithm in which particles are clustered into jets in the E-scheme (i.e., the jet four-momentum is computed as the sum of the particle four-momenta). The radius parameter is chosen to be $R = 0.6$. This is large enough for a jet to include a sufficient amount of soft and hard radiation around the jet axis, thereby improving the properties of pQCD calculations at fixed order in $\alpha_{\rm S}$, and it is small enough to avoid excessive contributions from the underlying event [27]. An inclusive dijet event sample is extracted by selecting all events with two or more jets, where the two leading-$p_{\rm T}$ jets have $p_{\rm T} > p_{\rm T\,min}$. The dijet phase space is further specified in terms of the variables $y_{\rm boost}$ and y^*, computed from the rapidities, y_1 and y_2, of the two leading-$p_{\rm T}$ jets as $y_{\rm boost} = (y_1 + y_2)/2$ and $y^* = |y_1 - y_2|/2$, respectively.[1] In $2 \to 2$ processes, the variable $y_{\rm boost}$ specifies the longitudinal boost between the dijet and the proton-proton center-of-mass frames, and y^* (which is longitudinally boost invariant) represents the absolute value of the jet rapidities in the dijet center-of-mass frame. The dijet phase space is restricted to $|y_{\rm boost}| < y_{\rm boost}^{\rm max}$ and $y^* < y^*_{\rm max}$. The variable $H_{\rm T}$ is defined as the scalar sum of the jet $p_{\rm T}$ for all jets i with $p_{{\rm T}i} > p_{\rm T\,min}$ and $|y_i - y_{\rm boost}| < y^*_{\rm max}$. Furthermore, the leading-$p_{\rm T}$ jet is required to have $p_{\rm T1} > H_{\rm T}/3$. The values of the parameters $p_{\rm T\,min}$, $y_{\rm boost}^{\rm max}$, and $y^*_{\rm max}$ ensure that jets are well measured in the detector within $|y| < 2.5$ and that contributions from nonperturbative corrections and pileup (additional proton-proton interactions within the same or nearby bunch crossings) are small. The requirement $p_{\rm T1} > H_{\rm T}/3$ ensures (for a given $H_{\rm T}$) a well-defined minimum $p_{\rm T1}$ which allows single-jet triggers to be used in the measurement. It also reduces the contributions from events with four or more jets, and therefore pQCD corrections from higher orders in $\alpha_{\rm S}$. The values of all parameters are specified in Table I. The quantity $R_{\Delta\phi}$ is defined in this inclusive dijet event sample as the ratio

$$R_{\Delta\phi}(H_{\rm T}, y^*, \Delta\phi_{\rm max}) = \frac{\frac{d^2\sigma_{\rm dijet}(\Delta\phi_{\rm dijet}<\Delta\phi_{\rm max})}{dH_{\rm T}dy^*}}{\frac{d^2\sigma_{\rm dijet}(\text{inclusive})}{dH_{\rm T}dy^*}}, \quad (1)$$

where the denominator is the inclusive dijet cross section in the phase space defined above, in bins of the variables $H_{\rm T}$ and y^*. The numerator is given by the subset of the denominator for which $\Delta\phi_{\rm dijet}$ of the two leading-$p_{\rm T}$ jets obeys $\Delta\phi_{\rm dijet} < \Delta\phi_{\rm max}$. The measurement of the y^* dependence of $R_{\Delta\phi}$ allows a test of the rapidity dependence of the pQCD matrix elements. The value of $\Delta\phi_{\rm max}$ is directly related to the hardness of the jet(s) produced in addition to the two leading-$p_{\rm T}$ jets in the event. The transverse momentum sum $H_{\rm T}$ is one possible choice that can be related to the scale at which $\alpha_{\rm S}$ is probed. The measurement is made as a function of $H_{\rm T}$ in three different

TABLE I. The values of the parameters and the requirements that define the analysis phase space for the inclusive dijet event sample.

Variable	Value
$p_{\rm T\,min}$	100 GeV
$y_{\rm boost}^{\rm max}$	0.5
$y^*_{\rm max}$	2.0
$p_{\rm T1}/H_{\rm T}$	>1/3

TABLE II. The $H_{\rm T}$, y^*, and $\Delta\phi_{\rm max}$ regions in which $R_{\Delta\phi}(H_{\rm T}, y^*, \Delta\phi_{\rm max})$ is measured.

Quantity	Value
$H_{\rm T}$ bin boundaries (in TeV)	0.45, 0.6, 0.75, 0.9, 1.1, 1.4, 1.8, 2.2, 2.7, 4.0
y^* regions	0.0–0.5, 0.5–1.0, 1.0–2.0
$\Delta\phi_{\rm max}$ values	$7\pi/8$, $5\pi/6$, $3\pi/4$, $2\pi/3$

[1]The ATLAS experiment uses a right-handed coordinate system, where the origin is given by the nominal interaction point (IP) in the center of the detector. The x axis points from the IP to the center of the LHC ring, the y axis points upward, and the z axis along the proton beam direction. Cylindrical coordinates (r, ϕ) are used in the transverse plane, ϕ being the azimuthal angle around the beam pipe. The rapidity y is defined as $y = \frac{1}{2}\ln\frac{E+p_z}{E-p_z}$, and the pseudorapidity in terms of the polar angle θ as $\eta = -\ln\tan(\theta/2)$.

y^* regions and for four different values of $\Delta\phi_{\max}$ (see Table II).

III. THEORETICAL PREDICTIONS

The theoretical predictions in this analysis are obtained from perturbative calculations at fixed order in α_S with additional corrections for nonperturbative effects.

The pQCD calculations are carried out using NLOJET++ [28,29] interfaced to FASTNLO [30,31] based on the matrix elements for massless quarks in the $\overline{\mathrm{MS}}$ scheme [32]. The renormalization and factorization scales are set to $\mu_R = \mu_F = \mu_0$ with $\mu_0 = H_T/2$. In inclusive dijet production at leading order (LO) in pQCD this choice is equivalent to other common choices: $\mu_0 = \bar{p}_T = (p_{T1} + p_{T2})/2$ and $\mu_0 = p_{T1}$. The evolution of α_S is computed using the numerical solution of the next-to-leading-logarithmic (2-loop) approximation of the RGE.

The pQCD predictions for the ratio $R_{\Delta\phi}$ are obtained from the ratio of the cross sections in the numerator and denominator in Eq. (1), computed to the same relative order (both either to NLO or to LO). The pQCD predictions for the cross section in the denominator by NLOJET++ are available up to NLO. For $\Delta\phi_{\max} = 7\pi/8, 5\pi/6, 3\pi/4$ ($2\pi/3$) the numerator is a three-jet (four-jet) quantity for which the pQCD predictions in NLOJET++ are available up to NLO (LO) [21].

The PDFs are taken from the global analyses MMHT2014 (NLO) [33,34], CT14 (NLO) [35], and NNPDFv2.3 (NLO) [36].[2] For additional studies, the PDF sets ABMP16 (NNLO) [38][3] and HERAPDF 2.0 (NLO) [39] are used, which were obtained using data from selected processes only. All of these PDF sets were obtained for a series of discrete $\alpha_S(m_Z)$ values, in increments of $\Delta\alpha_S(m_Z) = 0.001$ (or $\Delta\alpha_S(m_Z) = 0.002$ for NNPDFv2.3). In all calculations in this paper, the PDF sets are consistently chosen to correspond to the value of $\alpha_S(m_Z)$ used in the matrix elements. The extraction of α_S from the experimental $R_{\Delta\phi}$ data requires a continuous dependence of the pQCD calculations on $\alpha_S(m_Z)$. This is obtained by cubic interpolation (linear extrapolation) for $\alpha_S(m_Z)$ values inside (outside) the ranges provided by the PDF sets. The central predictions that are compared to the data use $\alpha_S(m_Z) = 0.118$, which is close to the current world average, and the MMHT2014 PDFs. The MMHT2014 PDFs also provide the largest range of $\alpha_S(m_Z)$ values ($0.108 \le \alpha_S(m_Z) \le 0.128$). For these reasons, the MMHT2014 PDFs are used to obtain the central results in the α_S determinations.

[2]The NNPDFv3.0 PDFs [37] are available only for a rather limited $\alpha_S(m_Z)$ range (0.115–0.121); therefore, the older NNPDFv2.3 results are employed.

[3]The ABMP16 analysis does not provide NLO PDF sets for a series of $\alpha_S(m_Z)$ values; their NNLO PDF sets are therefore used.

The uncertainties of the perturbative calculation are estimated from the scale dependence (as an estimate of missing higher-order pQCD corrections) and the PDF uncertainties. The former is evaluated from independent variations of μ_R and μ_F between $\mu_0/2$ and $2\mu_0$ (with the restriction $0.5 \le \mu_R/\mu_F \le 2.0$). The PDF-induced uncertainty is computed by propagating the MMHT2014 PDF uncertainties. In addition, a "PDF set" uncertainty is included as the envelope of the differences of the results obtained with CT14, NNPDFv2.3, ABMP16, and HERAPDF 2.0, relative to those obtained with MMHT2014.

The pQCD predictions based on matrix elements for massless quarks also depend on the number of quark flavors, in gluon splitting ($g \to q\bar{q}$), n_f, which affects the tree-level matrix elements and their real and virtual corrections, as well as the RGE predictions and the PDFs obtained from global data analyses. The central results in this analysis are obtained for a consistent choice $n_f = 5$ in all of these contributions. Studies of the effects of using $n_f = 6$ in the matrix elements and the RGE, as documented in Appendix A, show that the corresponding effects for $R_{\Delta\phi}$ are between -1% and $+2\%$ over the whole kinematic range of this measurement. Appendix A also includes a study of the contributions from the $t\bar{t}$ production process, concluding that the effects on $R_{\Delta\phi}$ are less than 0.5% over the whole analysis phase space.

The corrections due to nonperturbative effects, related to hadronization and the underlying event, were obtained in Ref. [17], using the event generators PYTHIA 6.426 [40] and HERWIG 6.520 [41,42]. An estimate of the model uncertainty is obtained from a study of the dependence on the generator's parameter settings (tunes), based on the PYTHIA tunes AMBT1 [43], DW [44], A [45], and S-Global [46], which differ in the parameter settings and the implementations of the parton-shower and underlying-event models. All model predictions for the total nonperturbative corrections lie below 2% (4%) for $\Delta\phi_{\max} = 7\pi/8$ and $5\pi/6$ ($\Delta\phi_{\max} = 3\pi/4$ and $2\pi/3$), and the different models agree within 2% (5%) for $\Delta\phi_{\max} = 7\pi/8$ and $5\pi/6$ ($\Delta\phi_{\max} = 3\pi/4$ and $2\pi/3$).

For this analysis, the central results are taken to be the average values obtained from PYTHIA with tunes AMBT1 and DW. The corresponding uncertainty is taken to be half of the difference (the numerical values are provided in Ref. [47]). The results obtained with PYTHIA tunes A and S-Global as well as HERWIG are used to study systematic uncertainties.

IV. ATLAS DETECTOR

ATLAS is a general-purpose detector consisting of an inner tracking detector, a calorimeter system, a muon spectrometer, and magnet systems. A detailed description of the ATLAS detector is given in Ref. [47]. The main components used in the $R_{\Delta\phi}$ measurement are the inner detector, the calorimeters, and the trigger system.

The position of the pp interaction is determined from charged-particle tracks reconstructed in the inner detector, located inside a superconducting solenoid that provides a 2 T axial magnetic field. The inner detector, covering the region $|\eta| < 2.5$, consists of layers of silicon pixels, silicon microstrips, and transition radiation tracking detectors.

Jet energies and directions are measured in the three electromagnetic and four hadronic calorimeters with a coverage of $|\eta| < 4.9$. The electromagnetic liquid argon (LAr) calorimeters cover $|\eta| < 1.475$ (barrel), $1.375 < |\eta| < 3.2$ (endcap), and $3.1 < |\eta| < 4.9$ (forward). The regions $|\eta| < 0.8$ (barrel) and $0.8 < |\eta| < 1.7$ (extended barrel) are covered by scintillator/steel sampling hadronic calorimeters, while the regions $1.5 < |\eta| < 3.2$ and $3.1 < |\eta| < 4.9$ are covered by the hadronic endcap with LAr/Cu calorimeter modules, and the hadronic forward calorimeter with LAr/W modules.

During 2012, for pp collisions, the ATLAS trigger system was divided into three levels, labeled L1, L2, and the event filter (EF) [48,49]. The L1 trigger is hardware-based, while L2 and EF are software based and impose increasingly refined selections designed to identify events of interest. The jet trigger identifies electromagnetically and hadronically interacting particles by reconstructing the energy deposited in the calorimeters. The L1 jet trigger uses a sliding window of $\Delta\eta \times \Delta\phi = 0.8 \times 0.8$ to find jets and requires these to have transverse energies E_{T} above a given threshold, measured at the electromagnetic scale. Jets triggered by L1 are passed to the L2 jet trigger, which reconstructs jets in the same region using a simple cone jet algorithm with a cone size of 0.4 in (η, ϕ) space. Events are accepted if a L2 jet is above a given E_{T} threshold. In events which pass L2, a full event reconstruction is performed by the EF. The jet EF constructs topological clusters [50] from which jets are then formed, using the anti-k_t jet algorithm with a radius parameter of $R = 0.4$. These jets are then calibrated to the hadronic scale. Events for this analysis are collected either with single-jet triggers with different minimum E_{T} requirements or with multijet triggers based on a single high-E_{T} jet plus some amount of H_{T} (the scalar E_{T} sum) of the multijet system. The trigger efficiencies are determined relative to fully efficient reference triggers, and each trigger is used above an H_{T} threshold where it is more than 98% efficient. The triggers used for the different H_{T} regions in the offline analysis are listed in Table III.

Single-jet triggers select events if any jet with $|\eta| < 3.2$ is above the E_{T} thresholds at L1, L2, and the EF. Due to their high rates, the single-jet triggers studied are highly prescaled during data-taking. Multijet triggers select events if an appropriate high-E_{T} jet is identified and the H_{T} value, summed over all jets at the EF with $|\eta| < 3.2$ and $E_{\mathrm{T}} > 45$ GeV, is above a given threshold. The additional H_{T} requirement significantly reduces the selected event rate, and lower prescales can be applied. The integrated luminosity of the data sample collected with the highest threshold triggers is 20.2 ± 0.4 fb^{-1}.

TABLE III. The triggers used to select the multijet events in the different H_{T} ranges in the offline analysis, and the corresponding integrated luminosities.

H_{T} range [GeV]	Trigger type	Integrated luminosity [pb^{-1}]
450–600	Single-jet	9.6 ± 0.2
600–750	Single-jet	36 ± 1
750–900	Multi-jet	546 ± 11
>900	Multi-jet	$(20.2 \pm 0.4) \times 10^3$

The detector response for the measured quantities is determined using a detailed simulation of the ATLAS detector in GEANT 4 [51,52]. The particle-level events, subjected to the detector simulation, were produced by the PYTHIA event generator [53] (version 8.160) with CT10 PDFs. The PYTHIA parameters were set according to the AU2 tune [54]. The "particle-level" jets are defined based on the four-momenta of the generated stable particles (as recommended in Ref. [24], with a proper lifetime τ satisfying $c\tau > 10$ mm, including muons and neutrinos from hadron decays). The "detector-level" jets are defined based on the four-momenta of the simulated detector objects.

V. MEASUREMENT PROCEDURE

The inclusive dijet events used for the measurement of $R_{\Delta\phi}$ were collected between April and December 2012 by the ATLAS detector in proton-proton collisions at $\sqrt{s} = 8$ TeV. All events used in this measurement are required to satisfy data-quality criteria which include stable beam conditions and stable operation of the tracking systems, calorimeters, solenoid, and trigger system. Events that pass the trigger selections described above are included in the sample if they contain at least one primary collision vertex with at least two associated tracks with $p_{\mathrm{T}} > 400$ MeV, in order to reject contributions due to cosmic-ray events and beam background. The primary vertex with highest $\sum p_{\mathrm{T}}^2$ of associated tracks is taken as the event vertex.

Jets are reconstructed offline using the anti-k_t jet algorithm with a radius parameter $R = 0.6$. Input to the jet algorithm consists of locally calibrated three-dimensional topological clusters [50] formed from sums of calorimeter cell energies, corrected for local calorimeter response, dead material, and out-of-cluster losses for pions. The jets are further corrected for pileup contributions and then calibrated to the hadronic scale, as detailed in the following. The pileup correction is applied to account for the effects on the jet response from additional interactions within the same proton bunch crossing ("in-time pileup") and from interactions in bunch crossings preceding or following the one of interest ("out-of-time pileup"). Energy is subtracted from each jet, based upon the energy density in the event and the measured area of the jet [55]. The jet energy is then adjusted by a small residual correction depending on the average pileup conditions for the event. This calibration restores the calorimeter energy scale, on average, to a reference point where pileup is not present [56]. Jets are then calibrated using an energy- and η-dependent correction to the hadronic scale with constants derived from data and Monte Carlo samples of jets produced in multi-jet processes. A residual calibration, based on a combination of several *in situ* techniques, is applied to take into account differences between data and Monte Carlo simulation. In the central region of the detector, the uncertainty in the jet energy calibration is derived from the transverse momentum balance in $Z+\text{jet}$, $\gamma+\text{jet}$ or multijet events measured *in situ*, by propagating the known uncertainties of the energies of the reference objects to the jet energies. The energy uncertainties for the central region are then propagated to the forward region by studying the transverse momentum balance in dijet events with one central and one forward jet [57]. The energy calibration uncertainty in the high-p_{T} range is estimated using the *in situ* measurement of the response to single isolated hadrons [58]. The jet energy calibration's total uncertainty is decomposed into 57 uncorrelated contributions, of which each is fully correlated in p_{T}. The corresponding uncertainty in jet p_{T} is between 1% and 4% in the central region ($|\eta| < 1.8$), and increases to 5% in the forward region ($1.8 < |\eta| < 4.5$).

The jet energy resolution has been measured in the data using the bisector method in dijet events [59–61] and the Monte Carlo simulation is seen to be in good agreement with the data. The uncertainty in the jet energy resolution is affected by selection parameters for jets, such as the amount of nearby jet activity, and depends on the η and p_{T} values of the jets. Further details about the determinations of the jet energy scale and resolution are given in Refs. [58,59,62].

The angular resolution of jets is obtained in the Monte Carlo simulation by matching particle-level jets with detector-level jets, when their distance in $\Delta R = \sqrt{(\Delta y^2 + \Delta\phi^2)}$ is smaller than the jet radius parameter. The jet η and ϕ resolutions are obtained from a Gaussian fit to the distributions of the difference between the detector-level and particle-level values of the corresponding quantity. The difference between the angular resolutions determined from different Monte Carlo simulations is taken as a systematic uncertainty for the measurement result, which is about 10%–15% for $p_{\mathrm{T}} < 150$ GeV and decreases to about 1% for $p_{\mathrm{T}} > 400$ GeV. The bias in jet η and ϕ is found to be negligible.

All jets within the whole detector acceptance, $|\eta| < 4.9$, are considered in the analysis. Data-quality requirements are applied to each reconstructed jet according to its properties, to reject spurious jets not originating from hard-scattering events. In each H_{T} bin, events from a single trigger are used and the same trigger is used for the numerator and the denominator of $R_{\Delta\phi}$. In order to test the stability of the measurement results, the event sample is divided into subsamples with different pileup conditions. The $R_{\Delta\phi}$ results for different pileup conditions are compatible within the statistical uncertainties without any systematic trends. The measurement is also tested for variations resulting from loosening the requirements on the event- and jet-data-quality conditions, and the observed variations are also consistent within the statistical uncertainties.

The distributions of $R_{\Delta\phi}(H_{\mathrm{T}}, y^*, \Delta\phi_{\max})$ are corrected for experimental effects, including detector resolutions and inefficiencies, using the simulation. To ensure that the simulation describes all relevant distributions, including the p_{T} and y distributions of the jets, the generated events are reweighted, based on the properties of the generated jets, to match these distributions in data, and to match the H_{T} dependence of the observed inclusive dijet cross section as well as the $R_{\Delta\phi}$ distributions and their H_{T} dependence. To minimize migrations between H_{T} bins due to resolution effects, the bin widths are chosen to be larger than the detector resolution. The bin purities, defined as the fraction of all reconstructed events that are generated in the same bin, are 65%–85% for $\Delta\phi_{\max} = 7\pi/8$ and $5\pi/6$, and 50%–75% for $\Delta\phi_{\max} = 3\pi/4$ and $2\pi/3$. The bin efficiencies, defined as the fraction of all generated events that are reconstructed in the same bin, have values in the same ranges as the bin purities. The corrections are obtained bin by bin from the generated Pythia events as the ratio of the $R_{\Delta\phi}$ results for the particle-level jets and the detector-level jets. These corrections are typically between 0% and 3%, and never outside the range from -10% to $+10\%$. Uncertainties in these corrections due to the modeling of the migrations by the simulation are estimated from the changes of the correction factors when varying the reweighting function. In most parts of the phase space, these uncertainties are below 1%. The results from the bin-by-bin correction procedure were compared to the results when using a Bayesian iterative unfolding procedure [63], and the two results agree within their statistical uncertainties.

The uncertainties of the $R_{\Delta\phi}$ measurements include two sources of statistical uncertainty and 62 sources of systematic uncertainty. The statistical uncertainties arise from the data and from the correction factors. The systematic uncertainties are from the correction factors (two independent sources, related to variations of the reweighting of the generated events), the jet energy calibration (57 independent sources), the jet energy resolution, and the jet η and ϕ resolutions. To avoid double counting of statistical fluctuations, the H_{T} dependence of the uncertainty distributions is smoothed by fitting either linear or quadratic functions in $\log(H_{\mathrm{T}}/\mathrm{GeV})$. From all 62 sources of experimental correlated uncertainties, the dominant systematic uncertainties are due to the jet energy calibration. For $\Delta\phi_{\max} = 7\pi/8$ and $5\pi/6$ the jet energy calibration uncertainties are typically between 1.0% and 1.5% and always less than 3.1%. For smaller values of $\Delta\phi_{\max}$ they can be as large as 4% (for $\Delta\phi_{\max} = 3\pi/4$) or 9% (for $\Delta\phi_{\max} = 2\pi/3$).

VI. MEASUREMENT RESULTS

The measurement results for $R_{\Delta\phi}(H_T, y^*, \Delta\phi_{\max})$ are corrected to the particle level and presented as a function of H_T, in different regions of y^* and for different $\Delta\phi_{\max}$ requirements. The results are listed in Appendix B in Tables VI–IX, and displayed in Fig. 1, at the arithmetic center of the H_T bins. At fixed (y^*, $\Delta\phi_{\max}$), $R_{\Delta\phi}(H_T, y^*, \Delta\phi_{\max})$ decreases with increasing H_T and increases with increasing y^* at fixed (H_T, $\Delta\phi_{\max}$). At fixed (H_T, y^*), $R_{\Delta\phi}$ decreases with decreasing $\Delta\phi_{\max}$.

Theoretical predictions based on NLO pQCD (for $\Delta\phi_{\max} = 7\pi/8$, $5\pi/6$, and $3\pi/4$) or LO (for $\Delta\phi_{\max} = 2\pi/3$) with corrections for nonperturbative effects, as described in Sec. III, are compared to the data. The ratios of data to the theoretical predictions are displayed in Fig. 2. To provide further information about the convergence of the pQCD calculation, the inverse of the NLO K-factors are also shown (defined as the ratio of predictions for $R_{\Delta\phi}$ at NLO and LO, $K = R^{\rm NLO}_{\Delta\phi}/R^{\rm LO}_{\Delta\phi}$). In all kinematical regions, the data are described by the theoretical predictions, even for $\Delta\phi_{\max} = 2\pi/3$, where the predictions are only based on LO pQCD and have uncertainties of about 20% (dominated by the dependence on μ_R and μ_F). The data for $\Delta\phi_{\max} = 7\pi/8$ and $5\pi/6$ allow the most stringent tests of the theoretical predictions, since for these $\Delta\phi_{\max}$ values the theoretical uncertainties are typically less than ±5%.

VII. SELECTION OF DATA POINTS FOR THE α_S EXTRACTION

The extraction of $\alpha_S(Q)$ at different scales $Q = H_T/2$ is based on a combination of data points in different kinematic regions of y^* and $\Delta\phi_{\max}$, with the same H_T. The data points are chosen according to the following criteria.

(1) Data points are used only from kinematic regions in which the pQCD predictions appear to be most reliable, as judged by the renormalization and factorization scale dependence, and by the NLO K-factors.
(2) For simplicity, data points are only combined in the α_S extraction if they are statistically independent, i.e., if their accessible phase space does not overlap.
(3) The preferred data points are those for which the cancellation of the PDFs between the numerator and the denominator in $R_{\Delta\phi}$ is largest.
(4) The experimental uncertainty at large H_T is limited by the sample size. If the above criteria give equal preference to two or more data sets with overlapping phase space, the data points with smaller statistical uncertainties are used to test the RGE at the largest possible momentum transfers with the highest precision.

Based on criterion (1), the data points obtained for $\Delta\phi_{\max} = 2\pi/3$ are excluded, as the pQCD predictions in NLOJET++ are only available at LO. Furthermore, it is

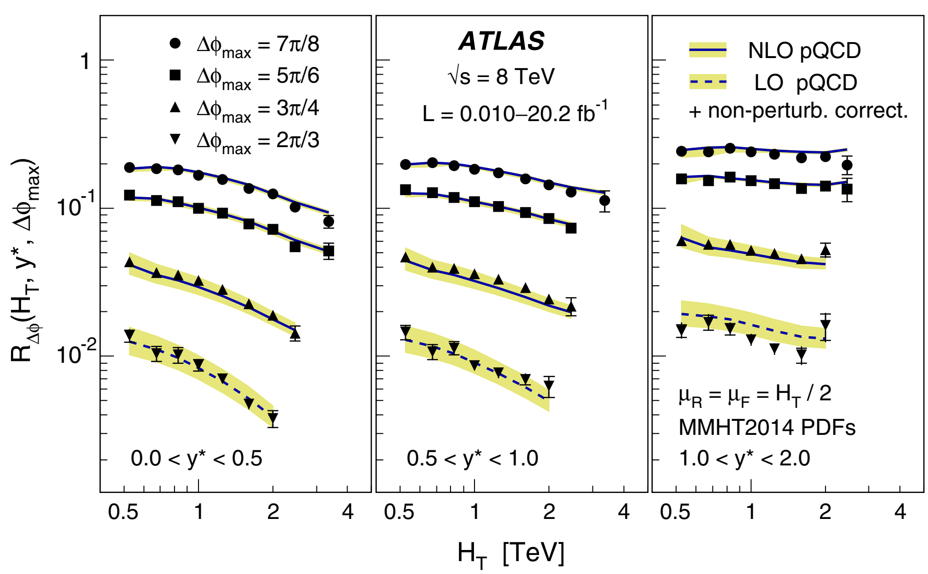

FIG. 1. The measurement of $R_{\Delta\phi}(H_T, y^*, \Delta\phi_{\max})$ as a function of H_T in three regions of y^* and for four choices of $\Delta\phi_{\max}$. The inner error bars indicate the statistical uncertainties, and the sum in quadrature of statistical and systematic uncertainties is displayed by the total error bars. The theoretical predictions, based on pQCD at NLO (for $\Delta\phi_{\max} = 7\pi/8$, $5\pi/6$, and $3\pi/4$) and LO (for $\Delta\phi_{\max} = 2\pi/3$) are shown as solid and dashed lines, respectively. The shaded bands display the PDF uncertainties and the scale dependence, added in quadrature.

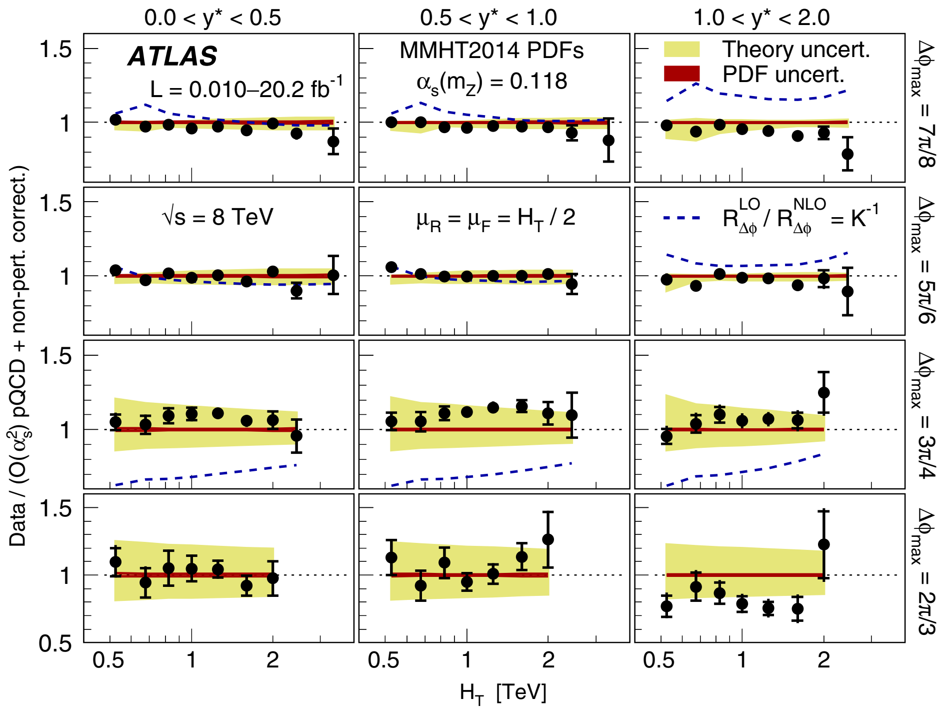

FIG. 2. The ratios of the $R_{\Delta\phi}$ measurements and the theoretical predictions obtained for MMHT2014 PDFs and $\alpha_S(m_Z) = 0.118$. The ratios are shown as a function of H_T, in different regions of y^* (columns) and for different $\Delta\phi_{\max}$ (rows). The inner error bars indicate the statistical uncertainties and the sum in quadrature of statistical and systematic uncertainties is displayed by the total error bars. The theoretical uncertainty is the sum in quadrature of the uncertainties due to the PDFs and the scale dependence. The inverse of the NLO K-factor is indicated by the dashed line.

observed that the points for $\Delta\phi_{\max} = 3\pi/4$ have a large scale dependence, which is typically between $+15\%$ and -10%. For the remaining data points with $\Delta\phi_{\max} = 7\pi/8$ and $5\pi/6$ at larger y^* ($1 < y^* < 2$), the NLO corrections are negative and (with a size of 5%–23%) larger than those at smaller y^*, indicating potentially larger corrections from not yet calculated higher orders. The conclusion from criterion (1) is therefore that the pQCD predictions are most reliable in the four kinematic regions $0 < y^* < 0.5$ and $0.5 < y^* < 1$, for $\Delta\phi_{\max} = 7\pi/8$ and $\Delta\phi_{\max} = 5\pi/6$, where the NLO K-factors are typically within $\pm 5\%$ of unity.

The requirement of statistically independent data points according to criterion (2) means that the data points from different y^* regions can be combined, but not those with different $\Delta\phi_{\max}$. The choice whether to use the data with $\Delta\phi_{\max} = 7\pi/8$ or $5\pi/6$ (in either case combining the data for $0 < y^* < 0.5$ and $0.5 < y^* < 1$) is therefore based on criteria (3) and (4).

The cancellation of the PDFs, as addressed in criterion (3), is largest for those data points for which the phase space of the numerator in Eq. (1) is closest to that of the denominator. Since the numerator of $R_{\Delta\phi}$ is a subset of the denominator, this applies more to the data at larger values of $\Delta\phi_{\max}$. For those points, the fractional contributions from different partonic subprocesses ($gg \to$ jets, $gq \to$ jets, $qq \to$ jets), and the ranges in the accessible proton momentum fraction x are more similar for the numerator and denominator, resulting in a larger cancellation of PDFs in $R_{\Delta\phi}$. This argument, based on the third criterion, leads to the same conclusion as the suggestion of criterion (4), to use the data set with smallest statistical uncertainty.

Based on the four criteria, α_S is therefore extracted combining the data points in the rapidity regions $0 < y^* < 0.5$ and $0.5 < y^* < 1$ for $\Delta\phi_{\max} = 7\pi/8$. Extractions of α_S from the data points in other kinematical regions in y^* and $\Delta\phi_{\max}$ are used to investigate the dependence of the final results on those choices.

VIII. DETERMINATION OF α_S

The $R_{\Delta\phi}$ measurements in the selected kinematic regions are used to determine α_S and to test the QCD predictions for its running as a function of the scale $Q = H_T/2$. The α_S results are extracted by using MINUIT [64], to minimize the χ^2 function specified in Appendix C. In this approach, the experimental and theoretical uncertainties that are correlated between all data points are treated in the Hessian method [65] by including a nuisance parameter for each uncertainty source, as described in Appendix C. The only exceptions are the uncertainties due to the PDF set and the $\mu_{R,F}$ dependence of the pQCD calculation. These uncertainties are determined from the variations of the α_S results,

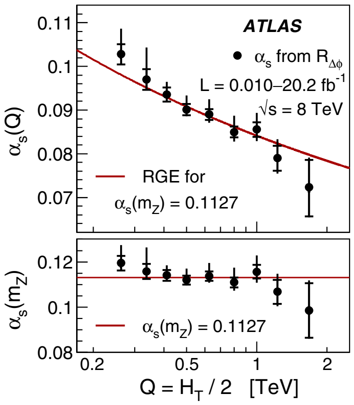

FIG. 3. The α_S results determined from the $R_{\Delta\phi}$ data for $\Delta\phi_{\max} = 7\pi/8$ in the y^* regions $0 < y^* < 0.5$ and $0.5 < y^* < 1.0$ in the range of $262 < Q < 1675$ GeV. The inner error bars indicate the experimental uncertainties and the sum in quadrature of experimental and theoretical uncertainties is displayed by the total error bars. The $\alpha_S(Q)$ results (top) are displayed together with the prediction of the RGE for the $\alpha_S(m_Z)$ result obtained in this analysis. The individual $\alpha_S(Q)$ values are then evolved to $Q = m_Z$ (bottom).

when repeating the α_S extractions for different PDF sets and for variations of the scales $\mu_{R,F}$ as described in Sec. III.

Results of $\alpha_S(Q)$ (with $Q = H_T/2$, taken at the arithmetic centers of the H_T bins) are determined from the $R_{\Delta\phi}$ data for $\Delta\phi_{\max} = 7\pi/8$, combining the data points in the two y^* regions of $0 < y^* < 0.5$ and $0.5 < y^* < 1.0$. Nine $\alpha_S(Q)$ values are determined in the range $262 < Q \leq 1675$ GeV. A single χ^2 minimization provides the uncertainties due to the statistical uncertainties, the experimental correlated uncertainties, the uncertainties due to the nonperturbative corrections, and the MMHT2014 PDF uncertainty. Separate χ^2 minimizations are made for variations of μ_R and μ_F (in the ranges described in Sec. III), and also for the CT14, NNPDFv2.3, ABMP16, and HERAPDF 2.0 PDF sets. The largest individual variations are used to quantify the uncertainty due to the scale dependence and the PDF set, respectively. The so-defined PDF set uncertainty may partially double count some of the uncertainties already taken into account by the MMHT2014 PDF uncertainties, but it may also include some additional systematic uncertainties due to different approaches in the PDF determinations. The $\alpha_S(Q)$ results are displayed in Fig. 3 and listed in Table IV.

In addition, assuming the validity of the RGE, all 18 data points in $0 < y^* < 0.5$ and $0.5 < y^* < 1.0$ for $\Delta\phi_{\max} = 7\pi/8$ are used to extract a combined $\alpha_S(m_Z)$ result. The combined fit (for MMHT2014 PDFs at the default scale) gives $\chi^2 = 21.7$ for 17 degrees of freedom and a result of $\alpha_S(m_Z) = 0.1127$ (the uncertainties are detailed in Table V). The fit is then repeated for the CT14, NNPDFv2.3, ABMP16, and HERAPDF 2.0 PDF sets, for which the $\alpha_S(m_Z)$ results differ by $+0.0001$, $+0.0022$, $+0.0026$, and $+0.0029$, respectively. Fits for various choices of μ_R and μ_F result in variations of the $\alpha_S(m_Z)$ results between -0.0019 and $+0.0052$.

Further dependence of the α_S results on some of the analysis choices is investigated in a series of systematic studies.

(i) *Changing the $\Delta\phi_{\max}$ requirement.*—Based on the criteria outlined in Sec. VII it was decided to use the data for $\Delta\phi_{\max} = 7\pi/8$ in the α_S analysis. If, instead, the data with $\Delta\phi_{\max} = 5\pi/6$ are used, the $\alpha_S(m_Z)$ result changes by $+0.0052$ to $\alpha_S(m_Z) = 0.1179$, with an uncertainty of $+0.0065$ and -0.0045 due to the scale dependence.

(ii) *Extending the y^* region.*—For the central α_S results, the data points with $1 < y^* < 2$ are excluded. If $\alpha_S(m_Z)$ is determined only from the data points for $1 < y^* < 2$ (with $\Delta\phi_{\max} = 7\pi/8$) the $\alpha_S(m_Z)$ result changes by -0.0018, with an increased scale dependence, to $\alpha_S(m_Z) = 0.1109^{+0.0071}_{-0.0031}$ with $\chi^2 = 13.8$ for 7 degrees of freedom. If the data points for $1 < y^* < 2$ are combined with those

TABLE IV. The results for $\alpha_S(Q)$ determined from the $R_{\Delta\phi}$ data for $\Delta\phi_{\max} = 7\pi/8$ with $0 < y^* < 0.5$ and $0.5 < y^* < 1.0$. All uncertainties have been multiplied by a factor of 10^3.

Q [GeV]	$\alpha_S(Q)$	Total uncertainty	Statistical	Experimental correlated	Nonperturbative corrections	MMHT2014 uncertainty	PDF set	$\mu_{R,F}$ variation
262.5	0.1029	$^{+6.0}_{-2.8}$	± 1.6	$^{+1.6}_{-1.7}$	$^{+0.4}_{-0.4}$	$^{+0.4}_{-0.4}$	$^{+1.4}_{-0.9}$	$^{+5.3}_{-0.2}$
337.5	0.0970	$^{+8.0}_{-2.6}$	± 1.8	$^{+1.5}_{-1.5}$	$^{+0.4}_{-0.4}$	$^{+0.3}_{-0.3}$	$^{+3.0}_{-0.5}$	$^{+7.0}_{-0.7}$
412.5	0.0936	$^{+4.0}_{-2.2}$	± 0.9	$^{+1.3}_{-1.3}$	$^{+0.3}_{-0.3}$	$^{+0.3}_{-0.3}$	$^{+2.6}_{-1.4}$	$^{+2.5}_{-0.2}$
500.0	0.0901	$^{+3.7}_{-1.5}$	± 0.6	$^{+1.2}_{-1.2}$	$^{+0.2}_{-0.2}$	$^{+0.3}_{-0.3}$	$^{+1.9}_{-0.3}$	$^{+2.9}_{-0.6}$
625.0	0.0890	$^{+3.9}_{-1.8}$	± 0.5	$^{+1.1}_{-1.1}$	$^{+0.1}_{-0.1}$	$^{+0.3}_{-0.4}$	$^{+1.7}_{-0.3}$	$^{+3.3}_{-1.3}$
800.0	0.0850	$^{+5.9}_{-2.2}$	± 0.6	$^{+1.0}_{-1.1}$	$^{+0.1}_{-0.1}$	$^{+0.4}_{-0.4}$	$^{+4.6}_{-0.2}$	$^{+3.5}_{-1.8}$
1000	0.0856	$^{+4.0}_{-2.7}$	± 1.2	$^{+1.1}_{-1.1}$	$^{+0.1}_{-0.1}$	$^{+0.4}_{-0.4}$	$^{+1.4}_{-0.4}$	$^{+3.4}_{-2.0}$
1225	0.0790	$^{+4.6}_{-3.5}$	± 2.5	$^{+1.2}_{-1.2}$	$^{+0.1}_{-0.1}$	$^{+0.5}_{-0.5}$	$^{+1.6}_{-0.4}$	$^{+3.2}_{-1.9}$
1675	0.0723	$^{+7.0}_{-8.6}$	± 6.1	$^{+1.3}_{-1.2}$	$< \pm 0.1$	$^{+0.5}_{-0.5}$	$^{+1.7}_{-5.1}$	$^{+2.8}_{-1.6}$

TABLE V. Fit result for $\alpha_S(m_Z)$, determined from the $R_{\Delta\phi}$ data for $\Delta\phi_{\max} = 7\pi/8$ with $0.0 < y^* < 0.5$ and $0.5 < y^* < 1.0$. All uncertainties have been multiplied by a factor of 10^3.

$\alpha_S(m_Z)$	Total uncertainty	Statistical	Experimental correlated	Nonperturbative corrections	MMHT2014 uncertainty	PDF set	$\mu_{R,F}$ variation
0.1127	$^{+6.3}_{-2.7}$	± 0.5	$^{+1.8}_{-1.7}$	$^{+0.3}_{-0.1}$	$^{+0.6}_{-0.6}$	$^{+2.9}_{-0.0}$	$^{+5.2}_{-1.9}$

for $0 < y^* < 0.5$ and $0.5 < y^* < 1$, the result is $\alpha_S(m_Z) = 0.1135^{+0.0051}_{-0.0025}$.

(iii) *Smoothing the systematic uncertainties.*—In the experimental measurement, the systematic uncertainties that are correlated between different data points were smoothed in order to avoid double counting of statistical fluctuations. For this purpose, the systematic uncertainties were fitted with a linear function in $\log(H_T/\mathrm{GeV})$. If, alternatively, a quadratic function is used, the central $\alpha_S(m_Z)$ result changes by −0.0006, and the experimental uncertainty is changed from $^{+0.0018}_{-0.0017}$ to $^{+0.0017}_{-0.0016}$.

(iv) *Stronger correlations of experimental uncertainties.*—The largest experimental uncertainties are due to the jet energy calibration. These are represented by contributions from 57 independent sources. Some of the correlations are estimated on the basis of prior assumptions. In a study of the systematic effects these assumptions are varied, resulting in an alternative scenario with stronger correlations between some of these sources. This changes the combined $\alpha_S(m_Z)$ result by −0.0004, while the experimental correlated uncertainty is reduced from $^{+0.0018}_{-0.0017}$ to $^{+0.0012}_{-0.0013}$.

(v) *Treatment of nonperturbative corrections.*—The central α_S results are obtained using the average values of the nonperturbative corrections from Pythia tunes ABT1 and DW, and the spread between the average and the individual models is taken as a correlated uncertainty, which is treated in the Hessian approach by fitting a corresponding nuisance parameter. Alternatively, the $\alpha_S(m_Z)$ result is also extracted by fixing the values for the nonperturbative corrections to the individual model predictions from Herwig (default) and Pythia with tunes AMBT1, DW, S Global, and A, and to unity (corresponding to zero nonperturbative corrections). The corresponding changes of the $\alpha_S(m_Z)$ result for the different choices are between −0.0004 and +0.0011.

(vi) *Choice of $n_f = 6$ versus $n_f = 5$.*—The choice of $n_f = 6$ corresponds to the rather extreme approximation in which the top quark is included as a massless quark in the pQCD calculation. The effect of using $n_f = 6$ instead of $n_f = 5$ in the pQCD matrix elements and the RGE and the corresponding impact on $R_{\Delta\phi}$ are discussed in Appendix A. The effects on the extracted α_S results are also studied and are found to be between +1.3% (at low H_T) and −1.1% (at high H_T) for the nine $\alpha_S(Q)$ results. The combined $\alpha_S(m_Z)$ result changes by −0.0006 from 0.1127 (for $n_f = 5$) to 0.1121 (for $n_f = 6$).

(vii) *A scan of the renormalization scale dependence.*—Unlike all other uncertainties which are treated in the Hessian approach, the uncertainty due to the renormalization and factorization scale dependence is obtained from individual fits in which both scales are set to fixed values. To ensure that the largest variation may not occur at intermediate values, a scan of the renormalization scale dependence in finer steps is made. For each of the three variations of μ_F by factors of $x_{\mu_F} = 0.5, 1.0, 2.0$, the renormalization scale is varied by nine logarithmically equal-spaced factors of $x_{\mu_R} = 0.5$, 0.596, 0.708, 0.841, 1.0, 1.189, 1.413, 1.679, and 2.0.

It is seen that the largest upward variation (of +0.0052) is obtained for the correlated variation $x_{\mu_R} = x_{\mu_F} = 2.0$. The lowest variation (of −0.0027) is obtained for the anti-correlated variation $x_{\mu_R} = 0.5$ and $x_{\mu_F} = 2.0$, which is, however, outside the range $0.5 \leq x_{\mu_R}/x_{\mu_F} \leq 2$. The lowest variation within this range (−0.0014) is obtained for $x_{\mu_R} = 0.5$ and $x_{\mu_F} = 1.0$.

(viii) *Effects of the Hessian method.*—In the Hessian approach, a fit can explore the multidimensional uncertainty space to find the χ^2 minimum at values of the nuisance parameters associated to the sources of systematic uncertainties, that do not represent the best knowledge of the corresponding sources. While in this analysis the shifts of the nuisance parameters are all small, it is still interesting to study their effects on the α_S fit results. Therefore, the $\alpha_S(m_Z)$ extraction is repeated, initially including the uncorrelated (i.e., statistical) uncertainties only. Then, step by step, the experimental correlated uncertainties, the uncertainties of the nonperturbative corrections, and the PDF uncertainties are included. These fits produce $\alpha_S(m_Z)$ results that differ by less than ±0.0004 from the central result.

These systematic studies show that the α_S results are rather independent of the analysis choices and demonstrate the stability of the α_S extraction procedure. These variations are not treated as additional uncertainties because their resulting effects are smaller than the other theoretical uncertainties. The largest variation of the $\alpha_S(m_Z)$ result, by $+0.0052$, is obtained when using the data with $\Delta\phi_{\max} = 5\pi/6$ instead of $\Delta\phi_{\max} = 7\pi/8$. This difference may be due to different higher-order corrections to the NLO pQCD results for different $\Delta\phi_{\max}$ values. This assumption is consistent with the observed scale dependence of the $\alpha_S(m_Z)$ results, within which the results for both choices of $\Delta\phi_{\max}$ agree ($0.1127 + 0.0052$ versus $0.1179 - 0.0045$ for $\Delta\phi_{\max} = 5\pi/6$ and $7\pi/8$, respectively). It is therefore concluded from the systematic studies that no further uncertainties need to be assigned.

The final result from the combined fit is $\alpha_S(m_Z) = 0.1127^{+0.0063}_{-0.0027}$ with the individual uncertainty contributions given in Table V. This result and the corresponding RGE prediction are also shown in Fig. 3. For all α_S results in Tables IV and V, the uncertainties are dominated by the μ_R dependence of the NLO pQCD calculation.

Within the uncertainties, the $\alpha_S(m_Z)$ result is consistent with the current world average value of $\alpha_S(m_Z) = 0.1181 \pm 0.0011$ [16] and with recent α_S results from multijet cross-section ratio measurements in hadron collisions, namely from the D0 measurement of $R_{\Delta R}$ [10] ($\alpha_S(m_Z) = 0.1191^{+0.0048}_{-0.0071}$), and from the CMS measurements of $R_{3/2}$ [11] ($\alpha_S(m_Z) = 0.1148 \pm 0.0055$), the inclusive jet cross section [12,13] ($\alpha_S(m_Z) = 0.1185^{+0.0063}_{-0.0042}$, $\alpha_S(m_Z) = 0.1164^{+0.0060}_{-0.0043}$), and the three-jet cross section [14] ($\alpha_S(m_Z) = 0.1171^{+0.0074}_{-0.0049}$), and the ATLAS measurement of transverse energy–energy correlations [15] ($\alpha_S(m_Z) = 0.1162^{+0.0085}_{-0.0071}$), with comparable uncertainties. The compatibility of the results of this analysis, based on the measurements of $R_{\Delta\phi}$, with the world average value of $\alpha_S(m_Z)$ is demonstrated in Appendix D.

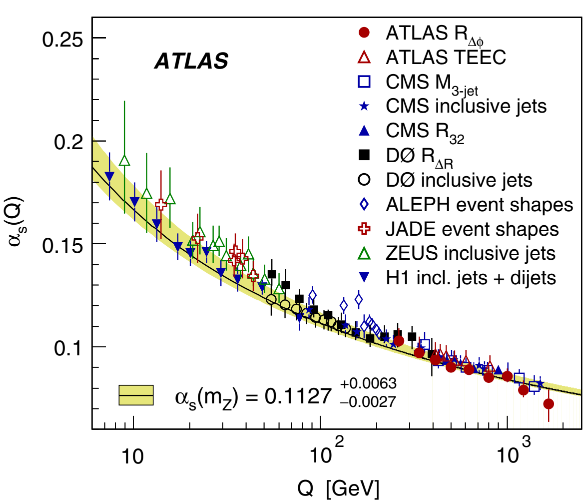

FIG. 4. The $\alpha_S(Q)$ results from this analysis in the range of $262 < Q < 1675$ GeV, compared to the results of previous α_S determinations from jet data in other experiments at $5 < Q < 1508$ GeV [4–7,9–15]. Also shown is the prediction of the RGE for the $\alpha_S(m_Z)$ result obtained from the $R_{\Delta\phi}$ data in this analysis.

The individual $\alpha_S(Q)$ results are compared in Fig. 4 with previously published α_S results obtained from jet measurements [4–7,9–15] and with the RGE prediction for the combined $\alpha_S(m_Z)$ result obtained in this analysis. The new results agree with previous $\alpha_S(Q)$ results in the region of overlap, and extend the pQCD tests to momentum transfers up to 1.6 TeV, where RGE predictions are consistent with the $\alpha_S(Q)$ results, as discussed in Appendix E.

IX. SUMMARY

The multijet cross-section ratio $R_{\Delta\phi}$ is measured at the LHC. The quantity $R_{\Delta\phi}$ specifies the fraction of the inclusive dijet events in which the azimuthal opening angle of the two jets with the highest transverse momenta is less than a given value of the parameter $\Delta\phi_{\max}$. The $R_{\Delta\phi}$ results, measured in 20.2 fb^{-1} of pp collisions at $\sqrt{s} = 8$ TeV with the ATLAS detector, are presented as a function of three variables: the total transverse momentum H_T, the dijet rapidity interval y^*, and the parameter $\Delta\phi_{\max}$. The H_T and y^* dependences of the data are well described by theoretical predictions based on NLO pQCD (for $\Delta\phi_{\max} = 7\pi/8$, $5\pi/6$, and $3\pi/4$), or LO pQCD (for $\Delta\phi_{\max} = 2\pi/3$), with corrections for non-perturbative effects. Based on the data points for $\Delta\phi_{\max} = 7\pi/8$ with $0 < y^* < 0.5$ and $0.5 < y^* < 1$, nine α_S results are determined, at a scale of $Q = H_T/2$, over the range of $262 < Q < 1675$ GeV. The $\alpha_S(Q)$ results are consistent with the predictions of the RGE, and a combined analysis results in a value of $\alpha_S(m_Z) = 0.1127^{+0.0063}_{-0.0027}$, where the uncertainty is dominated by the scale dependence of the NLO pQCD predictions.

ACKNOWLEDGMENTS

We thank CERN for the very successful operation of the LHC, as well as the support staff from our institutions without whom ATLAS could not be operated efficiently. We acknowledge the support of ANPCyT, Argentina; YerPhI, Armenia; ARC, Australia; BMWFW and FWF, Austria; ANAS, Azerbaijan; SSTC, Belarus; CNPq and FAPESP, Brazil; NSERC, NRC and CFI, Canada; CERN; CONICYT, Chile; CAS, MOST and NSFC, China; COLCIENCIAS, Colombia; MSMT CR, MPO CR and VSC CR, Czech Republic; DNRF and DNSRC, Denmark; IN2P3-CNRS, CEA-DRF/IRFU, France; SRNSFG, Georgia; BMBF, HGF, and MPG, Germany; GSRT, Greece; RGC, Hong Kong SAR, China; ISF, I-CORE and Benoziyo Center, Israel; INFN, Italy; MEXT and JSPS, Japan; CNRST, Morocco; NWO, Netherlands; RCN, Norway; MNiSW and NCN, Poland; FCT, Portugal; MNE/IFA, Romania; MES of Russia and NRC KI, Russian Federation; JINR; MESTD, Serbia; MSSR, Slovakia; ARRS and MIZŠ, Slovenia; DST/NRF, South Africa; MINECO, Spain; SRC and Wallenberg Foundation, Sweden; SERI, SNSF and Cantons of Bern and Geneva, Switzerland; MOST, Taiwan; TAEK, Turkey; STFC, United Kingdom; DOE and NSF, United States of America. In addition, individual groups and members have received support from BCKDF, the Canada Council, CANARIE, CRC, Compute Canada, FQRNT, and the Ontario Innovation Trust, Canada; EPLANET, ERC, ERDF, FP7, Horizon 2020 and Marie Skłodowska-Curie Actions, European Union; Investissements d'Avenir Labex and Idex, ANR, Région Auvergne and Fondation Partager le Savoir, France; DFG and AvH Foundation, Germany; Herakleitos, Thales and Aristeia programmes co-financed by EU-ESF and the Greek NSRF; BSF, GIF and Minerva, Israel; BRF, Norway; CERCA Programme Generalitat de Catalunya, Generalitat Valenciana, Spain; the Royal Society and Leverhulme Trust, United Kingdom. The crucial computing support from all WLCG partners is acknowledged gratefully, in particular from CERN, the ATLAS Tier-1 facilities at TRIUMF (Canada), NDGF (Denmark, Norway, Sweden), CC-IN2P3 (France), KIT/GridKA (Germany), INFN-CNAF (Italy), NL-T1 (Netherlands), PIC (Spain), ASGC (Taiwan), RAL (UK) and BNL (USA), the Tier-2 facilities worldwide and large non-WLCG resource providers. Major contributors of computing resources are listed in Ref. [66].

APPENDIX A: EFFECTS OF TOP QUARK CONTRIBUTIONS ON THE pQCD PREDICTIONS

There are two ways in which contributions from top quarks affect the pQCD predictions for $R_{\Delta\phi}$. First, the pQCD predictions based on matrix elements for massless quarks also depend on the number of quark flavors in gluon splitting ($g \to q\bar{q}$), n_{f}, which affects the tree-level matrix elements and their real and virtual corrections, as well as the RGE predictions. The pQCD predictions for the central analysis are obtained for $n_{\mathrm{f}} = 5$. The effects for the measured quantity $R_{\Delta\phi}$ for the choice $n_{\mathrm{f}} = 6$ are computed in this Appendix. Second, since the decay products of hadronically decaying (anti)top quarks are sometimes reconstructed as multiple jets, the $\mathcal{O}(\alpha_{\mathrm{S}}^2)$ $t\bar{t}$ production process also contributes to three-jet topologies. Since this contribution is of lower order in α_{S} as compared to the pQCD $\mathcal{O}(\alpha_{\mathrm{S}}^3)$ three-jet production processes, it is a "super-leading" contribution, which is formally more important. This potentially large contribution and the corresponding effects for $R_{\Delta\phi}$ are also estimated in this Appendix.

In a pQCD calculation in which quark masses are properly taken into account, the contributions from the massive top quark arise naturally at higher momentum transfers, according to the available phase space. In calculations based on matrix elements for massless quarks, n_{f} is a parameter in the calculation. For jet production at the LHC, the alternatives are $n_{\mathrm{f}} = 5$, i.e., ignoring the contributions from $g \to t\bar{t}$ processes (which is the central choice for this analysis), or $n_{\mathrm{f}} = 6$, i.e., treating the top quark as a sixth massless quark. The relative difference between the two alternatives is evaluated from the effects due to the RGE and the matrix elements. For this purpose, the 2-loop solution of the RGE for $n_{\mathrm{f}} = 5$ is replaced by the 2-loop solutions for $n_{\mathrm{f}} = 5$ and $n_{\mathrm{f}} = 6$ with 1-loop matching [67] at the pole mass of the top quark $m_{\mathrm{top}}^{\mathrm{pole}}$, assuming that $m_{\mathrm{top}}^{\mathrm{pole}}$ is equal to the world average of the measured "Monte Carlo mass" of 173.21 GeV [16]. In addition, the matrix elements are recomputed for $n_{\mathrm{f}} = 6$. For a fixed value of $\alpha_{\mathrm{S}}(m_Z) = 0.118$, the corresponding effects for the pQCD predictions for $R_{\Delta\phi}$ are in the range of -1% to $+2\%$.

The effects on $R_{\Delta\phi}$ due to the contributions from hadronic decays of $t\bar{t}$ final states are estimated using POWHEG-BOX [68] (for the pQCD matrix elements) interfaced with PYTHIA (for the parton shower, underlying event, and hadronization) and CTEQ6L1 PDFs [69]. It is seen that the $t\bar{t}$ process contributes 0.003–0.2% to the denominator of $R_{\Delta\phi}$ (the inclusive dijet cross section), and 0.006%–0.5% to the numerator (with $\Delta\phi_{\max} = 7\pi/8$). The effects for the ratio $R_{\Delta\phi}$ are 0%–0.5% in the analysis phase space, and there are no systematic trends in the considered distributions within the statistical uncertainties of the generated POWHEG-BOX event sample. Since this effect is about four to eight times smaller than the typical uncertainty due to the renormalization scale dependence, the corresponding effects on α_{S} are not investigated further.

APPENDIX B: DATA TABLES

The results of the $R_{\Delta\phi}$ measurements are listed in Tables VI–IX, together with their relative statistical and systematic uncertainties.

TABLE VI. The $R_{\Delta\phi}$ measurement results for $\Delta\phi_{\max} = 7\pi/8$ with their relative statistical and systematic uncertainties.

H_T [GeV]	y^*	$R_{\Delta\phi}$	Statistical uncertainties [%]	Systematic uncertainties [%]	
450–600	0.0–0.5	1.88×10^{-1}	±2.2	+1.8	−1.7
600–750	0.0–0.5	1.85×10^{-1}	±2.2	+1.6	−1.5
750–900	0.0–0.5	1.82×10^{-1}	±1.3	+1.4	−1.4
900–1100	0.0–0.5	1.67×10^{-1}	±0.9	+1.3	−1.3
1100–1400	0.0–0.5	1.56×10^{-1}	±0.7	+1.2	−1.2
1400–1800	0.0–0.5	1.36×10^{-1}	±1.0	+1.2	−1.2
1800–2200	0.0–0.5	1.25×10^{-1}	±1.9	+1.2	−1.3
2200–2700	0.0–0.5	1.02×10^{-1}	±4.1	+1.3	−1.4
2700–4000	0.0–0.5	0.82×10^{-1}	±9.9	+1.5	−1.7
450–600	0.5–1.0	1.97×10^{-1}	±2.2	+1.5	−1.6
600–750	0.5–1.0	2.04×10^{-1}	±2.3	+1.3	−1.4
750–900	0.5–1.0	1.94×10^{-1}	±1.3	+1.2	−1.3
900–1100	0.5–1.0	1.83×10^{-1}	±0.8	+1.2	−1.2
1100–1400	0.5–1.0	1.73×10^{-1}	±0.8	+1.3	−1.2
1400–1800	0.5–1.0	1.59×10^{-1}	±1.1	+1.4	−1.3
1800–2200	0.5–1.0	1.44×10^{-1}	±2.3	+1.7	−1.5
2200–2700	0.5–1.0	1.28×10^{-1}	±5.4	+1.9	−1.7
2700–4000	0.5–1.0	1.13×10^{-1}	±16	+2.4	−2.0
450–600	1.0–2.0	2.42×10^{-1}	±2.3	+2.3	−1.0
600–750	1.0–2.0	2.40×10^{-1}	±2.5	+1.9	−1.1
750–900	1.0–2.0	2.54×10^{-1}	±1.5	+1.7	−1.2
900–1100	1.0–2.0	2.40×10^{-1}	±1.1	+1.6	−1.4
1100–1400	1.0–2.0	2.33×10^{-1}	±1.0	+1.6	−1.7
1400–1800	1.0–2.0	2.18×10^{-1}	±1.8	+1.6	−2.2
1800–2200	1.0–2.0	2.22×10^{-1}	±4.4	+1.6	−2.7
2200–2700	1.0–2.0	1.96×10^{-1}	±14	+1.7	−3.1

TABLE VII. The $R_{\Delta\phi}$ measurement results for $\Delta\phi_{\max} = 5\pi/6$ with their relative statistical and systematic uncertainties.

H_T [GeV]	y^*	$R_{\Delta\phi}$	Statistical uncertainties [%]	Systematic uncertainties [%]	
450–600	0.0–0.5	1.22×10^{-1}	±2.8	+2.0	−1.9
600–750	0.0–0.5	1.13×10^{-1}	±2.9	+1.7	−1.7
750–900	0.0–0.5	1.10×10^{-1}	±1.7	+1.5	−1.6
900–1100	0.0–0.5	1.00×10^{-1}	±1.3	+1.4	−1.5
1100–1400	0.0–0.5	0.92×10^{-1}	±1.0	+1.2	−1.5
1400–1800	0.0–0.5	0.78×10^{-1}	±1.4	+1.2	−1.5
1800–2200	0.0–0.5	0.72×10^{-1}	±2.6	+1.2	−1.7
2200–2700	0.0–0.5	0.55×10^{-1}	±5.7	+1.3	−1.9
2700–4000	0.0–0.5	0.51×10^{-1}	±13	+1.6	−2.3
450–600	0.5–1.0	1.33×10^{-1}	±2.9	+1.5	−1.8
600–750	0.5–1.0	1.27×10^{-1}	±3.1	+1.4	−1.5
750–900	0.5–1.0	1.18×10^{-1}	±1.8	+1.3	−1.3
900–1100	0.5–1.0	1.11×10^{-1}	±1.2	+1.3	−1.2
1100–1400	0.5–1.0	1.03×10^{-1}	±1.2	+1.4	−1.2
1400–1800	0.5–1.0	0.93×10^{-1}	±1.5	+1.6	−1.3
1800–2200	0.5–1.0	0.85×10^{-1}	±3.2	+1.9	−1.4
2200–2700	0.5–1.0	0.74×10^{-1}	±7.3	+2.2	−1.6

(Table continued)

TABLE VII. *(Continued)*

H_T [GeV]	y^*	$R_{\Delta\phi}$	Statistical uncertainties [%]	Systematic uncertainties [%]	
450–600	1.0–2.0	1.58×10^{-1}	±2.9	+3.1	−1.0
600–750	1.0–2.0	1.54×10^{-1}	±3.3	+2.5	−0.9
750–900	1.0–2.0	1.62×10^{-1}	±2.3	+2.1	−1.1
900–1100	1.0–2.0	1.53×10^{-1}	±1.6	+1.9	−1.5
1100–1400	1.0–2.0	1.47×10^{-1}	±1.4	+1.8	−2.2
1400–1800	1.0–2.0	1.36×10^{-1}	±2.6	+1.8	−3.1
1800–2200	1.0–2.0	1.41×10^{-1}	±5.8	+1.9	−3.9
2200–2700	1.0–2.0	1.35×10^{-1}	±18	+2.0	−4.7

TABLE VIII. The $R_{\Delta\phi}$ measurement results for $\Delta\phi_{\max} = 3\pi/4$ with their relative statistical and systematic uncertainties.

H_T [GeV]	y^*	$R_{\Delta\phi}$	Statistical uncertainties [%]	Systematic uncertainties [%]	
450–600	0.0–0.5	4.35×10^{-2}	±5.0	+3.4	−2.4
600–750	0.0–0.5	3.67×10^{-2}	±5.9	+3.0	−2.1
750–900	0.0–0.5	3.55×10^{-2}	±4.6	+2.6	−1.9
900–1100	0.0–0.5	3.24×10^{-2}	±3.9	+2.3	−1.8
1100–1400	0.0–0.5	2.84×10^{-2}	±2.5	+2.0	−1.8
1400–1800	0.0–0.5	2.27×10^{-2}	±3.2	+1.8	−2.0
1800–2200	0.0–0.5	1.89×10^{-2}	±5.5	+1.8	−2.2
2200–2700	0.0–0.5	1.43×10^{-2}	±12	+1.9	−2.5
450–600	0.5–1.0	4.68×10^{-2}	±5.5	+2.2	−2.6
600–750	0.5–1.0	4.01×10^{-2}	±6.1	+1.8	−1.9
750–900	0.5–1.0	3.92×10^{-2}	±4.1	+1.6	−1.6
900–1100	0.5–1.0	3.61×10^{-2}	±2.9	+1.5	−1.4
1100–1400	0.5–1.0	3.31×10^{-2}	±3.3	+1.6	−1.3
1400–1800	0.5–1.0	2.90×10^{-2}	±3.4	+2.1	−1.3
1800–2200	0.5–1.0	2.44×10^{-2}	±6.7	+2.5	−1.5
2200–2700	0.5–1.0	2.17×10^{-2}	±14	+3.0	−1.8
450–600	1.0–2.0	6.02×10^{-2}	±5.1	+5.8	−2.5
600–750	1.0–2.0	5.68×10^{-2}	±5.7	+4.8	−2.4
750–900	1.0–2.0	5.71×10^{-2}	±4.6	+4.1	−2.7
900–1100	1.0–2.0	5.19×10^{-2}	±3.4	+3.7	−3.2
1100–1400	1.0–2.0	4.95×10^{-2}	±2.7	+3.5	−4.0
1400–1800	1.0–2.0	4.56×10^{-2}	±5.0	+3.7	−5.0
1800–2200	1.0–2.0	5.25×10^{-2}	±11	+4.1	−6.1

TABLE IX. The $R_{\Delta\phi}$ measurement results for $\Delta\phi_{\max} = 2\pi/3$ with their relative statistical and systematic uncertainties.

H_T [GeV]	y^*	$R_{\Delta\phi}$	Statistical uncertainties [%]	Systematic uncertainties [%]	
450–600	0.0–0.5	1.37×10^{-2}	±9.5	+6.3	−4.1
600–750	0.0–0.5	1.05×10^{-2}	±11	+5.4	−3.6
750–900	0.0–0.5	1.02×10^{-2}	±12	+4.7	−3.3
900–1100	0.0–0.5	0.87×10^{-2}	±8.9	+4.1	−3.2
1100–1400	0.0–0.5	0.70×10^{-2}	±6.0	+3.5	−3.2
1400–1800	0.0–0.5	0.48×10^{-2}	±7.8	+3.2	−3.3
1800–2200	0.0–0.5	0.38×10^{-2}	±13	+3.2	−3.7

(Table continued)

TABLE IX. (Continued)

H_T [GeV]	y^*	$R_{\Delta\phi}$	Statistical uncertainties [%]	Systematic uncertainties [%]	
450–600	0.5–1.0	1.45×10^{-2}	±11	+3.9	−4.4
600–750	0.5–1.0	1.07×10^{-2}	±12	+2.7	−2.5
750–900	0.5–1.0	1.14×10^{-2}	±11	+2.1	−1.8
900–1100	0.5–1.0	0.86×10^{-2}	±6.8	+2.2	−1.8
1100–1400	0.5–1.0	0.77×10^{-2}	±7.1	+2.8	−2.3
1400–1800	0.5–1.0	0.70×10^{-2}	±8.6	+3.8	−3.2
1800–2200	0.5–1.0	0.63×10^{-2}	±16	+4.8	−4.2
450–600	1.0–2.0	1.49×10^{-2}	±10	+9.0	−5.1
600–750	1.0–2.0	1.70×10^{-2}	±11	+7.4	−3.8
750–900	1.0–2.0	1.53×10^{-2}	±8.9	+6.5	−3.7
900–1100	1.0–2.0	1.29×10^{-2}	±7.5	+6.2	−4.3
1100–1400	1.0–2.0	1.12×10^{-2}	±6.6	+6.6	−5.9
1400–1800	1.0–2.0	1.02×10^{-2}	±12	+7.6	−8.0
1800–2200	1.0–2.0	1.61×10^{-2}	±20	+8.8	−10

APPENDIX C: DEFINITION OF χ^2

Given is a set of experimental measurement results in bins i of a given quantity with central measurement results d_i with statistical and uncorrelated systematic uncertainties $\sigma_{i,\mathrm{stat}}$ and $\sigma_{i,\mathrm{uncorr}}$, respectively. The experimental measurements are affected by various sources of correlated uncertainties, and $\delta_{ij}(\epsilon_j)$ specifies the uncertainty of measurement i due to the source j, where ϵ_j is a Gaussian distributed random variable with zero expectation value and unit width. The $\delta_{ij}(\epsilon_j)$ specify the dependence of the measured result i on the variation of the correlated uncertainty source j by ϵ_j standard deviations, where $\epsilon_j = 0$ corresponds to the central value of the measurement (i.e., $\delta_{ij}(\epsilon_j = 0) = 0$), while the relative uncertainties corresponding to plus/minus one standard deviation are given by $\delta_{ij}(\epsilon_j = \pm 1) = \Delta d_{ij}^{\pm}$. From the central measurement result and the relative uncertainties $\Delta d_{ij}^{\pm}$, the continuous ϵ_j dependence of $\delta_{ij}(\epsilon_j)$ can be obtained using quadratic interpolation

$$\delta_{ij}(\epsilon_j) = \epsilon_j \frac{\Delta d_{ij}^{+} - \Delta d_{ij}^{-}}{2} + \epsilon_j^2 \frac{\Delta d_{ij}^{+} + \Delta d_{ij}^{-}}{2}. \quad \text{(C1)}$$

The theoretical prediction $t_i(\alpha_S)$ for bin i depends on the value of α_S. Furthermore, the theoretical predictions are also affected by sources of correlated uncertainties; $\delta_{ik}(\lambda_k)$ specifies the relative uncertainty of t_i due to the source k. Like the ϵ_j, the λ_j are also treated as Gaussian distributed random variables with zero expectation value and unity width. It is assumed that the theoretical predictions can be obtained with statistical uncertainties which are negligible as compared to the statistical uncertainties of the measurements.

The continuous dependence of the relative uncertainty $\delta_{ik}(\lambda_k)$ can be obtained through quadratic interpolation between the central result t_i and the results $t_{ik}^{\pm}$ obtained by variations corresponding to plus/minus one standard deviation due to source k

$$\delta_{ik}(\lambda_k) = \lambda_k \frac{t_{ik}^{+} - t_{ik}^{-}}{2t_i} + \lambda_k^2 \left(\frac{t_{ik}^{+} + t_{ik}^{-}}{2t_i} - 1 \right). \quad \text{(C2)}$$

The χ^2 used in the α_S extraction is then computed as

$$\chi^2(\alpha_S, \vec{\epsilon}, \vec{\lambda}) = \sum_i \frac{\left[d_i - t_i(\alpha_S) \frac{(1+\sum_k \delta_{ik}(\lambda_k))}{(1+\sum_j \delta_{ij}(\epsilon_j))} \right]^2}{\sigma_{i,\mathrm{stat}}^2 + \sigma_{i,\mathrm{uncorr}}^2} + \sum_j \epsilon_j^2 + \sum_k \lambda_k^2, \quad \text{(C3)}$$

where i runs over all data points, j runs over all sources of experimental correlated uncertainties, and k over all theoretical correlated uncertainties. The fit result of α_S is determined by minimizing χ^2 with respect to α_S and the "nuisance parameters" ϵ_j and λ_k.

APPENDIX D: ON THE COMPATIBILITY OF THE $R_{\Delta\phi}$ DATA AND THE WORLD AVERAGE OF $\alpha_S(m_Z)$

The $\alpha_S(m_Z)$ result in Table V is lower than the world average value by approximately one standard deviation. In this Appendix, the consistency of the world average of $\alpha_S(m_Z)$ and the $R_{\Delta\phi}$ data is investigated using the χ^2 values. The χ^2 values are computed according to Appendix C, using the 18 data points with $\Delta\phi_{\max} = 7\pi/8$, and $0.0 < y^* < 0.5$ and $0.5 < y^* < 1.0$. The theoretical predictions are computed for the fixed value of $\alpha_S(m_Z) = 0.1181$. The computation of χ^2 uses the Hessian method for the treatment of all uncertainties except for the PDF set uncertainty

TABLE X. The χ^2 values between the 18 data points and the theoretical predictions when $\alpha_S(m_Z)$ is fixed to the world average value of $\alpha_S(m_Z) = 0.1181$ (third column) and when it is a free fitted parameter (fourth column) for variations of the scales μ_R and μ_F around the central choice $\mu_R = \mu_F = \mu_0 = H_T/2$.

μ_R/μ_0	μ_F/μ_0	χ^2 for $\alpha_S(m_Z) = 0.1181$	χ^2 for $\alpha_S(m_Z)$ free fit parameter
0.5	0.5	62.4	50.9
0.5	1.0	56.3	39.6
1.0	0.5	31.6	23.6
1.0	1.0	29.7	21.7
1.0	2.0	28.4	20.8
2.0	1.0	19.2	19.0
2.0	2.0	19.3	19.3

and the scale dependence, so the χ^2 values do not reflect these theoretical uncertainties. Therefore, a series of χ^2 values is computed for possible combinations of variations of μ_R and μ_F around the central choice $\mu_R = \mu_F = \mu_0 = H_T/2$. The results are displayed in Table X and compared to the χ^2 values obtained when $\alpha_S(m_Z)$ is a free fit parameter.

When $\alpha_S(m_Z)$ is fixed to the world average, the χ^2 value for the central scale choice is slightly higher than the one obtained for a free $\alpha_S(m_Z)$, and also higher than the expectation of $\chi^2 = N_{dof} \pm \sqrt{2 \cdot N_{dof}}$, where $N_{dof} = 18$ when $\alpha_S(m_Z)$ is fixed or 17 when it is a free fit parameter. However, the χ^2 definition does not take into account the theoretical uncertainty due to the scale dependence. When the renormalization scale is increased by a factor of two, to $\mu_R = 2\mu_0$, lower χ^2 values are obtained, which are similar in size to the ones obtained for a free $\alpha_S(m_Z)$, and close to the expectation (the dependence on the factorization scale is rather small). Since these χ^2 values are well within the range of the expectation, it is concluded that, within their uncertainties, the theoretical predictions for the world average value of $\alpha_S(m_Z)$ are consistent with the $R_{\Delta\phi}$ data.

APPENDIX E: ON THE COMPATIBILITY OF THE RGE AND THE SLOPE OF THE $\alpha_S(Q)$ RESULTS

It is natural to ask whether the observed Q dependence (i.e., the running) of the $\alpha_S(Q)$ results shown in Fig. 3 is described by the RGE or instead exhibits significant deviations at the highest Q values, possibly indicating signals of physics beyond the Standard Model. The consistency of the RGE predictions with the observed slope is investigated in this Appendix. The RGE prediction would be in agreement with the observed Q dependence of the $\alpha_S(Q)$ results if the latter, when evolved to m_Z, give $\alpha_S(m_Z)$ values that are independent of Q. For this purpose, a linear function in $\log_{10}(Q/1\text{ GeV})$, $f(Q) = c + m \cdot \log_{10}(Q/1\text{ GeV})$, is fitted to the nine $\alpha_S(m_Z)$ points in Fig. 3 (bottom) and their statistical uncertainties. Here the correlated systematic uncertainties are not taken into account as their correlations are nontrivial since the individual $\alpha_S(Q)$ results are obtained in separate fits, with different optimizations for the nuisance parameters. The fit results for the slope parameter m and its uncertainty are displayed in Table XI for a fit to the $\alpha_S(m_Z)$ points at all nine Q values, and also for fits to different subsets of the $\alpha_S(m_Z)$ points, omitting points either at lower or higher Q.

TABLE XI. Fit of a linear function in $\log_{10}(Q/\text{GeV})$ to the nine extracted $\alpha_S(Q)$ results with their statistical uncertainties.

$\alpha_S(Q)$ points included in fit	Q range (GeV)	Fit result for slope parameter
1–9	225–2000	$(-0.89 \pm 0.35) \times 10^{-2}$
2–9	300–2000	$(-0.52 \pm 0.33) \times 10^{-2}$
3–9	375–2000	$(-0.39 \pm 0.28) \times 10^{-2}$
4–9	450–2000	$(-0.20 \pm 0.29) \times 10^{-2}$
5–9	550–2000	$(-1.19 \pm 0.35) \times 10^{-2}$
6–9	700–2000	$(+0.35 \pm 0.51) \times 10^{-2}$
1–9	225–2000	$(-0.89 \pm 0.35) \times 10^{-2}$
1–8	225–1350	$(-0.85 \pm 0.43) \times 10^{-2}$
1–7	225–1100	$(-0.78 \pm 0.32) \times 10^{-2}$
1–6	225–900	$(-1.14 \pm 0.28) \times 10^{-2}$
1–5	225–700	$(-1.01 \pm 0.31) \times 10^{-2}$
1–4	225–550	$(-2.55 \pm 0.41) \times 10^{-2}$

As documented in Table XI, a fit to all nine $\alpha_S(m_Z)$ points gives a slope that differs from zero by more than its uncertainty. Fits to groups of data points, however, show that the significance of this slope arises from the two points at lowest Q. Omitting the $\alpha_S(m_Z)$ point at lowest Q (fitting points Nos. 2–9), or the two points at lowest Q (fitting points # 3–9), both give fit results for which the slope parameter is more consistent with zero, while the $\alpha_S(m_Z)$ results change by less than ± 0.0001. On the other hand, omitting the $\alpha_S(Q)$ points at highest Q (fitting points Nos. 1–8 or Nos. 1–7) does not affect the significance of the slope. It is therefore concluded that the high-Q behavior of the $\alpha_S(Q)$ results is consistent with the RGE and that the small differences at lowest Q do not affect the combined $\alpha_S(m_Z)$ result.

[1] H. D. Politzer, Reliable Perturbative Results for Strong Interactions?, Phys. Rev. Lett. **30**, 1346 (1973).

[2] D. J. Gross and F. Wilczek, Asymptotically free gauge theories. 1, Phys. Rev. D **8**, 3633 (1973).

[3] H1 Collaboration, Measurement of jet production cross sections in deep-inelastic ep scattering at HERA, Eur. Phys. J. C **77**, 215 (2017).

[4] H1 Collaboration, Determination of the strong coupling constant $\alpha_s(m_Z)$ in next-to-next-to-leading order QCD using H1 jet cross section measurements, Eur. Phys. J. C **77**, 791 (2017).

[5] ZEUS Collaboration, Inclusive-jet photoproduction at HERA and determination of α_s, Nucl. Phys. **B864**, 1 (2012).

[6] S. Bethke, S. Kluth, C. Pahl, and J. Schieck, Determination of the strong coupling α_s from hadronic event shapes with $\mathcal{O}(\alpha_s^3)$ and resummed QCD predictions using JADE data, Eur. Phys. J. C **64**, 351 (2009).

[7] G. Dissertori, A. Gehrmann-De Ridder, T. Gehrmann, E. W. N. Glover, G. Heinrich, G. Luisoni, and H. Stenzel, Determination of the strong coupling constant using matched NNLO + NLLA predictions for hadronic event shapes in e +e- annihilations, J. High Energy Phys. 08 (2009) 036.

[8] CDF Collaboration, Measurement of the Strong Coupling Constant from Inclusive Jet Production at the Tevatron $\bar{p}p$ Collider, Phys. Rev. Lett. **88**, 042001 (2002).

[9] D0 Collaboration, Determination of the strong coupling constant from the inclusive jet cross section in $p\bar{p}$ collisions at $\sqrt{s} = 1.96$ TeV, Phys. Rev. D **80**, 111107 (2009).

[10] D0 Collaboration, Measurement of angular correlations of jets at $\sqrt{s} = 1.96$ TeV and determination of the strong coupling at high momentum transfers, Phys. Lett. B **718**, 56 (2012).

[11] CMS Collaboration, Measurement of the ratio of the inclusive 3-jet cross section to the inclusive 2-jet cross section in pp collisions at $\sqrt{s} = 7$ TeV and first determination of the strong coupling constant in the TeV range, Eur. Phys. J. C **73**, 2604 (2013).

[12] CMS Collaboration, Constraints on parton distribution functions and extraction of the strong coupling constant from the inclusive jet cross section in pp collisions at $\sqrt{s} = 7$ TeV, Eur. Phys. J. C **75**, 288 (2015).

[13] CMS Collaboration, Measurement and QCD analysis of double-differential inclusive jet cross sections in pp collisions at $\sqrt{s} = 8$ TeV and cross section ratios to 2.76 and 7 TeV, J. High Energy Phys. 03 (2017) 156.

[14] CMS Collaboration, Measurement of the inclusive 3-jet production differential cross section in proton–proton collisions at 7 TeV and determination of the strong coupling constant in the TeV range, Eur. Phys. J. C **75**, 186 (2015).

[15] ATLAS Collaboration, Determination of the strong coupling constant α_s from transverse energy–energy correlations in multijet events at $\sqrt{s} = 8$ TeV using the ATLAS detector, Eur. Phys. J. C **77**, 872 (2017).

[16] C. Patrignani *et al.*, Review of particle physics, Chin. Phys. C **40**, 100001 (2016).

[17] M. Wobisch, K. Chakravarthula, R. Dhullipudi, L. Sawyer, and M. Tamsett, A new quantity for studies of dijet azimuthal decorrelations, J. High Energy Phys. 01 (2013) 172.

[18] D0 Collaboration, Measurement of Dijet Azimuthal Decorrelations at Central Rapidities in $p\bar{p}$ Collisions at $\sqrt{s} = 1.96$ TeV, Phys. Rev. Lett. **94**, 221801 (2005).

[19] CMS Collaboration, Dijet Azimuthal Decorrelations in pp Collisions at $\sqrt{s} = 7$ TeV, Phys. Rev. Lett. **106**, 122003 (2011).

[20] ATLAS Collaboration, Measurement of Dijet Azimuthal Decorrelations in pp Collisions at $\sqrt{s} = 7$ TeV, Phys. Rev. Lett. **106**, 172002 (2011).

[21] M. Wobisch and K. Rabbertz, Dijet azimuthal decorrelations for $\Delta\phi_{\mathrm{dijet}} < 2\pi/3$ in perturbative QCD, J. High Energy Phys. 12 (2015) 024.

[22] D0 Collaboration, Measurement of the combined rapidity and p_T dependence of dijet azimuthal decorrelations in $p\bar{p}$ collisions at $\sqrt{s} = 1.96$ TeV, Phys. Lett. B **721**, 212 (2013).

[23] ATLAS Collaboration, Luminosity determination in pp collisions at $\sqrt{s} = 8$ TeV using the ATLAS detector at the LHC, Eur. Phys. J. C **76**, 653 (2016).

[24] C. Buttar *et al.*, Standard Model Handles and Candles Working Group, Tools and jets summary report, arXiv: 0803.0678.

[25] M. Cacciari and G. P. Salam, Dispelling the N^3 myth for the k_t jet-finder, Phys. Lett. B **641**, 57 (2006).

[26] M. Cacciari, G. P. Salam, and G. Soyez, The anti-k_t jet clustering algorithm, J. High Energy Phys. 04 (2008) 063.

[27] G. Soyez, Optimal jet radius in kinematic dijet reconstruction, J. High Energy Phys. 07 (2010) 075.

[28] Z. Nagy, Next-to-leading order calculation of three jet observables in hadron hadron collision, Phys. Rev. D **68**, 094002 (2003).

[29] Z. Nagy, Three jet cross-sections in hadron hadron collisions at next-to-leading order, Phys. Rev. Lett. **88**, 122003 (2002).

[30] T. Kluge, K. Rabbertz, and M. Wobisch, FastNLO: Fast pQCD calculations for PDF fits, arXiv:hep-ph/0609285.

[31] M. Wobisch, D. Britzger, T. Kluge, K. Rabbertz, and F. Stober, Theory-data comparisons for jet measurements in hadron-induced processes, arXiv:1109.1310.

[32] W. A. Bardeen, A. J. Buras, D. W. Duke, and T. Muta, Deep-inelastic scattering beyond the leading order in asymptotically free gauge theories, Phys. Rev. D **18**, 3998 (1978).

[33] L. A. Harland-Lang, A. D. Martin, P. Motylinski, and R. S. Thorne, Parton distributions in the LHC era: MMHT 2014 PDFs, Eur. Phys. J. C **75**, 204 (2015).

[34] L. A. Harland-Lang, A. D. Martin, P. Motylinski, and R. S. Thorne, Uncertainties on α_s in the MMHT2014 global PDF analysis and implications for SM predictions, Eur. Phys. J. C **75**, 435 (2015).

[35] S. Dulat, T.-J. Hou, J. Gao, M. Guzzi, J. Huston, P. Nadolsky, J. Pumplin, C. Schmidt, D. Stump, and C.-P. Yuan, New parton distribution functions from a global analysis of quantum chromodynamics, Phys. Rev. D **93**, 033006 (2016).

[36] R. D. Ball, V. Bertone, F. Cerutti, L. Del Debbio, S. Forte, A. Guffanti, J. I. Latorre, J. Rojo, and M. Ubiali, Impact of heavy quark masses on parton distributions and LHC phenomenology, Nucl. Phys. **B849**, 296 (2011).

[37] R. D. Ball *et al.*, Parton distributions for the LHC Run II, J. High Energy Phys. 04 (2015) 040.

[38] S. Alekhin, J. Blümlein, S. Moch, and R. Placakyte, Parton distribution functions, α_s and heavy-quark masses for LHC run II, Phys. Rev. D **96**, 014011 (2017).
[39] H1 and ZEUS Collaborations, Combination of measurements of inclusive deep inelastic $e^{\pm}p$ scattering cross sections and QCD analysis of HERA data, Eur. Phys. J. C **75**, 580 (2015).
[40] T. Sjöstrand, P. Edén, C. Friberg, L. Lönnblad, G. Miu, S. Mrenna, and E. Norrbin, High-energy physics event generation with PYTHIA 6.1, Comput. Phys. Commun. **135**, 238 (2001).
[41] G. Corcella, I. G. Knowles, G. Marchesini, S. Moretti, K. Odagiri, P. Richardson, M. H. Seymour, and B. R. Webber, HERWIG 6: An event generator for hadron emission reactions with interfering gluons (including supersymmetric processes), J. High Energy Phys. 01 (2001) 010.
[42] G. Corcella *et al.*, HERWIG 6.5 release note, arXiv:hep-ph/0210213.
[43] ATLAS Collaboration, Charged particle multiplicities in pp interactions at $\sqrt{s} = 0.9$ and 7 TeV in a diffractive limited phase-space measured with the ATLAS detector at the LHC and new PYTHIA6 tune, CERN Report No. ATLAS-CONF-2010-031, 2010, https://cds.cern.ch/record/1277665.
[44] M. G. Albrow *et al.*, Tevatron-for-LHC Report of the QCD Working Group, arXiv:hep-ph/0610012.
[45] R. Field, Min-bias and the underlying event at the Tevatron and the LHC, Proceedings of Fermilab ME/MC Tuning Workshop, Fermilab, 2002 (unpublished).
[46] H. Schulz and P. Z. Skands, Energy scaling of minimum-bias tunes, Eur. Phys. J. C **71**, 1644 (2011).
[47] ATLAS Collaboration, The ATLAS experiment at the CERN Large Hadron Collider, J. Instrum. **3**, S08003 (2008).
[48] ATLAS Collaboration, Performance of the ATLAS trigger system in 2010, Eur. Phys. J. C **72**, 1849 (2012).
[49] ATLAS Collaboration, The performance of the jet trigger for the ATLAS detector during 2011 data taking, Eur. Phys. J. C **76**, 526 (2016).
[50] ATLAS Collaboration, Topological cell clustering in the ATLAS calorimeters and its performance in LHC Run 1, Eur. Phys. J. C **77**, 490 (2017).
[51] S. Agostinelli *et al.*, GEANT4: A simulation toolkit, Nucl. Instrum. Methods Phys. Res., Sect. A **506**, 250 (2003).
[52] ATLAS Collaboration, The ATLAS simulation infrastructure, Eur. Phys. J. C **70**, 823 (2010).
[53] T. Sjöstrand, S. Mrenna, and P. Z. Skands, A brief introduction to PYTHIA 8.1, Comput. Phys. Commun. **178**, 852 (2008).
[54] ATLAS Collaboration, Summary of ATLAS Pythia 8 tunes, CERN Report No. ATL-PHYS-PUB-2012-003, 2012, https://cds.cern.ch/record/1474107.
[55] M. Cacciari and G. P. Salam, Pileup subtraction using jet areas, Phys. Lett. B **659**, 119 (2008).
[56] ATLAS Collaboration, Performance of pile-up mitigation techniques for jets in pp collisions at $\sqrt{s} = 8$ TeV using the ATLAS detector, Eur. Phys. J. C **76**, 581 (2016).
[57] ATLAS Collaboration, Monte Carlo calibration and combination of in-situ measurements of jet energy scale, jet energy resolution and jet mass in ATLAS, CERN Report No. ATLAS-CONF-2015-037, 2015, https://cds.cern.ch/record/2044941.
[58] ATLAS Collaboration, A measurement of the calorimeter response to single hadrons and determination of the jet energy scale uncertainty using LHC Run-1 pp-collision data with the ATLAS detector, Eur. Phys. J. C **77**, 26 (2017).
[59] ATLAS Collaboration, Data-driven determination of the energy scale and resolution of jets reconstructed in the ATLAS calorimeters using dijet and multijet events at $\sqrt{s} = 8$ TeV, CERN Report No. ATLAS-CONF-2015-017, 2015, https://cds.cern.ch/record/2008678.
[60] ATLAS Collaboration, Jet energy resolution in proton-proton collisions at $\sqrt{s} = 7$ TeV recorded in 2010 with the ATLAS detector, Eur. Phys. J. C **73**, 2306 (2013).
[61] ATLAS Collaboration, Determination of the jet energy scale and resolution at ATLAS using Z/γ-jet events in data at $\sqrt{s} = 8$ TeV, CERN Report No. ATLAS-CONF-2015-057, 2015, https://cds.cern.ch/record/2059846.
[62] ATLAS Collaboration, Jet global sequential corrections with the ATLAS detector in proton-proton collisions at $\sqrt{s} = 8$ TeV, CERN Report No. ATLAS-CONF-2015-002, 2015, https://cds.cern.ch/record/2001682.
[63] G. D'Agostini, A Multidimensional unfolding method based on Bayes' theorem, Nucl. Instrum. Methods Phys. Res., Sect. A **362**, 487 (1995).
[64] F. James and M. Roos, Minuit: A system for function minimization and analysis of the parameter errors and correlations, Comput. Phys. Commun. **10**, 343 (1975).
[65] T. Carli *et al.*, Experimental determination of Parton Distributions, in *Proceedings of HERA and the LHC: A workshop on the implications of HERA for LHC physics: Proceedings Part A*, edited by G. Altarelli *et al.*, 2005, arXiv:hep-ph/0601012.
[66] ATLAS Collaboration, ATLAS computing acknowledgements, CERN Report No. ATL-GEN-PUB-2016-002, https://cds.cern.ch/record/2202407.
[67] K. G. Chetyrkin, B. A. Kniehl, and M. Steinhauser, Strong Coupling Constant with Flavor Thresholds at Four Loops in the MS Scheme, Phys. Rev. Lett. **79**, 2184 (1997).
[68] P. Nason, A new method for combining NLO QCD with shower Monte Carlo algorithms, J. High Energy Phys. 11 (2004) 040.
[69] J. Pumplin, D. R. Stump, J. Huston, H.-L. Lai, P. Nadolsky, and W.-K. Tung, New generation of parton distributions with uncertainties from global QCD analysis, J. High Energy Phys. 07 (2002) 012.

M. Aaboud,[34d] G. Aad,[99] B. Abbott,[124] O. Abdinov,[13,a] B. Abeloos,[128] S. H. Abidi,[165] O. S. AbouZeid,[143] N. L. Abraham,[153] H. Abramowicz,[159] H. Abreu,[158] R. Abreu,[127] Y. Abulaiti,[43a,43b] B. S. Acharya,[64a,64b,b] S. Adachi,[161] L. Adamczyk,[81a] J. Adelman,[119] M. Adersberger,[112] T. Adye,[141] A. A. Affolder,[143] Y. Afik,[158] T. Agatonovic-Jovin,[16] C. Agheorghiesei,[27c]

J. A. Aguilar-Saavedra,[136f,136a] F. Ahmadov,[77,c] G. Aielli,[71a,71b] S. Akatsuka,[83] H. Akerstedt,[43a,43b] T. P. A. Åkesson,[94] E. Akilli,[52] A. V. Akimov,[108] G. L. Alberghi,[23b,23a] J. Albert,[174] P. Albicocco,[49] M. J. Alconada Verzini,[86] S. Alderweireldt,[117] M. Aleksa,[35] I. N. Aleksandrov,[77] C. Alexa,[27b] G. Alexander,[159] T. Alexopoulos,[10] M. Alhroob,[124] B. Ali,[138] G. Alimonti,[66a] J. Alison,[36] S. P. Alkire,[38] B. M. M. Allbrooke,[153] B. W. Allen,[127] P. P. Allport,[21] A. Aloisio,[67a,67b] A. Alonso,[39] F. Alonso,[86] C. Alpigiani,[145] A. A. Alshehri,[55] M. I. Alstaty,[99] B. Alvarez Gonzalez,[35] D. Álvarez Piqueras,[172] M. G. Alviggi,[67a,67b] B. T. Amadio,[18] Y. Amaral Coutinho,[78b] C. Amelung,[26] D. Amidei,[103] S. P. Amor Dos Santos,[136a,136c] S. Amoroso,[35] G. Amundsen,[26] C. Anastopoulos,[146] L. S. Ancu,[52] N. Andari,[21] T. Andeen,[11] C. F. Anders,[59b] J. K. Anders,[88] K. J. Anderson,[36] A. Andreazza,[66a,66b] V. Andrei,[59a] S. Angelidakis,[37] I. Angelozzi,[118] A. Angerami,[38] A. V. Anisenkov,[120b,120a] N. Anjos,[14] A. Annovi,[69a] C. Antel,[59a] M. Antonelli,[49] A. Antonov,[110,a] D. J. A. Antrim,[169] F. Anulli,[70a] M. Aoki,[79] L. Aperio Bella,[35] G. Arabidze,[104] Y. Arai,[79] J. P. Araque,[136a] V. Araujo Ferraz,[78b] A. T. H. Arce,[47] R. E. Ardell,[91] F. A. Arduh,[86] J-F. Arguin,[107] S. Argyropoulos,[75] M. Arik,[12c] A. J. Armbruster,[35] L. J. Armitage,[90] O. Arnaez,[165] H. Arnold,[50] M. Arratia,[31] O. Arslan,[24] A. Artamonov,[109,a] G. Artoni,[131] S. Artz,[97] S. Asai,[161] N. Asbah,[44] A. Ashkenazi,[159] L. Asquith,[153] K. Assamagan,[29] R. Astalos,[28a] M. Atkinson,[171] N. B. Atlay,[148] K. Augsten,[138] G. Avolio,[35] B. Axen,[18] M. K. Ayoub,[15a] G. Azuelos,[107,d] A. E. Baas,[59a] M. J. Baca,[21] H. Bachacou,[142] K. Bachas,[65a,65b] M. Backes,[131] P. Bagnaia,[70a,70b] M. Bahmani,[82] H. Bahrasemani,[149] J. T. Baines,[141] M. Bajic,[39] O. K. Baker,[181] P. J. Bakker,[118] E. M. Baldin,[120b,120a] P. Balek,[178] F. Balli,[142] W. K. Balunas,[133] E. Banas,[82] A. Bandyopadhyay,[24] S. Banerjee,[179,e] A. A. E. Bannoura,[180] L. Barak,[159] E. L. Barberio,[102] D. Barberis,[53b,53a] M. Barbero,[99] T. Barillari,[113] M-S. Barisits,[35] J. Barkeloo,[127] T. Barklow,[150] N. Barlow,[31] S. L. Barnes,[58c] B. M. Barnett,[141] R. M. Barnett,[18] Z. Barnovska-Blenessy,[58a] A. Baroncelli,[72a] G. Barone,[26] A. J. Barr,[131] L. Barranco Navarro,[172] F. Barreiro,[96] J. Barreiro Guimarães da Costa,[15a] R. Bartoldus,[150] A. E. Barton,[87] P. Bartos,[28a] A. Basalaev,[134] A. Bassalat,[128] R. L. Bates,[55] S. J. Batista,[165] J. R. Batley,[31] M. Battaglia,[143] M. Bauce,[70a,70b] F. Bauer,[142] H. S. Bawa,[150,f] J. B. Beacham,[122] M. D. Beattie,[87] T. Beau,[132] P. H. Beauchemin,[168] P. Bechtle,[24] H. C. Beck,[51] H. P. Beck,[20,g] K. Becker,[131] M. Becker,[97] C. Becot,[121] A. Beddall,[12d] A. J. Beddall,[12a] V. A. Bednyakov,[77] M. Bedognetti,[118] C. P. Bee,[152] T. A. Beermann,[35] M. Begalli,[78b] M. Begel,[29] J. K. Behr,[44] A. S. Bell,[92] G. Bella,[159] L. Bellagamba,[23b] A. Bellerive,[33] M. Bellomo,[158] K. Belotskiy,[110] O. Beltramello,[35] N. L. Belyaev,[110] O. Benary,[159,a] D. Benchekroun,[34a] M. Bender,[112] N. Benekos,[10] Y. Benhammou,[159] E. Benhar Noccioli,[181] J. Benitez,[75] D. P. Benjamin,[47] M. Benoit,[52] J. R. Bensinger,[26] S. Bentvelsen,[118] L. Beresford,[131] M. Beretta,[49] D. Berge,[118] E. Bergeaas Kuutmann,[170] N. Berger,[5] J. Beringer,[18] S. Berlendis,[56] N. R. Bernard,[100] G. Bernardi,[132] C. Bernius,[150] F. U. Bernlochner,[24] T. Berry,[91] P. Berta,[97] C. Bertella,[15a] G. Bertoli,[43a,43b] I. A. Bertram,[87] C. Bertsche,[44] D. Bertsche,[124] G. J. Besjes,[39] O. Bessidskaia Bylund,[43a,43b] M. Bessner,[44] N. Besson,[142] A. Bethani,[98] S. Bethke,[113] A. Betti,[24] A. J. Bevan,[90] J. Beyer,[113] R. M. Bianchi,[135] O. Biebel,[112] D. Biedermann,[19] R. Bielski,[98] K. Bierwagen,[97] N. V. Biesuz,[69a,69b] M. Biglietti,[72a] T. R. V. Billoud,[107] H. Bilokon,[49] M. Bindi,[51] A. Bingul,[12d] C. Bini,[70a,70b] S. Biondi,[23b,23a] T. Bisanz,[51] C. Bittrich,[46] D. M. Bjergaard,[47] J. E. Black,[150] K. M. Black,[25] R. E. Blair,[6] T. Blazek,[28a] I. Bloch,[44] C. Blocker,[26] A. Blue,[55] W. Blum,[97,a] U. Blumenschein,[90] Blunier,[144a] G. J. Bobbink,[118] V. S. Bobrovnikov,[120b,120a] S. S. Bocchetta,[94] A. Bocci,[47] C. Bock,[112] M. Boehler,[50] D. Boerner,[180] D. Bogavac,[112] A. G. Bogdanchikov,[120b,120a] C. Bohm,[43a] V. Boisvert,[91] P. Bokan,[170] T. Bold,[81a] A. S. Boldyrev,[111] A. E. Bolz,[59b] M. Bomben,[132] M. Bona,[90] M. Boonekamp,[142] A. Borisov,[140] G. Borissov,[87] J. Bortfeldt,[35] D. Bortoletto,[131] V. Bortolotto,[61a,61b,61c] D. Boscherini,[23b] M. Bosman,[14] J. D. Bossio Sola,[30] J. Boudreau,[135] J. Bouffard,[2] E. V. Bouhova-Thacker,[87] D. Boumediene,[37] C. Bourdarios,[128] S. K. Boutle,[55] A. Boveia,[122] J. Boyd,[35] I. R. Boyko,[77] A. J. Bozson,[91] J. Bracinik,[21] A. Brandt,[8] G. Brandt,[51] O. Brandt,[59a] F. Braren,[44] U. Bratzler,[162] B. Brau,[100] J. E. Brau,[127] W. D. Breaden Madden,[55] K. Brendlinger,[44] A. J. Brennan,[102] L. Brenner,[118] R. Brenner,[170] S. Bressler,[178] D. L. Briglin,[21] T. M. Bristow,[48] D. Britton,[55] D. Britzger,[44] I. Brock,[24] R. Brock,[104] G. Brooijmans,[38] T. Brooks,[91] W. K. Brooks,[144b] J. Brosamer,[18] E. Brost,[119] J. H. Broughton,[21] P. A. Bruckman de Renstrom,[82] D. Bruncko,[28b] A. Bruni,[23b] G. Bruni,[23b] L. S. Bruni,[118] S. Bruno,[71a,71b] B. H. Brunt,[31] M. Bruschi,[23b] N. Bruscino,[135] P. Bryant,[36] L. Bryngemark,[44] T. Buanes,[17] Q. Buat,[149] P. Buchholz,[148] A. G. Buckley,[55] I. A. Budagov,[77] M. K. Bugge,[130] F. Bührer,[50] O. Bulekov,[110] D. Bullock,[8] T. J. Burch,[119] S. Burdin,[88] C. D. Burgard,[50] A. M. Burger,[5] B. Burghgrave,[119] K. Burka,[82] S. Burke,[141] I. Burmeister,[45] J. T. P. Burr,[131] E. Busato,[37] D. Büscher,[50] V. Büscher,[97] P. Bussey,[55] J. M. Butler,[25] C. M. Buttar,[55] J. M. Butterworth,[92] P. Butti,[35] W. Buttinger,[29] A. Buzatu,[155] A. R. Buzykaev,[120b,120a] S. Cabrera Urbán,[172] D. Caforio,[138] H. Cai,[171] V. M. M. Cairo,[40b,40a] O. Cakir,[4a] N. Calace,[52] P. Calafiura,[18] A. Calandri,[99] G. Calderini,[132] P. Calfayan,[63] G. Callea,[40b,40a] L. P. Caloba,[78b] S. Calvente Lopez,[96] D. Calvet,[37] S. Calvet,[37] T. P. Calvet,[99] R. Camacho Toro,[36] S. Camarda,[35] P. Camarri,[71a,71b] D. Cameron,[130]

R. Caminal Armadans,[171] C. Camincher,[56] S. Campana,[35] M. Campanelli,[92] A. Camplani,[66a,66b] A. Campoverde,[148] V. Canale,[67a,67b] M. Cano Bret,[58c] J. Cantero,[125] T. Cao,[159] M. D. M. Capeans Garrido,[35] I. Caprini,[27b] M. Caprini,[27b] M. Capua,[40b,40a] R. M. Carbone,[38] R. Cardarelli,[71a] F. C. Cardillo,[50] I. Carli,[139] T. Carli,[35] G. Carlino,[67a] B. T. Carlson,[135] L. Carminati,[66a,66b] R. M. D. Carney,[43a,43b] S. Caron,[117] E. Carquin,[144b] S. Carrá,[66a,66b] G. D. Carrillo-Montoya,[35] D. Casadei,[21] M. P. Casado,[14,h] M. Casolino,[14] D. W. Casper,[169] R. Castelijn,[118] V. Castillo Gimenez,[172] N. F. Castro,[136a] A. Catinaccio,[35] J. R. Catmore,[130] A. Cattai,[35] J. Caudron,[24] V. Cavaliere,[171] E. Cavallaro,[14] D. Cavalli,[66a] M. Cavalli-Sforza,[14] V. Cavasinni,[69a,69b] E. Celebi,[12b] F. Ceradini,[72a,72b] L. Cerda Alberich,[172] A. S. Cerqueira,[78a] A. Cerri,[153] L. Cerrito,[71a,71b] F. Cerutti,[18] A. Cervelli,[23b,23a] S. A. Cetin,[12b] A. Chafaq,[34a] D. Chakraborty,[119] S. K. Chan,[57] W. S. Chan,[118] Y. L. Chan,[61a] P. Chang,[171] J. D. Chapman,[31] D. G. Charlton,[21] C. C. Chau,[33] C. A. Chavez Barajas,[153] S. Che,[122] S. Cheatham,[64a,64c] A. Chegwidden,[104] S. Chekanov,[6] S. V. Chekulaev,[166a] G. A. Chelkov,[77,i] M. A. Chelstowska,[35] C. Chen,[58a] C. H. Chen,[76] H. Chen,[29] J. Chen,[58a] S. Chen,[161] S. J. Chen,[15c] X. Chen,[15b,j] Y. Chen,[80] H. C. Cheng,[103] H. J. Cheng,[15d] A. Cheplakov,[77] E. Cheremushkina,[140] R. Cherkaoui El Moursli,[34e] E. Cheu,[7] K. Cheung,[62] L. Chevalier,[142] V. Chiarella,[49] G. Chiarelli,[69a] G. Chiodini,[65a] A. S. Chisholm,[35] A. Chitan,[27b] Y. H. Chiu,[174] M. V. Chizhov,[77] K. Choi,[63] A. R. Chomont,[37] S. Chouridou,[160] Y. S. Chow,[61a] V. Christodoulou,[92] M. C. Chu,[61a] J. Chudoba,[137] A. J. Chuinard,[101] J. J. Chwastowski,[82] L. Chytka,[126] A. K. Ciftci,[4a] D. Cinca,[45] V. Cindro,[89] I. A. Cioară,[24] A. Ciocio,[18] F. Cirotto,[67a,67b] Z. H. Citron,[178] M. Citterio,[66a] M. Ciubancan,[27b] A. Clark,[52] B. L. Clark,[57] M. R. Clark,[38] P. J. Clark,[48] R. N. Clarke,[18] C. Clement,[43a,43b] Y. Coadou,[99] M. Cobal,[64a,64c] A. Coccaro,[52] J. Cochran,[76] L. Colasurdo,[117] B. Cole,[38] A. P. Colijn,[118] J. Collot,[56] T. Colombo,[169] P. Conde Muiño,[136a,136b] E. Coniavitis,[50] S. H. Connell,[32b] I. A. Connelly,[98] S. Constantinescu,[27b] G. Conti,[35] F. Conventi,[67a,k] M. Cooke,[18] A. M. Cooper-Sarkar,[131] F. Cormier,[173] K. J. R. Cormier,[165] M. Corradi,[70a,70b] F. Corriveau,[101,l] A. Cortes-Gonzalez,[35] G. Costa,[66a] M. J. Costa,[172] D. Costanzo,[146] G. Cottin,[31] G. Cowan,[91] B. E. Cox,[98] K. Cranmer,[121] S. J. Crawley,[55] R. A. Creager,[133] G. Cree,[33] S. Crépé-Renaudin,[56] F. Crescioli,[132] W. A. Cribbs,[43a,43b] M. Cristinziani,[24] V. Croft,[121] G. Crosetti,[40b,40a] A. Cueto,[96] T. Cuhadar Donszelmann,[146] A. R. Cukierman,[150] J. Cummings,[181] M. Curatolo,[49] J. Cúth,[97] S. Czekierda,[82] P. Czodrowski,[35] M. J. Da Cunha Sargedas De Sousa,[136a,136b] C. Da Via,[98] W. Dabrowski,[81a] T. Dado,[28a,m] T. Dai,[103] O. Dale,[17] F. Dallaire,[107] C. Dallapiccola,[100] M. Dam,[39] G. D'amen,[23b,23a] J. R. Dandoy,[133] M. F. Daneri,[30] N. P. Dang,[179,e] A. C. Daniells,[21] N. D. Dann,[98] M. Danninger,[173] M. Dano Hoffmann,[142] V. Dao,[152] G. Darbo,[53b] S. Darmora,[8] J. Dassoulas,[3] A. Dattagupta,[127] T. Daubney,[44] S. D'Auria,[55] W. Davey,[24] C. David,[44] T. Davidek,[139] D. R. Davis,[47] P. Davison,[92] E. Dawe,[102] I. Dawson,[146] K. De,[8] R. De Asmundis,[67a] A. De Benedetti,[124] S. De Castro,[23b,23a] S. De Cecco,[132] N. De Groot,[117] P. de Jong,[118] H. De la Torre,[104] F. De Lorenzi,[76] A. De Maria,[51,n] D. De Pedis,[70a] A. De Salvo,[70a] U. De Sanctis,[71a,71b] A. De Santo,[153] K. De Vasconcelos Corga,[99] J. B. De Vivie De Regie,[128] R. Debbe,[29] C. Debenedetti,[143] D. V. Dedovich,[77] N. Dehghanian,[3] I. Deigaard,[118] M. Del Gaudio,[40b,40a] J. Del Peso,[96] D. Delgove,[128] F. Deliot,[142] C. M. Delitzsch,[7] M. Della Pietra,[67a,67b] D. Della Volpe,[52] A. Dell'Acqua,[35] L. Dell'Asta,[25] M. Dell'Orso,[69a,69b] M. Delmastro,[5] C. Delporte,[128] P. A. Delsart,[56] D. A. DeMarco,[165] S. Demers,[181] M. Demichev,[77] A. Demilly,[132] S. P. Denisov,[140] D. Denysiuk,[142] L. D'Eramo,[132] D. Derendarz,[82] J. E. Derkaoui,[34d] F. Derue,[132] P. Dervan,[88] K. Desch,[24] C. Deterre,[44] K. Dette,[165] M. R. Devesa,[30] P. O. Deviveiros,[35] A. Dewhurst,[141] S. Dhaliwal,[26] F. A. Di Bello,[52] A. Di Ciaccio,[71a,71b] L. Di Ciaccio,[5] W. K. Di Clemente,[133] C. Di Donato,[67a,67b] A. Di Girolamo,[35] B. Di Girolamo,[35] B. Di Micco,[72a,72b] R. Di Nardo,[35] K. F. Di Petrillo,[57] A. Di Simone,[50] R. Di Sipio,[165] D. Di Valentino,[33] C. Diaconu,[99] M. Diamond,[165] F. A. Dias,[39] M. A. Diaz,[144a] E. B. Diehl,[103] J. Dietrich,[19] S. Díez Cornell,[44] A. Dimitrievska,[16] J. Dingfelder,[24] P. Dita,[27b] S. Dita,[27b] F. Dittus,[35] F. Djama,[99] T. Djobava,[157b] J. I. Djuvsland,[59a] M. A. B. Do Vale,[78c] D. Dobos,[35] M. Dobre,[27b] D. Dodsworth,[26] C. Doglioni,[94] J. Dolejsi,[139] Z. Dolezal,[139] M. Donadelli,[78d] S. Donati,[69a,69b] P. Dondero,[68a,68b] J. Donini,[37] M. D'Onofrio,[88] J. Dopke,[141] A. Doria,[67a] M. T. Dova,[86] A. T. Doyle,[55] E. Drechsler,[51] M. Dris,[10] Y. Du,[58b] J. Duarte-Campderros,[159] A. Dubreuil,[52] E. Duchovni,[178] G. Duckeck,[112] A. Ducourthial,[132] O. A. Ducu,[107,o] D. Duda,[118] A. Dudarev,[35] A. C. Dudder,[97] E. M. Duffield,[18] L. Duflot,[128] M. Dührssen,[35] C. Dülsen,[180] M. Dumancic,[178] A. E. Dumitriu,[27b,p] A. K. Duncan,[55] M. Dunford,[59a] A. Duperrin,[99] H. Duran Yildiz,[4a] M. Düren,[54] A. Durglishvili,[157b] D. Duschinger,[46] B. Dutta,[44] D. Duvnjak,[1] M. Dyndal,[44] B. S. Dziedzic,[82] C. Eckardt,[44] K. M. Ecker,[113] R. C. Edgar,[103] T. Eifert,[35] G. Eigen,[17] K. Einsweiler,[18] T. Ekelof,[170] M. El Kacimi,[34c] R. El Kosseifi,[99] V. Ellajosyula,[99] M. Ellert,[170] S. Elles,[5] F. Ellinghaus,[180] A. A. Elliot,[174] N. Ellis,[35] J. Elmsheuser,[29] M. Elsing,[35] D. Emeliyanov,[141] Y. Enari,[161] O. C. Endner,[97] J. S. Ennis,[176] M. B. Epland,[47] J. Erdmann,[45] A. Ereditato,[20] M. Ernst,[29] S. Errede,[171] M. Escalier,[128] C. Escobar,[172] B. Esposito,[49] O. Estrada Pastor,[172] A. I. Etienvre,[142] E. Etzion,[159] H. Evans,[63] A. Ezhilov,[134] M. Ezzi,[34e] F. Fabbri,[23b,23a] L. Fabbri,[23b,23a]

V. Fabiani,[117] G. Facini,[92] R. M. Fakhrutdinov,[140] S. Falciano,[70a] R. J. Falla,[92] J. Faltova,[35] Y. Fang,[15a] M. Fanti,[66a,66b] A. Farbin,[8] A. Farilla,[72a] C. Farina,[135] E. M. Farina,[68a,68b] T. Farooque,[104] S. Farrell,[18] S. M. Farrington,[176] P. Farthouat,[35] F. Fassi,[34e] P. Fassnacht,[35] D. Fassouliotis,[9] M. Faucci Giannelli,[48] A. Favareto,[53b,53a] W. J. Fawcett,[131] L. Fayard,[128] O. L. Fedin,[134,q] W. Fedorko,[173] S. Feigl,[130] L. Feligioni,[99] C. Feng,[58b] E. J. Feng,[35] M. J. Fenton,[55] A. B. Fenyuk,[140] L. Feremenga,[8] P. Fernandez Martinez,[172] S. Fernandez Perez,[14] J. Ferrando,[44] A. Ferrari,[170] P. Ferrari,[118] R. Ferrari,[68a] D. E. Ferreira de Lima,[59b] A. Ferrer,[172] D. Ferrere,[52] C. Ferretti,[103] F. Fiedler,[97] M. Filipuzzi,[44] A. Filipčič,[89] F. Filthaut,[117] M. Fincke-Keeler,[174] K. D. Finelli,[154] M. C. N. Fiolhais,[136a,136c,r] L. Fiorini,[172] A. Fischer,[2] C. Fischer,[14] J. Fischer,[180] W. C. Fisher,[104] N. Flaschel,[44] I. Fleck,[148] P. Fleischmann,[103] R. R. M. Fletcher,[133] T. Flick,[180] B. M. Flierl,[112] L. R. Flores Castillo,[61a] M. J. Flowerdew,[113] G. T. Forcolin,[98] A. Formica,[142] F. A. Förster,[14] A. C. Forti,[98] A. G. Foster,[21] D. Fournier,[128] H. Fox,[87] S. Fracchia,[146] P. Francavilla,[132] M. Franchini,[23b,23a] S. Franchino,[59a] D. Francis,[35] L. Franconi,[130] M. Franklin,[57] M. Frate,[169] M. Fraternali,[68a,68b] D. Freeborn,[92] S. M. Fressard-Batraneanu,[35] B. Freund,[107] D. Froidevaux,[35] J. A. Frost,[131] C. Fukunaga,[162] T. Fusayasu,[114] J. Fuster,[172] O. Gabizon,[158] A. Gabrielli,[23b,23a] A. Gabrielli,[18] G. P. Gach,[81a] S. Gadatsch,[35] S. Gadomski,[52] G. Gagliardi,[53b,53a] L. G. Gagnon,[107] C. Galea,[117] B. Galhardo,[136a,136c] E. J. Gallas,[131] B. J. Gallop,[141] P. Gallus,[138] G. Galster,[39] K. K. Gan,[122] S. Ganguly,[37] Y. Gao,[88] Y. S. Gao,[150,f] C. García,[172] J. E. García Navarro,[172] J. A. García Pascual,[15a] M. Garcia-Sciveres,[18] R. W. Gardner,[36] N. Garelli,[150] V. Garonne,[130] A. Gascon Bravo,[44] K. Gasnikova,[44] C. Gatti,[49] A. Gaudiello,[53b,53a] G. Gaudio,[68a] I. L. Gavrilenko,[108] C. Gay,[173] G. Gaycken,[24] E. N. Gazis,[10] C. N. P. Gee,[141] J. Geisen,[51] M. Geisen,[97] M. P. Geisler,[59a] K. Gellerstedt,[43a,43b] C. Gemme,[53b] M. H. Genest,[56] C. Geng,[103] S. Gentile,[70a,70b] C. Gentsos,[160] S. George,[91] D. Gerbaudo,[14] G. Gessner,[45] S. Ghasemi,[148] M. Ghneimat,[24] B. Giacobbe,[23b] S. Giagu,[70a,70b] N. Giangiacomi,[23b,23a] P. Giannetti,[69a] S. M. Gibson,[91] M. Gignac,[173] M. Gilchriese,[18] D. Gillberg,[33] G. Gilles,[180] D. M. Gingrich,[3,d] M. P. Giordani,[64a,64c] F. M. Giorgi,[23b] P. F. Giraud,[142] P. Giromini,[57] G. Giugliarelli,[64a,64c] D. Giugni,[66a] F. Giuli,[131] C. Giuliani,[113] M. Giulini,[59b] B. K. Gjelsten,[130] S. Gkaitatzis,[160] I. Gkialas,[9,s] E. L. Gkougkousis,[14] P. Gkountoumis,[10] L. K. Gladilin,[111] C. Glasman,[96] J. Glatzer,[14] P. C. F. Glaysher,[44] A. Glazov,[44] M. Goblirsch-Kolb,[26] J. Godlewski,[82] S. Goldfarb,[102] T. Golling,[52] D. Golubkov,[140] A. Gomes,[136a,136b,136d] R. Goncalves Gama,[78b] J. Goncalves Pinto Firmino Da Costa,[142] R. Gonçalo,[136a] G. Gonella,[50] L. Gonella,[21] A. Gongadze,[77] S. González de la Hoz,[172] S. Gonzalez-Sevilla,[52] L. Goossens,[35] P. A. Gorbounov,[109] H. A. Gordon,[29] I. Gorelov,[116] B. Gorini,[35] E. Gorini,[65a,65b] A. Gorišek,[89] A. T. Goshaw,[47] C. Gössling,[45] M. I. Gostkin,[77] C. A. Gottardo,[24] C. R. Goudet,[128] D. Goujdami,[34c] A. G. Goussiou,[145] N. Govender,[32b,t] E. Gozani,[158] I. Grabowska-Bold,[81a] P. O. J. Gradin,[170] J. Gramling,[169] E. Gramstad,[130] S. Grancagnolo,[19] V. Gratchev,[134] P. M. Gravila,[27f] C. Gray,[55] H. M. Gray,[18] Z. D. Greenwood,[93,u] C. Grefe,[24] K. Gregersen,[92] I. M. Gregor,[44] P. Grenier,[150] K. Grevtsov,[5] J. Griffiths,[8] A. A. Grillo,[143] K. Grimm,[87] S. Grinstein,[14,v] Ph. Gris,[37] J.-F. Grivaz,[128] S. Groh,[97] E. Gross,[178] J. Grosse-Knetter,[51] G. C. Grossi,[93] Z. J. Grout,[92] A. Grummer,[116] L. Guan,[103] W. Guan,[179] J. Guenther,[35] F. Guescini,[166a] D. Guest,[169] O. Gueta,[159] B. Gui,[122] E. Guido,[53b,53a] T. Guillemin,[5] S. Guindon,[35] U. Gul,[55] C. Gumpert,[35] J. Guo,[58c] W. Guo,[103] Y. Guo,[58a,w] R. Gupta,[41] S. Gupta,[131] S. Gurbuz,[12c] G. Gustavino,[124] B. J. Gutelman,[158] P. Gutierrez,[124] N. G. Gutierrez Ortiz,[92] C. Gutschow,[92] C. Guyot,[142] M. P. Guzik,[81a] C. Gwenlan,[131] C. B. Gwilliam,[88] A. Haas,[121] C. Haber,[18] H. K. Hadavand,[8] N. Haddad,[34e] A. Hadef,[99] S. Hageböck,[24] M. Hagihara,[167] H. Hakobyan,[182,a] M. Haleem,[44] J. Haley,[125] G. Halladjian,[104] G. D. Hallewell,[99] K. Hamacher,[180] P. Hamal,[126] K. Hamano,[174] A. Hamilton,[32a] G. N. Hamity,[146] P. G. Hamnett,[44] L. Han,[58a] S. Han,[15d] K. Hanagaki,[79,x] K. Hanawa,[161] M. Hance,[143] B. Haney,[133] P. Hanke,[59a] J. B. Hansen,[39] J. D. Hansen,[39] M. C. Hansen,[24] P. H. Hansen,[39] K. Hara,[167] A. S. Hard,[179] T. Harenberg,[180] F. Hariri,[128] S. Harkusha,[105] P. F. Harrison,[176] N. M. Hartmann,[112] Y. Hasegawa,[147] A. Hasib,[48] S. Hassani,[142] S. Haug,[20] R. Hauser,[104] L. Hauswald,[46] L. B. Havener,[38] M. Havranek,[138] C. M. Hawkes,[21] R. J. Hawkings,[35] D. Hayakawa,[163] D. Hayden,[104] C. P. Hays,[131] J. M. Hays,[90] H. S. Hayward,[88] S. J. Haywood,[141] S. J. Head,[21] T. Heck,[97] V. Hedberg,[94] L. Heelan,[8] S. Heer,[24] K. K. Heidegger,[50] S. Heim,[44] T. Heim,[18] B. Heinemann,[44,y] J. J. Heinrich,[112] L. Heinrich,[121] C. Heinz,[54] J. Hejbal,[137] L. Helary,[35] A. Held,[173] S. Hellman,[43a,43b] C. Helsens,[35] R. C. W. Henderson,[87] Y. Heng,[179] S. Henkelmann,[173] A. M. Henriques Correia,[35] S. Henrot-Versille,[128] G. H. Herbert,[19] H. Herde,[26] V. Herget,[175] Y. Hernández Jiménez,[32c] H. Herr,[97] G. Herten,[50] R. Hertenberger,[112] L. Hervas,[35] T. C. Herwig,[133] G. G. Hesketh,[92] N. P. Hessey,[166a] J. W. Hetherly,[41] S. Higashino,[79] E. Higón-Rodriguez,[172] K. Hildebrand,[36] E. Hill,[174] J. C. Hill,[31] K. H. Hiller,[44] S. J. Hillier,[21] M. Hils,[46] I. Hinchliffe,[18] M. Hirose,[50] D. Hirschbuehl,[180] B. Hiti,[89] O. Hladik,[137] X. Hoad,[48] J. Hobbs,[152] N. Hod,[166a] M. C. Hodgkinson,[146] P. Hodgson,[146] A. Hoecker,[35] M. R. Hoeferkamp,[116] F. Hoenig,[112] D. Hohn,[24] T. R. Holmes,[36] M. Homann,[45] S. Honda,[167] T. Honda,[79] T. M. Hong,[135] B. H. Hooberman,[171] W. H. Hopkins,[127] Y. Horii,[115] A. J. Horton,[149] J-Y. Hostachy,[56] A. Hostiuc,[145]

S. Hou,[155] A. Hoummada,[34a] J. Howarth,[98] J. Hoya,[86] M. Hrabovsky,[126] J. Hrdinka,[35] I. Hristova,[19] J. Hrivnac,[128] A. Hrynevich,[106] T. Hryn'ova,[5] P. J. Hsu,[62] S.-C. Hsu,[145] Q. Hu,[58a] S. Hu,[58c] Y. Huang,[15a] Z. Hubacek,[138] F. Hubaut,[99] F. Huegging,[24] T. B. Huffman,[131] E. W. Hughes,[38] G. Hughes,[87] M. Huhtinen,[35] R. F. H. Hunter,[33] P. Huo,[152] N. Huseynov,[77,c] J. Huston,[104] J. Huth,[57] R. Hyneman,[103] G. Iacobucci,[52] G. Iakovidis,[29] I. Ibragimov,[148] L. Iconomidou-Fayard,[128] Z. Idrissi,[34e] P. Iengo,[35] O. Igonkina,[118,z] T. Iizawa,[177] Y. Ikegami,[79] M. Ikeno,[79] Y. Ilchenko,[11] D. Iliadis,[160] N. Ilic,[150] F. Iltzsche,[46] G. Introzzi,[68a,68b] P. Ioannou,[9,a] M. Iodice,[72a] K. Iordanidou,[38] V. Ippolito,[57] M. F. Isacson,[170] N. Ishijima,[129] M. Ishino,[161] M. Ishitsuka,[163] C. Issever,[131] S. Istin,[12c,aa] F. Ito,[167] J. M. Iturbe Ponce,[61a] R. Iuppa,[73a,73b] H. Iwasaki,[79] J. M. Izen,[42] V. Izzo,[67a] S. Jabbar,[3] P. Jackson,[1] R. M. Jacobs,[24] V. Jain,[2] K. B. Jakobi,[97] K. Jakobs,[50] S. Jakobsen,[74] T. Jakoubek,[137] D. O. Jamin,[125] D. K. Jana,[93] R. Jansky,[52] J. Janssen,[24] M. Janus,[51] P. A. Janus,[81a] G. Jarlskog,[94] N. Javadov,[77,c] T. Javůrek,[50] M. Javurkova,[50] F. Jeanneau,[142] L. Jeanty,[18] J. Jejelava,[157a,bb] A. Jelinskas,[176] P. Jenni,[50,cc] C. Jeske,[176] S. Jézéquel,[5] H. Ji,[179] J. Jia,[152] H. Jiang,[76] Y. Jiang,[58a] Z. Jiang,[150,dd] S. Jiggins,[92] J. Jimenez Pena,[172] S. Jin,[15a] A. Jinaru,[27b] O. Jinnouchi,[163] H. Jivan,[32c] P. Johansson,[146] K. A. Johns,[7] C. A. Johnson,[63] W. J. Johnson,[145] K. Jon-And,[43a,43b] R. W. L. Jones,[87] S. D. Jones,[153] S. Jones,[7] T. J. Jones,[88] J. Jongmanns,[59a] P. M. Jorge,[136a,136b] J. Jovicevic,[166a] X. Ju,[179] A. Juste Rozas,[14,v] A. Kaczmarska,[82] M. Kado,[128] H. Kagan,[122] M. Kagan,[150] S. J. Kahn,[99] T. Kaji,[177] E. Kajomovitz,[158] C. W. Kalderon,[94] A. Kaluza,[97] S. Kama,[41] A. Kamenshchikov,[140] N. Kanaya,[161] L. Kanjir,[89] V. A. Kantserov,[110] J. Kanzaki,[79] B. Kaplan,[121] L. S. Kaplan,[179] D. Kar,[32c] K. Karakostas,[10] N. Karastathis,[10] M. J. Kareem,[166b] E. Karentzos,[10] S. N. Karpov,[77] Z. M. Karpova,[77] K. Karthik,[121] V. Kartvelishvili,[87] A. N. Karyukhin,[140] K. Kasahara,[167] L. Kashif,[179] R. D. Kass,[122] A. Kastanas,[151] Y. Kataoka,[161] C. Kato,[161] A. Katre,[52] J. Katzy,[44] K. Kawade,[80] K. Kawagoe,[85] T. Kawamoto,[161] G. Kawamura,[51] E. F. Kay,[88] V. F. Kazanin,[120b,120a] R. Keeler,[174] R. Kehoe,[41] J. S. Keller,[33] E. Kellermann,[94] J. J. Kempster,[91] J. Kendrick,[21] H. Keoshkerian,[165] O. Kepka,[137] S. Kersten,[180] B. P. Kerševan,[89] R. A. Keyes,[101] M. Khader,[171] F. Khalil-Zada,[13] A. Khanov,[125] A. G. Kharlamov,[120b,120a] T. Kharlamova,[120b,120a] A. Khodinov,[164] T. J. Khoo,[52] V. Khovanskiy,[109,a] E. Khramov,[77] J. Khubua,[157b] S. Kido,[80] C. R. Kilby,[91] H. Y. Kim,[8] S. H. Kim,[167] Y. K. Kim,[36] N. Kimura,[160] O. M. Kind,[19] B. T. King,[88] D. Kirchmeier,[46] J. Kirk,[141] A. E. Kiryunin,[113] T. Kishimoto,[161] D. Kisielewska,[81a] V. Kitali,[44] O. Kivernyk,[5] E. Kladiva,[28b,a] T. Klapdor-Kleingrothaus,[50] M. H. Klein,[103] M. Klein,[88] U. Klein,[88] K. Kleinknecht,[97] P. Klimek,[119] A. Klimentov,[29] R. Klingenberg,[45,a] T. Klingl,[24] T. Klioutchnikova,[35] P. Kluit,[118] S. Kluth,[113] E. Kneringer,[74] E. B. F. G. Knoops,[99] A. Knue,[113] A. Kobayashi,[161] D. Kobayashi,[85] T. Kobayashi,[161] M. Kobel,[46] M. Kocian,[150] P. Kodys,[139] T. Koffas,[33] E. Koffeman,[118] M. K. Köhler,[178] N. M. Köhler,[113] T. Koi,[150] M. Kolb,[59b] I. Koletsou,[5] A. A. Komar,[108,a] T. Kondo,[79] N. Kondrashova,[58c] K. Köneke,[50] A. C. König,[117] T. Kono,[79,ee] R. Konoplich,[121,ff] N. Konstantinidis,[92] R. Kopeliansky,[63] S. Koperny,[81a] A. K. Kopp,[50] K. Korcyl,[82] K. Kordas,[160] A. Korn,[92] A. A. Korol,[120b,120a,gg] I. Korolkov,[14] E. V. Korolkova,[146] O. Kortner,[113] S. Kortner,[113] T. Kosek,[139] V. V. Kostyukhin,[24] A. Kotwal,[47] A. Koulouris,[10] A. Kourkoumeli-Charalampidi,[68a,68b] C. Kourkoumelis,[9] E. Kourlitis,[146] V. Kouskoura,[29] A. B. Kowalewska,[82] R. Kowalewski,[174] T. Z. Kowalski,[81a] C. Kozakai,[161] W. Kozanecki,[142] A. S. Kozhin,[140] V. A. Kramarenko,[111] G. Kramberger,[89] D. Krasnopevtsev,[110] M. W. Krasny,[132] A. Krasznahorkay,[35] D. Krauss,[113] J. A. Kremer,[81a] J. Kretzschmar,[88] K. Kreutzfeldt,[54] P. Krieger,[165] K. Krizka,[18] K. Kroeninger,[45] H. Kroha,[113] J. Kroll,[137] J. Kroll,[133] J. Kroseberg,[24] J. Krstic,[16] U. Kruchonak,[77] H. Krüger,[24] N. Krumnack,[76] M. C. Kruse,[47] T. Kubota,[102] H. Kucuk,[92] S. Kuday,[4b] J. T. Kuechler,[180] S. Kuehn,[35] A. Kugel,[59a] F. Kuger,[175] T. Kuhl,[44] V. Kukhtin,[77] R. Kukla,[99] Y. Kulchitsky,[105] S. Kuleshov,[144b] Y. P. Kulinich,[171] M. Kuna,[70a,70b] T. Kunigo,[83] A. Kupco,[137] T. Kupfer,[45] O. Kuprash,[159] H. Kurashige,[80] L. L. Kurchaninov,[166a] Y. A. Kurochkin,[105] M. G. Kurth,[15d] E. S. Kuwertz,[174] M. Kuze,[163] J. Kvita,[126] T. Kwan,[174] D. Kyriazopoulos,[146] A. La Rosa,[113] J. L. La Rosa Navarro,[78d] L. La Rotonda,[40b,40a] F. La Ruffa,[40b,40a] C. Lacasta,[172] F. Lacava,[70a,70b] J. Lacey,[44] D. P. J. Lack,[98] H. Lacker,[19] D. Lacour,[132] E. Ladygin,[77] R. Lafaye,[5] B. Laforge,[132] T. Lagouri,[32c] S. Lai,[51] S. Lammers,[63] W. Lampl,[7] E. Lançon,[29] U. Landgraf,[50] M. P. J. Landon,[90] M. C. Lanfermann,[52] V. S. Lang,[44] J. C. Lange,[14] R. J. Langenberg,[35] A. J. Lankford,[169] F. Lanni,[29] K. Lantzsch,[24] A. Lanza,[68a] A. Lapertosa,[53b,53a] S. Laplace,[132] J. F. Laporte,[142] T. Lari,[66a] F. Lasagni Manghi,[23b,23a] M. Lassnig,[35] T. S. Lau,[61a] P. Laurelli,[49] W. Lavrijsen,[18] A. T. Law,[143] P. Laycock,[88] T. Lazovich,[57] M. Lazzaroni,[66a,66b] B. Le,[102] O. Le Dortz,[132] E. Le Guirriec,[99] E. P. Le Quilleuc,[142] M. LeBlanc,[174] T. LeCompte,[6] F. Ledroit-Guillon,[56] C. A. Lee,[29] G. R. Lee,[144a] L. Lee,[57] S. C. Lee,[155] B. Lefebvre,[101] G. Lefebvre,[132] M. Lefebvre,[174] F. Legger,[112] C. Leggett,[18] G. Lehmann Miotto,[35] X. Lei,[7] W. A. Leight,[44] M. A. L. Leite,[78d] R. Leitner,[139] D. Lellouch,[178] B. Lemmer,[51] K. J. C. Leney,[92] T. Lenz,[24] B. Lenzi,[35] R. Leone,[7] S. Leone,[69a] C. Leonidopoulos,[48] G. Lerner,[153] C. Leroy,[107] R. Les,[165] A. A. J. Lesage,[142] C. G. Lester,[31] M. Levchenko,[134] J. Levêque,[5] D. Levin,[103] L. J. Levinson,[178] M. Levy,[21] D. Lewis,[90]

B. Li,[58a,w] C-Q. Li,[58a,hh] H. Li,[152] L. Li,[58c] Q. Li,[15d] Q. Y. Li,[58a] S. Li,[47] X. Li,[58c] Y. Li,[148] Z. Liang,[15a] B. Liberti,[71a] A. Liblong,[165] K. Lie,[61c] J. Liebal,[24] W. Liebig,[17] A. Limosani,[154] C. Y. Lin,[31] K. Lin,[104] S. C. Lin,[156] T. H. Lin,[97] R. A. Linck,[63] B. E. Lindquist,[152] A. L. Lionti,[52] E. Lipeles,[133] A. Lipniacka,[17] M. Lisovyi,[59b] T. M. Liss,[171,ii] A. Lister,[173] A. M. Litke,[143] B. Liu,[76] H. B. Liu,[29] H. Liu,[103] J. B. Liu,[58a] J. K. K. Liu,[131] J. Liu,[58b] K. Liu,[99] L. Liu,[171] M. Liu,[58a] Y. L. Liu,[58a] Y. W. Liu,[58a] M. Livan,[68a,68b] A. Lleres,[56] J. Llorente Merino,[15a] S. L. Lloyd,[90] C. Y. Lo,[61b] F. Lo Sterzo,[41] E. M. Lobodzinska,[44] P. Loch,[7] F. K. Loebinger,[98] K. M. Loew,[26] T. Lohse,[19] K. Lohwasser,[146] M. Lokajicek,[137] B. A. Long,[25] J. D. Long,[171] R. E. Long,[87] L. Longo,[65a,65b] K. A. Looper,[122] J. A. Lopez,[144b] I. Lopez Paz,[14] A. Lopez Solis,[132] J. Lorenz,[112] N. Lorenzo Martinez,[5] M. Losada,[22] P. J. Lösel,[112] A. Lösle,[50] X. Lou,[15a] A. Lounis,[128] J. Love,[6] P. A. Love,[87] H. Lu,[61a] N. Lu,[103] Y. J. Lu,[62] H. J. Lubatti,[145] C. Luci,[70a,70b] A. Lucotte,[56] C. Luedtke,[50] F. Luehring,[63] W. Lukas,[74] L. Luminari,[70a] O. Lundberg,[43a,43b] B. Lund-Jensen,[151] M. S. Lutz,[100] P. M. Luzi,[132] D. Lynn,[29] R. Lysak,[137] E. Lytken,[94] F. Lyu,[15a] V. Lyubushkin,[77] H. Ma,[29] L. L. Ma,[58b] Y. Ma,[58b] G. Maccarrone,[49] A. Macchiolo,[113] C. M. Macdonald,[146] J. Machado Miguens,[133,136b] D. Madaffari,[172] R. Madar,[37] W. F. Mader,[46] A. Madsen,[44] N. Madysa,[46] J. Maeda,[80] S. Maeland,[17] T. Maeno,[29] A. S. Maevskiy,[111] V. Magerl,[50] C. Maiani,[128] C. Maidantchik,[78b] T. Maier,[112] A. Maio,[136a,136b,136d] O. Majersky,[28a] S. Majewski,[127] Y. Makida,[79] N. Makovec,[128] B. Malaescu,[132] Pa. Malecki,[82] V. P. Maleev,[134] F. Malek,[56] U. Mallik,[75] D. Malon,[6] C. Malone,[31] S. Maltezos,[10] S. Malyukov,[35] J. Mamuzic,[172] G. Mancini,[49] I. Mandić,[89] J. Maneira,[136a,136b] L. Manhaes de Andrade Filho,[78a] J. Manjarres Ramos,[46] K. H. Mankinen,[94] A. Mann,[112] A. Manousos,[35] B. Mansoulie,[142] J. D. Mansour,[15a] R. Mantifel,[101] M. Mantoani,[51] S. Manzoni,[66a,66b] L. Mapelli,[35] G. Marceca,[30] L. March,[52] L. Marchese,[131] G. Marchiori,[132] M. Marcisovsky,[137] C. A. Marin Tobon,[35] M. Marjanovic,[37] D. E. Marley,[103] F. Marroquim,[78b] S. P. Marsden,[98] Z. Marshall,[18] M. U. F. Martensson,[170] S. Marti-Garcia,[172] C. B. Martin,[122] T. A. Martin,[176] V. J. Martin,[48] B. Martin dit Latour,[17] M. Martinez,[14,v] V. I. Martinez Outschoorn,[171] S. Martin-Haugh,[141] V. S. Martoiu,[27b] A. C. Martyniuk,[92] A. Marzin,[35] L. Masetti,[97] T. Mashimo,[161] R. Mashinistov,[108] J. Masik,[98] A. L. Maslennikov,[120b,120a] L. H. Mason,[102] L. Massa,[71a,71b] P. Mastrandrea,[5] A. Mastroberardino,[40b,40a] T. Masubuchi,[161] P. Mättig,[180] J. Maurer,[27b] B. Maček,[89] S. J. Maxfield,[88] D. A. Maximov,[120b,120a] R. Mazini,[155] I. Maznas,[160] S. M. Mazza,[66a,66b] N. C. Mc Fadden,[116] G. Mc Goldrick,[165] S. P. Mc Kee,[103] A. McCarn,[103] R. L. McCarthy,[152] T. G. McCarthy,[113] L. I. McClymont,[92] E. F. McDonald,[102] J. A. Mcfayden,[35] G. Mchedlidze,[51] S. J. McMahon,[141] P. C. McNamara,[102] C. J. McNicol,[176] R. A. McPherson,[174,l] S. Meehan,[145] T. M. Megy,[50] S. Mehlhase,[112] A. Mehta,[88] T. Meideck,[56] B. Meirose,[42] D. Melini,[172,jj] B. R. Mellado Garcia,[32c] J. D. Mellenthin,[51] M. Melo,[28a] F. Meloni,[20] A. Melzer,[24] S. B. Menary,[98] L. Meng,[88] X. T. Meng,[103] A. Mengarelli,[23b,23a] S. Menke,[113] E. Meoni,[40b,40a] S. Mergelmeyer,[19] C. Merlassino,[20] P. Mermod,[52] L. Merola,[67a,67b] C. Meroni,[66a] F. S. Merritt,[36] A. Messina,[70a,70b] J. Metcalfe,[6] A. S. Mete,[169] C. Meyer,[133] J. Meyer,[118] J-P. Meyer,[142] H. Meyer Zu Theenhausen,[59a] F. Miano,[153] R. P. Middleton,[141] S. Miglioranzi,[53b,53a] L. Mijović,[48] G. Mikenberg,[178] M. Mikestikova,[137] M. Mikuž,[89] M. Milesi,[102] A. Milic,[165] D. A. Millar,[90] D. W. Miller,[36] C. Mills,[48] A. Milov,[178] D. A. Milstead,[43a,43b] A. A. Minaenko,[140] Y. Minami,[161] I. A. Minashvili,[157b] A. I. Mincer,[121] B. Mindur,[81a] M. Mineev,[77] Y. Minegishi,[161] Y. Ming,[179] L. M. Mir,[14] A. Mirto,[65a,65b] K. P. Mistry,[133] T. Mitani,[177] J. Mitrevski,[112] V. A. Mitsou,[172] A. Miucci,[20] P. S. Miyagawa,[146] A. Mizukami,[79] J. U. Mjörnmark,[94] T. Mkrtchyan,[182] M. Mlynarikova,[139] T. Moa,[43a,43b] K. Mochizuki,[107] P. Mogg,[50] S. Mohapatra,[38] S. Molander,[43a,43b] R. Moles-Valls,[24] M. C. Mondragon,[104] K. Mönig,[44] J. Monk,[39] E. Monnier,[99] A. Montalbano,[152] J. Montejo Berlingen,[35] F. Monticelli,[86] S. Monzani,[66a] R. W. Moore,[3] N. Morange,[128] D. Moreno,[22] M. Moreno Llácer,[35] P. Morettini,[53b] S. Morgenstern,[35] D. Mori,[149] T. Mori,[161] M. Morii,[57] M. Morinaga,[177] V. Morisbak,[130] A. K. Morley,[35] G. Mornacchi,[35] J. D. Morris,[90] L. Morvaj,[152] P. Moschovakos,[10] M. Mosidze,[157b] H. J. Moss,[146] J. Moss,[150,kk] K. Motohashi,[163] R. Mount,[150] E. Mountricha,[29] E. J. W. Moyse,[100] S. Muanza,[99] F. Mueller,[113] J. Mueller,[135] R. S. P. Mueller,[112] D. Muenstermann,[87] P. Mullen,[55] G. A. Mullier,[20] F. J. Munoz Sanchez,[98] W. J. Murray,[176,141] H. Musheghyan,[35] M. Muškinja,[89] A. G. Myagkov,[140,ll] M. Myska,[138] B. P. Nachman,[18] O. Nackenhorst,[52] K. Nagai,[131] R. Nagai,[79,ee] K. Nagano,[79] Y. Nagasaka,[60] K. Nagata,[167] M. Nagel,[50] E. Nagy,[99] A. M. Nairz,[35] Y. Nakahama,[115] K. Nakamura,[79] T. Nakamura,[161] I. Nakano,[123] R. F. Naranjo Garcia,[44] R. Narayan,[11] D. I. Narrias Villar,[59a] I. Naryshkin,[134] T. Naumann,[44] G. Navarro,[22] R. Nayyar,[7] H. A. Neal,[103,a] P. Y. Nechaeva,[108] T. J. Neep,[142] A. Negri,[68a,68b] M. Negrini,[23b] S. Nektarijevic,[117] C. Nellist,[51] A. Nelson,[169] M. E. Nelson,[131] S. Nemecek,[137] P. Nemethy,[121] M. Nessi,[35,mm] M. S. Neubauer,[171] M. Neumann,[180] P. R. Newman,[21] T. Y. Ng,[61c] Y. S. Ng,[19] T. Nguyen Manh,[107] R. B. Nickerson,[131] R. Nicolaidou,[142] J. Nielsen,[143] N. Nikiforou,[11] V. Nikolaenko,[140,ll] I. Nikolic-Audit,[132] K. Nikolopoulos,[21] J. K. Nilsen,[130] P. Nilsson,[29] Y. Ninomiya,[161] A. Nisati,[70a] N. Nishu,[58c] R. Nisius,[113] I. Nitsche,[45] T. Nitta,[177] T. Nobe,[161] Y. Noguchi,[83]

M. Nomachi,[129] I. Nomidis,[33] M. A. Nomura,[29] T. Nooney,[90] M. Nordberg,[35] N. Norjoharuddeen,[131] O. Novgorodova,[46] M. Nozaki,[79] L. Nozka,[126] K. Ntekas,[169] E. Nurse,[92] F. Nuti,[102] F. G. Oakham,[33,d] H. Oberlack,[113] T. Obermann,[24] J. Ocariz,[132] A. Ochi,[80] I. Ochoa,[38] J. P. Ochoa-Ricoux,[144a] K. O'Connor,[26] S. Oda,[85] S. Odaka,[79] A. Oh,[98] S. H. Oh,[47] C. C. Ohm,[151] H. Ohman,[170] H. Oide,[53b,53a] H. Okawa,[167] Y. Okumura,[161] T. Okuyama,[79] A. Olariu,[27b] L. F. Oleiro Seabra,[136a] S. A. Olivares Pino,[144a] D. Oliveira Damazio,[29] A. Olszewski,[82] J. Olszowska,[82] D. C. O'Neil,[149] A. Onofre,[136a,136e] K. Onogi,[115] P. U. E. Onyisi,[11] H. Oppen,[130] M. J. Oreglia,[36] Y. Oren,[159] D. Orestano,[72a,72b] N. Orlando,[61b] A. A. O'Rourke,[44] R. S. Orr,[165] B. Osculati,[53b,53a,a] V. O'Shea,[55] R. Ospanov,[58a] G. Otero y Garzon,[30] H. Otono,[85] M. Ouchrif,[34d] F. Ould-Saada,[130] A. Ouraou,[142] K. P. Oussoren,[118] Q. Ouyang,[15a] M. Owen,[55] R. E. Owen,[21] V. E. Ozcan,[12c] N. Ozturk,[8] K. Pachal,[149] A. Pacheco Pages,[14] L. Pacheco Rodriguez,[142] C. Padilla Aranda,[14] S. Pagan Griso,[18] M. Paganini,[181] F. Paige,[29,a] G. Palacino,[63] S. Palazzo,[40b,40a] S. Palestini,[35] M. Palka,[81b] D. Pallin,[37] E.St. Panagiotopoulou,[10] I. Panagoulias,[10] C. E. Pandini,[52] J. G. Panduro Vazquez,[91] P. Pani,[35] S. Panitkin,[29] D. Pantea,[27b] L. Paolozzi,[52] T. D. Papadopoulou,[10] K. Papageorgiou,[9,s] A. Paramonov,[6] D. Paredes Hernandez,[181] A. J. Parker,[87] K. A. Parker,[44] M. A. Parker,[31] F. Parodi,[53b,53a] J. A. Parsons,[38] U. Parzefall,[50] V. R. Pascuzzi,[165] J. M. P. Pasner,[143] E. Pasqualucci,[70a] S. Passaggio,[53b] F. Pastore,[91] S. Pataraia,[97] J. R. Pater,[98] T. Pauly,[35] B. Pearson,[113] S. Pedraza Lopez,[172] R. Pedro,[136a,136b] S. V. Peleganchuk,[120b,120a] O. Penc,[137] C. Peng,[15d] H. Peng,[58a] J. Penwell,[63] B. S. Peralva,[78a] M. M. Perego,[142] D. V. Perepelitsa,[29] F. Peri,[19] L. Perini,[66a,66b] H. Pernegger,[35] S. Perrella,[67a,67b] R. Peschke,[44] V. D. Peshekhonov,[77,a] K. Peters,[44] R. F. Y. Peters,[98] B. A. Petersen,[35] T. C. Petersen,[39] E. Petit,[56] A. Petridis,[1] C. Petridou,[160] P. Petroff,[128] E. Petrolo,[70a] M. Petrov,[131] F. Petrucci,[72a,72b] N. E. Pettersson,[100] A. Peyaud,[142] R. Pezoa,[144b] F. H. Phillips,[104] P. W. Phillips,[141] G. Piacquadio,[152] E. Pianori,[176] A. Picazio,[100] E. Piccaro,[90] M. A. Pickering,[131] R. Piegaia,[30] J. E. Pilcher,[36] A. D. Pilkington,[98] M. Pinamonti,[71a,71b] J. L. Pinfold,[3] H. Pirumov,[44] M. Pitt,[178] L. Plazak,[28a] M.-A. Pleier,[29] V. Pleskot,[97] E. Plotnikova,[77] D. Pluth,[76] P. Podberezko,[120b,120a] R. Poettgen,[94] R. Poggi,[68a,68b] L. Poggioli,[128] I. Pogrebnyak,[104] D. Pohl,[24] I. Pokharel,[51] G. Polesello,[68a] A. Poley,[44] A. Policicchio,[40b,40a] R. Polifka,[35] A. Polini,[23b] C. S. Pollard,[55] V. Polychronakos,[29] K. Pommès,[35] D. Ponomarenko,[110] L. Pontecorvo,[70a] G. A. Popeneciu,[27d] D. M. Portillo Quintero,[132] S. Pospisil,[138] K. Potamianos,[44] I. N. Potrap,[77] C. J. Potter,[31] H. Potti,[11] T. Poulsen,[94] J. Poveda,[35] M. E. Pozo Astigarraga,[35] P. Pralavorio,[99] A. Pranko,[18] S. Prell,[76] D. Price,[98] M. Primavera,[65a] S. Prince,[101] N. Proklova,[110] K. Prokofiev,[61c] F. Prokoshin,[144b] S. Protopopescu,[29] J. Proudfoot,[6] M. Przybycien,[81a] A. Puri,[171] P. Puzo,[128] J. Qian,[103] G. Qin,[55] Y. Qin,[98] A. Quadt,[51] M. Queitsch-Maitland,[44] D. Quilty,[55] S. Raddum,[130] V. Radeka,[29] V. Radescu,[131] S. K. Radhakrishnan,[152] P. Radloff,[127] P. Rados,[102] F. Ragusa,[66a,66b] G. Rahal,[95] J. A. Raine,[98] S. Rajagopalan,[29] C. Rangel-Smith,[170] T. Rashid,[128] S. Raspopov,[5] M. G. Ratti,[66a,66b] D. M. Rauch,[44] F. Rauscher,[112] S. Rave,[97] I. Ravinovich,[178] J. H. Rawling,[98] M. Raymond,[35] A. L. Read,[130] N. P. Readioff,[56] M. Reale,[65a,65b] D. M. Rebuzzi,[68a,68b] A. Redelbach,[175] G. Redlinger,[29] R. Reece,[143] R. G. Reed,[32c] K. Reeves,[42] L. Rehnisch,[19] J. Reichert,[133] A. Reiss,[97] C. Rembser,[35] H. Ren,[15d] M. Rescigno,[70a] S. Resconi,[66a] E. D. Resseguie,[133] S. Rettie,[173] E. Reynolds,[21] O. L. Rezanova,[120b,120a] P. Reznicek,[139] R. Rezvani,[107] R. Richter,[113] S. Richter,[92] E. Richter-Was,[81b] O. Ricken,[24] M. Ridel,[132] P. Rieck,[113] C. J. Riegel,[180] J. Rieger,[51] O. Rifki,[124] M. Rijssenbeek,[152] A. Rimoldi,[68a,68b] M. Rimoldi,[20] L. Rinaldi,[23b] G. Ripellino,[151] B. Ristić,[35] E. Ritsch,[35] I. Riu,[14] F. Rizatdinova,[125] E. Rizvi,[90] C. Rizzi,[14] R. T. Roberts,[98] S. H. Robertson,[101,l] A. Robichaud-Veronneau,[101] D. Robinson,[31] J. E. M. Robinson,[44] A. Robson,[55] E. Rocco,[97] C. Roda,[69a,69b] Y. Rodina,[99,nn] S. Rodriguez Bosca,[172] A. Rodriguez Perez,[14] D. Rodriguez Rodriguez,[172] S. Roe,[35] C. S. Rogan,[57] O. Røhne,[130] J. Roloff,[57] A. Romaniouk,[110] M. Romano,[23b,23a] S. M. Romano Saez,[37] E. Romero Adam,[172] N. Rompotis,[88] M. Ronzani,[50] L. Roos,[132] S. Rosati,[70a] K. Rosbach,[50] P. Rose,[143] N-A. Rosien,[51] E. Rossi,[67a,67b] L. P. Rossi,[53b] J. H. N. Rosten,[31] R. Rosten,[145] M. Rotaru,[27b] J. Rothberg,[145] D. Rousseau,[128] A. Rozanov,[99] Y. Rozen,[158] X. Ruan,[32c] F. Rubbo,[150] F. Rühr,[50] A. Ruiz-Martinez,[33] Z. Rurikova,[50] N. A. Rusakovich,[77] H. L. Russell,[101] J. P. Rutherfoord,[7] N. Ruthmann,[35] Y. F. Ryabov,[134] M. Rybar,[171] G. Rybkin,[128] S. Ryu,[6] A. Ryzhov,[140] G. F. Rzehorz,[51] A. F. Saavedra,[154] G. Sabato,[118] S. Sacerdoti,[30] H. F-W. Sadrozinski,[143] R. Sadykov,[77] F. Safai Tehrani,[70a] P. Saha,[119] M. Sahinsoy,[59a] M. Saimpert,[44] M. Saito,[161] T. Saito,[161] H. Sakamoto,[161] Y. Sakurai,[177] G. Salamanna,[72a,72b] J. E. Salazar Loyola,[144b] D. Salek,[118] P. H. Sales De Bruin,[170] D. Salihagic,[113] A. Salnikov,[150] J. Salt,[172] D. Salvatore,[40b,40a] F. Salvatore,[153] A. Salvucci,[61a,61b,61c] A. Salzburger,[35] D. Sammel,[50] D. Sampsonidis,[160] D. Sampsonidou,[160] J. Sánchez,[172] V. Sanchez Martinez,[172] A. Sanchez Pineda,[64a,64c] H. Sandaker,[130] R. L. Sandbach,[90] C. O. Sander,[44] M. Sandhoff,[180] C. Sandoval,[22] D. P. C. Sankey,[141] M. Sannino,[53b,53a] Y. Sano,[115] A. Sansoni,[49] C. Santoni,[37] H. Santos,[136a] I. Santoyo Castillo,[153] A. Sapronov,[77] J. G. Saraiva,[136a,136d] B. Sarrazin,[24] O. Sasaki,[79] K. Sato,[167] E. Sauvan,[5] G. Savage,[91] P. Savard,[165,d] N. Savic,[113] C. Sawyer,[141] L. Sawyer,[93,u] J. Saxon,[36]

C. Sbarra,[23b] A. Sbrizzi,[23b,23a] T. Scanlon,[92] D. A. Scannicchio,[169] J. Schaarschmidt,[145] P. Schacht,[113] B. M. Schachtner,[112] D. Schaefer,[36] L. Schaefer,[133] R. Schaefer,[44] J. Schaeffer,[97] S. Schaepe,[24] S. Schaetzel,[59b] U. Schäfer,[97] A. C. Schaffer,[128] D. Schaile,[112] R. D. Schamberger,[152] V. A. Schegelsky,[134] D. Scheirich,[139] M. Schernau,[169] C. Schiavi,[53b,53a] S. Schier,[143] L. K. Schildgen,[24] C. Schillo,[50] M. Schioppa,[40b,40a] S. Schlenker,[35] K. R. Schmidt-Sommerfeld,[113] K. Schmieden,[35] C. Schmitt,[97] S. Schmitt,[44] S. Schmitz,[97] U. Schnoor,[50] L. Schoeffel,[142] A. Schoening,[59b] B. D. Schoenrock,[104] E. Schopf,[24] M. Schott,[97] J. F. P. Schouwenberg,[117] J. Schovancova,[35] S. Schramm,[52] N. Schuh,[97] A. Schulte,[97] M. J. Schultens,[24] H-C. Schultz-Coulon,[59a] H. Schulz,[19] M. Schumacher,[50] B. A. Schumm,[143] Ph. Schune,[142] A. Schwartzman,[150] T. A. Schwarz,[103] H. Schweiger,[98] Ph. Schwemling,[142] R. Schwienhorst,[104] A. Sciandra,[24] G. Sciolla,[26] M. Scornajenghi,[40b,40a] F. Scuri,[69a] F. Scutti,[102] J. Searcy,[103] P. Seema,[24] S. C. Seidel,[116] A. Seiden,[143] J. M. Seixas,[78b] G. Sekhniaidze,[67a] K. Sekhon,[103] S. J. Sekula,[41] N. Semprini-Cesari,[23b,23a] S. Senkin,[37] C. Serfon,[130] L. Serin,[128] L. Serkin,[64a,64b] M. Sessa,[72a,72b] R. Seuster,[174] H. Severini,[124] F. Sforza,[168] A. Sfyrla,[52] E. Shabalina,[51] N. W. Shaikh,[43a,43b] L. Y. Shan,[15a] R. Shang,[171] J. T. Shank,[25] M. Shapiro,[18] P. B. Shatalov,[109] K. Shaw,[64a,64b] S. M. Shaw,[98] A. Shcherbakova,[43a,43b] C. Y. Shehu,[153] Y. Shen,[124] N. Sherafati,[33] P. Sherwood,[92] L. Shi,[155,oo] S. Shimizu,[80] C. O. Shimmin,[181] M. Shimojima,[114] I. P. J. Shipsey,[131] S. Shirabe,[85] M. Shiyakova,[77] J. Shlomi,[178] A. Shmeleva,[108] D. Shoaleh Saadi,[107] M. J. Shochet,[36] S. Shojaii,[102] D. R. Shope,[124] S. Shrestha,[122] E. Shulga,[110] M. A. Shupe,[7] P. Sicho,[137] A. M. Sickles,[171] P. E. Sidebo,[151] E. Sideras Haddad,[32c] O. Sidiropoulou,[175] A. Sidoti,[23b,23a] F. Siegert,[46] Dj. Sijacki,[16] J. Silva,[136a,136d] S. B. Silverstein,[43a] V. Simak,[138] L. Simic,[77] S. Simion,[128] E. Simioni,[97] B. Simmons,[92] M. Simon,[97] P. Sinervo,[165] N. B. Sinev,[127] M. Sioli,[23b,23a] G. Siragusa,[175] I. Siral,[103] S.Yu. Sivoklokov,[111] J. Sjölin,[43a,43b] M. B. Skinner,[87] P. Skubic,[124] M. Slater,[21] T. Slavicek,[138] M. Slawinska,[82] K. Sliwa,[168] R. Slovak,[139] V. Smakhtin,[178] B. H. Smart,[5] J. Smiesko,[28a] N. Smirnov,[110] S.Yu. Smirnov,[110] Y. Smirnov,[110] L. N. Smirnova,[111] O. Smirnova,[94] J. W. Smith,[51] M. N. K. Smith,[38] R. W. Smith,[38] M. Smizanska,[87] K. Smolek,[138] A. A. Snesarev,[108] I. M. Snyder,[127] S. Snyder,[29] R. Sobie,[174,l] F. Socher,[46] A. Soffer,[159] A. Søgaard,[48] D. A. Soh,[155] G. Sokhrannyi,[89] C. A. Solans Sanchez,[35] M. Solar,[138] E. Yu. Soldatov,[110] U. Soldevila,[172] A. A. Solodkov,[140] A. Soloshenko,[77] O. V. Solovyanov,[140] V. Solovyev,[134] P. Sommer,[50] H. Son,[168] A. Sopczak,[138] D. Sosa,[59b] C. L. Sotiropoulou,[69a,69b] S. Sottocornola,[68a,68b] R. Soualah,[64a,64c,pp] A. M. Soukharev,[120b,120a] D. South,[44] B. C. Sowden,[91] S. Spagnolo,[65a,65b] M. Spalla,[69a,69b] M. Spangenberg,[176] F. Spanò,[91] D. Sperlich,[19] F. Spettel,[113] T. M. Spieker,[59a] R. Spighi,[23b] G. Spigo,[35] L. A. Spiller,[102] M. Spousta,[139] R. D. St. Denis,[55,a] A. Stabile,[66a,66b] R. Stamen,[59a] S. Stamm,[19] E. Stanecka,[82] R. W. Stanek,[6] C. Stanescu,[72a] M. M. Stanitzki,[44] B. Stapf,[118] S. Stapnes,[130] E. A. Starchenko,[140] G. H. Stark,[36] J. Stark,[56] S.H. Stark,[39] P. Staroba,[137] P. Starovoitov,[59a] S. Stärz,[35] R. Staszewski,[82] M. Stegler,[44] P. Steinberg,[29] B. Stelzer,[149] H. J. Stelzer,[35] O. Stelzer-Chilton,[166a] H. Stenzel,[54] G. A. Stewart,[55] M. C. Stockton,[127] M. Stoebe,[101] G. Stoicea,[27b] P. Stolte,[51] S. Stonjek,[113] A. R. Stradling,[8] A. Straessner,[46] M. E. Stramaglia,[20] J. Strandberg,[151] S. Strandberg,[43a,43b] M. Strauss,[124] P. Strizenec,[28b] R. Ströhmer,[175] D. M. Strom,[127] R. Stroynowski,[41] A. Strubig,[48] S. A. Stucci,[29] B. Stugu,[17] N. A. Styles,[44] D. Su,[150] J. Su,[135] R. Subramaniam,[93] S. Suchek,[59a] Y. Sugaya,[129] M. Suk,[138] V. V. Sulin,[108] D. M. S. Sultan,[73a,73b] S. Sultansoy,[4c] T. Sumida,[83] S. Sun,[57] X. Sun,[3] K. Suruliz,[153] C. J. E. Suster,[154] M. R. Sutton,[153] S. Suzuki,[79] M. Svatos,[137] M. Swiatlowski,[36] S. P. Swift,[2] I. Sykora,[28a] T. Sykora,[139] D. Ta,[50] K. Tackmann,[44,qq] J. Taenzer,[159] A. Taffard,[169] R. Tafirout,[166a] E. Tahirovic,[90] N. Taiblum,[159] H. Takai,[29] R. Takashima,[84] E. H. Takasugi,[113] K. Takeda,[80] T. Takeshita,[147] Y. Takubo,[79] M. Talby,[99] A. A. Talyshev,[120b,120a] M. C. Tamsett,[93] J. Tanaka,[161] M. Tanaka,[163] R. Tanaka,[128] S. Tanaka,[79] R. Tanioka,[80] B. B. Tannenwald,[122] S. Tapia Araya,[144b] S. Tapprogge,[97] S. Tarem,[158] G. F. Tartarelli,[66a] P. Tas,[139] M. Tasevsky,[137] T. Tashiro,[83] E. Tassi,[40b,40a] A. Tavares Delgado,[136a,136b] Y. Tayalati,[34e] A. C. Taylor,[116] A. J. Taylor,[48] G. N. Taylor,[102] P. T. E. Taylor,[102] W. Taylor,[166b] P. Teixeira-Dias,[91] D. Temple,[149] H. Ten Kate,[35] P. K. Teng,[155] J. J. Teoh,[129] F. Tepel,[180] S. Terada,[79] K. Terashi,[161] J. Terron,[96] S. Terzo,[14] M. Testa,[49] R. J. Teuscher,[165,l] T. Theveneaux-Pelzer,[99] F. Thiele,[39] J. P. Thomas,[21] J. Thomas-Wilsker,[91] A. S. Thompson,[55] P. D. Thompson,[21] L. A. Thomsen,[181] E. Thomson,[133] Y. Tian,[38] M. J. Tibbetts,[18] R. E. Ticse Torres,[99] V. O. Tikhomirov,[108,rr] Yu.A. Tikhonov,[120b,120a] S. Timoshenko,[110] P. Tipton,[181] S. Tisserant,[99] K. Todome,[163] S. Todorova-Nova,[5] S. Todt,[46] J. Tojo,[85] S. Tokár,[28a] K. Tokushuku,[79] E. Tolley,[122] L. Tomlinson,[98] M. Tomoto,[115] L. Tompkins,[150,dd] K. Toms,[116] B. Tong,[57] P. Tornambe,[50] E. Torrence,[127] H. Torres,[46] E. Torró Pastor,[145] J. Toth,[99,ss] F. Touchard,[99] D. R. Tovey,[146] C. J. Treado,[121] T. Trefzger,[175] F. Tresoldi,[153] A. Tricoli,[29] I. M. Trigger,[166a] S. Trincaz-Duvoid,[132] M. F. Tripiana,[14] W. Trischuk,[165] B. Trocmé,[56] A. Trofymov,[44] C. Troncon,[66a] M. Trottier-McDonald,[18] M. Trovatelli,[174] L. Truong,[32b] M. Trzebinski,[82] A. Trzupek,[82] K. W. Tsang,[61a] J.C-L. Tseng,[131] P. V. Tsiareshka,[105] G. Tsipolitis,[10] N. Tsirintanis,[9] S. Tsiskaridze,[14] V. Tsiskaridze,[50] E. G. Tskhadadze,[157a]

I. I. Tsukerman,[109] V. Tsulaia,[18] S. Tsuno,[79] D. Tsybychev,[152] Y. Tu,[61b] A. Tudorache,[27b] V. Tudorache,[27b] T. T. Tulbure,[27a] A. N. Tuna,[57] S. Turchikhin,[77] D. Turgeman,[178] I. Turk Cakir,[4b,tt] R. Turra,[66a] P. M. Tuts,[38] G. Ucchielli,[23b,23a] I. Ueda,[79] M. Ughetto,[43a,43b] F. Ukegawa,[167] G. Unal,[35] A. Undrus,[29] G. Unel,[169] F. C. Ungaro,[102] Y. Unno,[79] K. Uno,[161] C. Unverdorben,[112] J. Urban,[28b] P. Urquijo,[102] P. Urrejola,[97] G. Usai,[8] J. Usui,[79] L. Vacavant,[99] V. Vacek,[138] B. Vachon,[101] K. O. H. Vadla,[130] A. Vaidya,[92] C. Valderanis,[112] E. Valdes Santurio,[43a,43b] M. Valente,[52] S. Valentinetti,[23b,23a] A. Valero,[172] L. Valéry,[14] S. Valkar,[139] A. Vallier,[5] J. A. Valls Ferrer,[172] W. Van Den Wollenberg,[118] H. Van der Graaf,[118] P. Van Gemmeren,[6] J. Van Nieuwkoop,[149] I. Van Vulpen,[118] M. C. van Woerden,[118] M. Vanadia,[71a,71b] W. Vandelli,[35] A. Vaniachine,[164] P. Vankov,[118] G. Vardanyan,[182] R. Vari,[70a] E. W. Varnes,[7] C. Varni,[53b,53a] T. Varol,[41] D. Varouchas,[128] A. Vartapetian,[8] K. E. Varvell,[154] G. A. Vasquez,[144b] J. G. Vasquez,[181] F. Vazeille,[37] D. Vazquez Furelos,[14] T. Vazquez Schroeder,[101] J. Veatch,[51] V. Veeraraghavan,[7] L. M. Veloce,[165] F. Veloso,[136a,136c] S. Veneziano,[70a] A. Ventura,[65a,65b] M. Venturi,[174] N. Venturi,[35] A. Venturini,[26] V. Vercesi,[68a] M. Verducci,[72a,72b] W. Verkerke,[118] A. T. Vermeulen,[118] J. C. Vermeulen,[118] M. C. Vetterli,[149,d] N. Viaux Maira,[144b] O. Viazlo,[94] I. Vichou,[171,a] T. Vickey,[146] O. E. Vickey Boeriu,[146] G. H. A. Viehhauser,[131] S. Viel,[18] L. Vigani,[131] M. Villa,[23b,23a] M. Villaplana Perez,[66a,66b] E. Vilucchi,[49] M. G. Vincter,[33] V. B. Vinogradov,[77] A. Vishwakarma,[44] C. Vittori,[23b,23a] I. Vivarelli,[153] S. Vlachos,[10] M. Vogel,[180] P. Vokac,[138] G. Volpi,[14] H. von der Schmitt,[113] E. Von Toerne,[24] V. Vorobel,[139] K. Vorobev,[110] M. Vos,[172] R. Voss,[35] J. H. Vossebeld,[88] N. Vranjes,[16] M. Vranjes Milosavljevic,[16] V. Vrba,[138] M. Vreeswijk,[118] T. Šfiligoj,[89] R. Vuillermet,[35] I. Vukotic,[36] T. Ženiš,[28a] L. Živković,[16] P. Wagner,[24] W. Wagner,[180] J. Wagner-Kuhr,[112] H. Wahlberg,[86] S. Wahrmund,[46] J. Walder,[87] R. Walker,[112] W. Walkowiak,[148] V. Wallangen,[43a,43b] C. Wang,[15c] C. Wang,[58b,p] F. Wang,[179] H. Wang,[18] H. Wang,[3] J. Wang,[154] J. Wang,[44] Q. Wang,[124] R.-J. Wang,[132] R. Wang,[6] S. M. Wang,[155] T. Wang,[38] W. Wang,[155,uu] W. X. Wang,[58a,vv] Z. Wang,[58c] C. Wanotayaroj,[44] A. Warburton,[101] C. P. Ward,[31] D. R. Wardrope,[92] A. Washbrook,[48] P. M. Watkins,[21] A. T. Watson,[21] M. F. Watson,[21] G. Watts,[145] S. Watts,[98] B. M. Waugh,[92] A. F. Webb,[11] S. Webb,[97] M. S. Weber,[20] S. A. Weber,[33] S. M. Weber,[59a] S. W. Weber,[175] J. S. Webster,[6] A. R. Weidberg,[131] B. Weinert,[63] J. Weingarten,[51] M. Weirich,[97] C. Weiser,[50] H. Weits,[118] P. S. Wells,[35] T. Wenaus,[29] T. Wengler,[35] S. Wenig,[35] N. Wermes,[24] M. D. Werner,[76] P. Werner,[35] M. Wessels,[59a] T. D. Weston,[20] K. Whalen,[127] N. L. Whallon,[145] A. M. Wharton,[87] A. S. White,[103] A. White,[8] M. J. White,[1] R. White,[144b] D. Whiteson,[169] B. W. Whitmore,[87] F. J. Wickens,[141] W. Wiedenmann,[179] M. Wielers,[141] C. Wiglesworth,[39] L. A. M. Wiik-Fuchs,[50] A. Wildauer,[113] F. Wilk,[98] H. G. Wilkens,[35] H. H. Williams,[133] S. Williams,[31] C. Willis,[104] S. Willocq,[100] J. A. Wilson,[21] I. Wingerter-Seez,[5] E. Winkels,[153] F. Winklmeier,[127] O. J. Winston,[153] B. T. Winter,[24] M. Wittgen,[150] M. Wobisch,[93] T. M. H. Wolf,[118] R. Wolff,[99] M. W. Wolter,[82] H. Wolters,[136a,136c] V. W. S. Wong,[173] N. L. Woods,[143] S. D. Worm,[21] B. K. Wosiek,[82] J. Wotschack,[35] K. W. Woźniak,[82] M. Wu,[36] S. L. Wu,[179] X. Wu,[52] Y. Wu,[103] T. R. Wyatt,[98] B. M. Wynne,[48] S. Xella,[39] Z. Xi,[103] L. Xia,[15b] D. Xu,[15a] L. Xu,[29] T. Xu,[142] B. Yabsley,[154] S. Yacoob,[32a] D. Yamaguchi,[163] Y. Yamaguchi,[163] A. Yamamoto,[79] S. Yamamoto,[161] T. Yamanaka,[161] F. Yamane,[80] M. Yamatani,[161] Y. Yamazaki,[80] Z. Yan,[25] H. J. Yang,[58c,58d] H. T. Yang,[18] Y. Yang,[155] Z. Yang,[17] W-M. Yao,[18] Y. C. Yap,[44] Y. Yasu,[79] E. Yatsenko,[5] K. H. Yau Wong,[24] J. Ye,[41] S. Ye,[29] I. Yeletskikh,[77] E. Yigitbasi,[25] E. Yildirim,[97] K. Yorita,[177] K. Yoshihara,[133] C. J. S. Young,[35] C. Young,[150] J. Yu,[8] J. Yu,[76] S. P. Y. Yuen,[24] I. Yusuff,[31,ww] B. Zabinski,[82] G. Zacharis,[10] R. Zaidan,[14] A. M. Zaitsev,[140,ll] N. Zakharchuk,[44] J. Zalieckas,[17] A. Zaman,[152] S. Zambito,[57] D. Zanzi,[102] C. Zeitnitz,[180] G. Zemaityte,[131] A. Zemla,[81a] J. C. Zeng,[171] Q. Zeng,[150] O. Zenin,[140] D. Zerwas,[128] D. F. Zhang,[58b] D. Zhang,[103] F. Zhang,[179] G. Zhang,[58a,vv] H. Zhang,[128] J. Zhang,[6] L. Zhang,[50] L. Zhang,[58a] M. Zhang,[171] P. Zhang,[15c] R. Zhang,[58a,p] R. Zhang,[24] X. Zhang,[58b] Y. Zhang,[15d] Z. Zhang,[128] X. Zhao,[41] Y. Zhao,[58b,128,xx] Z. Zhao,[58a] A. Zhemchugov,[77] B. Zhou,[103] C. Zhou,[179] L. Zhou,[41] M. S. Zhou,[15d] M. Zhou,[152] N. Zhou,[15b] Y. Zhou,[7] C. G. Zhu,[58b] H. Zhu,[15a] J. Zhu,[103] Y. Zhu,[58a] X. Zhuang,[15a] K. Zhukov,[108] A. Zibell,[175] D. Zieminska,[63] N. I. Zimine,[77] C. Zimmermann,[97] S. Zimmermann,[50] Z. Zinonos,[113] M. Zinser,[97] M. Ziolkowski,[148] G. Zobernig,[179] A. Zoccoli,[23b,23a] R. Zou,[36] M. Zur Nedden,[19] and L. Zwalinski[35]

(ATLAS Collaboration)

[1]*Department of Physics, University of Adelaide, Adelaide, Australia*
[2]*Physics Department, SUNY Albany, Albany, New York, USA*
[3]*Department of Physics, University of Alberta, Edmonton, Alberta, Canada*
[4a]*Department of Physics, Ankara University, Ankara, Turkey*

[4b]Istanbul Aydin University, Istanbul, Turkey
[4c]Division of Physics, TOBB University of Economics and Technology, Ankara, Turkey
[5]LAPP, Université Grenoble Alpes, Université Savoie Mont Blanc, CNRS/IN2P3, Annecy, France
[6]High Energy Physics Division, Argonne National Laboratory, Argonne, Illinois, USA
[7]Department of Physics, University of Arizona, Tucson, Arizona, USA
[8]Department of Physics, University of Texas at Arlington, Arlington, Texas, USA
[9]Physics Department, National and Kapodistrian University of Athens, Athens, Greece
[10]Physics Department, National Technical University of Athens, Zografou, Greece
[11]Department of Physics, University of Texas at Austin, Austin, Texas, USA
[12a]Bahcesehir University, Faculty of Engineering and Natural Sciences, Istanbul, Turkey
[12b]Istanbul Bilgi University, Faculty of Engineering and Natural Sciences, Istanbul, Turkey
[12c]Department of Physics, Bogazici University, Istanbul, Turkey
[12d]Department of Physics Engineering, Gaziantep University, Gaziantep, Turkey
[13]Institute of Physics, Azerbaijan Academy of Sciences, Baku, Azerbaijan
[14]Institut de Física d'Altes Energies (IFAE), Barcelona Institute of Science and Technology, Barcelona, Spain
[15a]Institute of High Energy Physics, Chinese Academy of Sciences, Beijing, China
[15b]Physics Department, Tsinghua University, Beijing, China
[15c]Department of Physics, Nanjing University, Nanjing, China
[15d]University of Chinese Academy of Science (UCAS), Beijing, China
[16]Institute of Physics, University of Belgrade, Belgrade, Serbia
[17]Department for Physics and Technology, University of Bergen, Bergen, Norway
[18]Physics Division, Lawrence Berkeley National Laboratory and University of California, Berkeley, California, USA
[19]Institut für Physik, Humboldt Universität zu Berlin, Berlin, Germany
[20]Albert Einstein Center for Fundamental Physics and Laboratory for High Energy Physics, University of Bern, Bern, Switzerland
[21]School of Physics and Astronomy, University of Birmingham, Birmingham, United Kingdom
[22]Centro de Investigaciónes, Universidad Antonio Nariño, Bogota, Colombia
[23a]Dipartimento di Fisica e Astronomia, Università di Bologna, Bologna, Italy
[23b]INFN Sezione di Bologna, Italy
[24]Physikalisches Institut, Universität Bonn, Bonn, Germany
[25]Department of Physics, Boston University, Boston, Massachusetts, USA
[26]Department of Physics, Brandeis University, Waltham, Massachusetts, USA
[27a]Transilvania University of Brasov, Brasov, Romania
[27b]Horia Hulubei National Institute of Physics and Nuclear Engineering, Bucharest, Romania
[27c]Department of Physics, Alexandru Ioan Cuza University of Iasi, Iasi, Romania
[27d]National Institute for Research and Development of Isotopic and Molecular Technologies, Physics Department, Cluj-Napoca, Romania
[27e]University Politehnica Bucharest, Bucharest, Romania
[27f]West University in Timisoara, Timisoara, Romania
[28a]Faculty of Mathematics, Physics and Informatics, Comenius University, Bratislava, Slovak Republic
[28b]Department of Subnuclear Physics, Institute of Experimental Physics of the Slovak Academy of Sciences, Kosice, Slovak Republic
[29]Physics Department, Brookhaven National Laboratory, Upton, New York, USA
[30]Departamento de Física, Universidad de Buenos Aires, Buenos Aires, Argentina
[31]Cavendish Laboratory, University of Cambridge, Cambridge, United Kingdom
[32a]Department of Physics, University of Cape Town, Cape Town, South Africa
[32b]Department of Mechanical Engineering Science, University of Johannesburg, Johannesburg, South Africa
[32c]School of Physics, University of the Witwatersrand, Johannesburg, South Africa
[33]Department of Physics, Carleton University, Ottawa, Ontario, Canada
[34a]Faculté des Sciences Ain Chock, Réseau Universitaire de Physique des Hautes Energies - Université Hassan II, Casablanca, Morocco
[34b]Centre National de l'Energie des Sciences Techniques Nucleaires (CNESTEN), Rabat, Morocco
[34c]Faculté des Sciences Semlalia, Université Cadi Ayyad, LPHEA-Marrakech, Morocco
[34d]Faculté des Sciences, Université Mohamed Premier and LPTPM, Oujda, Morocco
[34e]Faculté des sciences, Université Mohammed V, Rabat, Morocco
[35]CERN, Geneva, Switzerland
[36]Enrico Fermi Institute, University of Chicago, Chicago, Illinois, USA

[37]LPC, Université Clermont Auvergne, CNRS/IN2P3, Clermont-Ferrand, France
[38]Nevis Laboratory, Columbia University, Irvington, New York, USA
[39]Niels Bohr Institute, University of Copenhagen, Copenhagen, Denmark
[40a]Dipartimento di Fisica, Università della Calabria, Rende, Italy
[40b]INFN Gruppo Collegato di Cosenza, Laboratori Nazionali di Frascati, Italy
[41]Physics Department, Southern Methodist University, Dallas, Texas, USA
[42]Physics Department, University of Texas at Dallas, Richardson, Texas, USA
[43a]Department of Physics, Stockholm University, Sweden
[43b]Oskar Klein Centre, Stockholm, Sweden
[44]Deutsches Elektronen-Synchrotron DESY, Hamburg and Zeuthen, Germany
[45]Lehrstuhl für Experimentelle Physik IV, Technische Universität Dortmund, Dortmund, Germany
[46]Institut für Kern- und Teilchenphysik, Technische Universität Dresden, Dresden, Germany
[47]Department of Physics, Duke University, Durham, North Carolina, USA
[48]SUPA - School of Physics and Astronomy, University of Edinburgh, Edinburgh, United Kingdom
[49]INFN e Laboratori Nazionali di Frascati, Frascati, Italy
[50]Physikalisches Institut, Albert-Ludwigs-Universität Freiburg, Freiburg, Germany
[51]II. Physikalisches Institut, Georg-August-Universität Göttingen, Göttingen, Germany
[52]Département de Physique Nucléaire et Corpusculaire, Université de Genève, Genève, Switzerland
[53a]Dipartimento di Fisica, Università di Genova, Genova, Italy
[53b]INFN Sezione di Genova, Italy
[54]II. Physikalisches Institut, Justus-Liebig-Universität Giessen, Giessen, Germany
[55]SUPA - School of Physics and Astronomy, University of Glasgow, Glasgow, United Kingdom
[56]LPSC, Université Grenoble Alpes, CNRS/IN2P3, Grenoble INP, Grenoble, France
[57]Laboratory for Particle Physics and Cosmology, Harvard University, Cambridge, Massachusetts, USA
[58a]Department of Modern Physics and State Key Laboratory of Particle Detection and Electronics, University of Science and Technology of China, Hefei, China
[58b]Institute of Frontier and Interdisciplinary Science and Key Laboratory of Particle Physics and Particle Irradiation (MOE), Shandong University, Qingdao, China
[58c]School of Physics and Astronomy, Shanghai Jiao Tong University, KLPPAC-MoE, SKLPPC, Shanghai, China
[58d]Tsung-Dao Lee Institute, Shanghai, China
[59a]Kirchhoff-Institut für Physik, Ruprecht-Karls-Universität Heidelberg, Heidelberg, Germany
[59b]Physikalisches Institut, Ruprecht-Karls-Universität Heidelberg, Heidelberg, Germany
[60]Faculty of Applied Information Science, Hiroshima Institute of Technology, Hiroshima, Japan
[61a]Department of Physics, Chinese University of Hong Kong, Shatin, N.T., Hong Kong, China
[61b]Department of Physics, University of Hong Kong, Hong Kong, China
[61c]Department of Physics and Institute for Advanced Study, Hong Kong University of Science and Technology, Clear Water Bay, Kowloon, Hong Kong, China
[62]Department of Physics, National Tsing Hua University, Hsinchu, Taiwan
[63]Department of Physics, Indiana University, Bloomington, Indiana, USA
[64a]INFN Gruppo Collegato di Udine, Sezione di Trieste, Udine, Italy
[64b]ICTP, Trieste, Italy
[64c]Dipartimento di Chimica, Fisica e Ambiente, Università di Udine, Udine, Italy
[65a]INFN Sezione di Lecce, Italy
[65b]Dipartimento di Matematica e Fisica, Università del Salento, Lecce, Italy
[66a]INFN Sezione di Milano, Italy
[66b]Dipartimento di Fisica, Università di Milano, Milano, Italy
[67a]INFN Sezione di Napoli, Italy
[67b]Dipartimento di Fisica, Università di Napoli, Napoli, Italy
[68a]INFN Sezione di Pavia, Italy
[68b]Dipartimento di Fisica, Università di Pavia, Pavia, Italy
[69a]INFN Sezione di Pisa, Italy
[69b]Dipartimento di Fisica E. Fermi, Università di Pisa, Pisa, Italy
[70a]INFN Sezione di Roma, Italy
[70b]Dipartimento di Fisica, Sapienza Università di Roma, Roma, Italy
[71a]INFN Sezione di Roma Tor Vergata, Italy
[71b]Dipartimento di Fisica, Università di Roma Tor Vergata, Roma, Italy
[72a]INFN Sezione di Roma Tre, Italy
[72b]Dipartimento di Matematica e Fisica, Università Roma Tre, Roma, Italy
[73a]INFN-TIFPA, Italy

[73b]Università degli Studi di Trento, Trento, Italy
[74]Institut für Astro- und Teilchenphysik, Leopold-Franzens-Universität, Innsbruck, Austria
[75]University of Iowa, Iowa City, Iowa, USA
[76]Department of Physics and Astronomy, Iowa State University, Ames, Iowa, USA
[77]Joint Institute for Nuclear Research, Dubna, Russia
[78a]Departamento de Engenharia Elétrica, Universidade Federal de Juiz de Fora (UFJF), Juiz de Fora, Brazil
[78b]Universidade Federal do Rio De Janeiro COPPE/EE/IF, Rio de Janeiro, Brazil
[78c]Universidade Federal de São João del Rei (UFSJ), São João del Rei, Brazil
[78d]Instituto de Física, Universidade de São Paulo, São Paulo, Brazil
[79]KEK, High Energy Accelerator Research Organization, Tsukuba, Japan
[80]Graduate School of Science, Kobe University, Kobe, Japan
[81a]AGH University of Science and Technology, Faculty of Physics and Applied Computer Science, Krakow, Poland
[81b]Marian Smoluchowski Institute of Physics, Jagiellonian University, Krakow, Poland
[82]Institute of Nuclear Physics Polish Academy of Sciences, Krakow, Poland
[83]Faculty of Science, Kyoto University, Kyoto, Japan
[84]Kyoto University of Education, Kyoto, Japan
[85]Research Center for Advanced Particle Physics and Department of Physics, Kyushu University, Fukuoka, Japan
[86]Instituto de Física La Plata, Universidad Nacional de La Plata and CONICET, La Plata, Argentina
[87]Physics Department, Lancaster University, Lancaster, United Kingdom
[88]Oliver Lodge Laboratory, University of Liverpool, Liverpool, United Kingdom
[89]Department of Experimental Particle Physics, Jožef Stefan Institute and Department of Physics, University of Ljubljana, Ljubljana, Slovenia
[90]School of Physics and Astronomy, Queen Mary University of London, London, United Kingdom
[91]Department of Physics, Royal Holloway University of London, Egham, United Kingdom
[92]Department of Physics and Astronomy, University College London, London, United Kingdom
[93]Louisiana Tech University, Ruston, Louisiana, USA
[94]Fysiska institutionen, Lunds universitet, Lund, Sweden
[95]Centre de Calcul de l'Institut National de Physique Nucléaire et de Physique des Particules (IN2P3), Villeurbanne, France
[96]Departamento de Física Teorica C-15 and CIAFF, Universidad Autónoma de Madrid, Madrid, Spain
[97]Institut für Physik, Universität Mainz, Mainz, Germany
[98]School of Physics and Astronomy, University of Manchester, Manchester, United Kingdom
[99]CPPM, Aix-Marseille Université, CNRS/IN2P3, Marseille, France
[100]Department of Physics, University of Massachusetts, Amherst, Massachusetts, USA
[101]Department of Physics, McGill University, Montreal, Quebec, Canada
[102]School of Physics, University of Melbourne, Victoria, Australia
[103]Department of Physics, University of Michigan, Ann Arbor, Michigan, USA
[104]Department of Physics and Astronomy, Michigan State University, East Lansing, Michigan, USA
[105]B.I. Stepanov Institute of Physics, National Academy of Sciences of Belarus, Minsk, Belarus
[106]Research Institute for Nuclear Problems of Byelorussian State University, Minsk, Belarus
[107]Group of Particle Physics, University of Montreal, Montreal, Quebec, Canada
[108]P.N. Lebedev Physical Institute of the Russian Academy of Sciences, Moscow, Russia
[109]Institute for Theoretical and Experimental Physics (ITEP), Moscow, Russia
[110]National Research Nuclear University MEPhI, Moscow, Russia
[111]D.V. Skobeltsyn Institute of Nuclear Physics, M.V. Lomonosov Moscow State University, Moscow, Russia
[112]Fakultät für Physik, Ludwig-Maximilians-Universität München, München, Germany
[113]Max-Planck-Institut für Physik (Werner-Heisenberg-Institut), München, Germany
[114]Nagasaki Institute of Applied Science, Nagasaki, Japan
[115]Graduate School of Science and Kobayashi-Maskawa Institute, Nagoya University, Nagoya, Japan
[116]Department of Physics and Astronomy, University of New Mexico, Albuquerque, New Mexico, USA
[117]Institute for Mathematics, Astrophysics and Particle Physics, Radboud University Nijmegen/Nikhef, Nijmegen, Netherlands
[118]Nikhef National Institute for Subatomic Physics and University of Amsterdam, Amsterdam, Netherlands
[119]Department of Physics, Northern Illinois University, DeKalb, Illinois, USA
[120a]Budker Institute of Nuclear Physics, SB RAS, Novosibirsk, Russia
[120b]Novosibirsk State University Novosibirsk, Russia

[121]Department of Physics, New York University, New York, New York, USA
[122]The Ohio State University, Columbus, Ohio, USA
[123]Faculty of Science, Okayama University, Okayama, Japan
[124]Homer L. Dodge Department of Physics and Astronomy, University of Oklahoma, Norman, Oklahoma, USA
[125]Department of Physics, Oklahoma State University, Stillwater, Oklahoma, USA
[126]Palacký University, RCPTM, Joint Laboratory of Optics, Olomouc, Czech Republic
[127]Center for High Energy Physics, University of Oregon, Eugene, Oregon, USA
[128]LAL, Université Paris-Sud, CNRS/IN2P3, Université Paris-Saclay, Orsay, France
[129]Graduate School of Science, Osaka University, Osaka, Japan
[130]Department of Physics, University of Oslo, Oslo, Norway
[131]Department of Physics, Oxford University, Oxford, United Kingdom
[132]LPNHE, Sorbonne Université, Paris Diderot Sorbonne Paris Cité, CNRS/IN2P3, Paris, France
[133]Department of Physics, University of Pennsylvania, Philadelphia, Pennsylvania, USA
[134]Konstantinov Nuclear Physics Institute of National Research Centre “Kurchatov Institute”, PNPI, St. Petersburg, Russia
[135]Department of Physics and Astronomy, University of Pittsburgh, Pittsburgh, Pennsylvania, USA
[136a]Laboratório de Instrumentação e Física Experimental de Partículas - LIP, Portugal
[136b]Departamento de Física, Faculdade de Ciências, Universidade de Lisboa, Lisboa, Portugal
[136c]Departamento de Física, Universidade de Coimbra, Coimbra, Portugal
[136d]Centro de Física Nuclear da Universidade de Lisboa, Lisboa, Portugal
[136e]Departamento de Física, Universidade do Minho, Braga, Portugal
[136f]Departamento de Física Teorica y del Cosmos, Universidad de Granada, Granada (Spain), Spain
[136g]Dep Física and CEFITEC of Faculdade de Ciências e Tecnologia, Universidade Nova de Lisboa, Caparica, Portugal
[137]Institute of Physics, Academy of Sciences of the Czech Republic, Prague, Czech Republic
[138]Czech Technical University in Prague, Prague, Czech Republic
[139]Charles University, Faculty of Mathematics and Physics, Prague, Czech Republic
[140]State Research Center Institute for High Energy Physics, NRC KI, Protvino, Russia
[141]Particle Physics Department, Rutherford Appleton Laboratory, Didcot, United Kingdom
[142]IRFU, CEA, Université Paris-Saclay, Gif-sur-Yvette, France
[143]Santa Cruz Institute for Particle Physics, University of California Santa Cruz, Santa Cruz, California, USA
[144a]Departamento de Física, Pontificia Universidad Católica de Chile, Santiago, Chile
[144b]Departamento de Física, Universidad Técnica Federico Santa María, Valparaíso, Chile
[145]Department of Physics, University of Washington, Seattle, Washington, USA
[146]Department of Physics and Astronomy, University of Sheffield, Sheffield, United Kingdom
[147]Department of Physics, Shinshu University, Nagano, Japan
[148]Department Physik, Universität Siegen, Siegen, Germany
[149]Department of Physics, Simon Fraser University, Burnaby, British Columbia, Canada
[150]SLAC National Accelerator Laboratory, Stanford, California, USA
[151]Physics Department, Royal Institute of Technology, Stockholm, Sweden
[152]Departments of Physics and Astronomy, Stony Brook University, Stony Brook, New York, USA
[153]Department of Physics and Astronomy, University of Sussex, Brighton, United Kingdom
[154]School of Physics, University of Sydney, Sydney, Australia
[155]Institute of Physics, Academia Sinica, Taipei, Taiwan
[156]Academia Sinica Grid Computing, Institute of Physics, Academia Sinica, Taipei, Taiwan
[157a]E. Andronikashvili Institute of Physics, Iv. Javakhishvili Tbilisi State University, Tbilisi, Georgia
[157b]High Energy Physics Institute, Tbilisi State University, Tbilisi, Georgia
[158]Department of Physics, Technion, Israel Institute of Technology, Haifa, Israel
[159]Raymond and Beverly Sackler School of Physics and Astronomy, Tel Aviv University, Tel Aviv, Israel
[160]Department of Physics, Aristotle University of Thessaloniki, Thessaloniki, Greece
[161]International Center for Elementary Particle Physics and Department of Physics, University of Tokyo, Tokyo, Japan
[162]Graduate School of Science and Technology, Tokyo Metropolitan University, Tokyo, Japan
[163]Department of Physics, Tokyo Institute of Technology, Tokyo, Japan
[164]Tomsk State University, Tomsk, Russia
[165]Department of Physics, University of Toronto, Toronto, Ontario, Canada
[166a]TRIUMF, Vancouver, British Columbia, Canada
[166b]Department of Physics and Astronomy, York University, Toronto, Ontario, Canada

[167]Division of Physics and Tomonaga Center for the History of the Universe, Faculty of Pure and Applied Sciences, University of Tsukuba, Tsukuba, Japan
[168]Department of Physics and Astronomy, Tufts University, Medford, Massachusetts, USA
[169]Department of Physics and Astronomy, University of California Irvine, Irvine, California, USA
[170]Department of Physics and Astronomy, University of Uppsala, Uppsala, Sweden
[171]Department of Physics, University of Illinois, Urbana, Illinois, USA
[172]Instituto de Física Corpuscular (IFIC), Centro Mixto Universidad de Valencia - CSIC, Valencia, Spain
[173]Department of Physics, University of British Columbia, Vancouver, British Columbia, Canada
[174]Department of Physics and Astronomy, University of Victoria, Victoria, British Columbia, Canada
[175]Fakultät für Physik und Astronomie, Julius-Maximilians-Universität Würzburg, Würzburg, Germany
[176]Department of Physics, University of Warwick, Coventry, United Kingdom
[177]Waseda University, Tokyo, Japan
[178]Department of Particle Physics, Weizmann Institute of Science, Rehovot, Israel
[179]Department of Physics, University of Wisconsin, Madison, Wisconsin, USA
[180]Fakultät für Mathematik und Naturwissenschaften, Fachgruppe Physik, Bergische Universität Wuppertal, Wuppertal, Germany
[181]Department of Physics, Yale University, New Haven, Connecticut, USA
[182]Yerevan Physics Institute, Yerevan, Armenia

[a]Deceased.
[b]Also at Department of Physics, King's College London, London, United Kingdom.
[c]Also at Institute of Physics, Azerbaijan Academy of Sciences, Baku, Azerbaijan.
[d]Also at TRIUMF, Vancouver, British Columbia, Canada.
[e]Also at Department of Physics and Astronomy, University of Louisville, Louisville, Kentucky, USA.
[f]Also at Department of Physics, California State University, Fresno, California, USA.
[g]Also at Department of Physics, University of Fribourg, Fribourg, Switzerland.
[h]Also at Departament de Fisica de la Universitat Autonoma de Barcelona, Barcelona, Spain.
[i]Also at Tomsk State University, Tomsk, and Moscow Institute of Physics and Technology State University, Dolgoprudny, Russia.
[j]Also at The Collaborative Innovation Center of Quantum Matter (CICQM), Beijing, China.
[k]Also at Universita di Napoli Parthenope, Napoli, Italy.
[l]Also at Institute of Particle Physics (IPP), Canada.
[m]Also at II. Physikalisches Institut, Georg-August-Universität Göttingen, Göttingen, Germany.
[n]Also at Dipartimento di Fisica E. Fermi, Università di Pisa, Pisa, Italy.
[o]Also at Horia Hulubei National Institute of Physics and Nuclear Engineering, Bucharest, Romania.
[p]Also at CPPM, Aix-Marseille Université, CNRS/IN2P3, Marseille, France.
[q]Also at Department of Physics, St. Petersburg State Polytechnical University, St. Petersburg, Russia.
[r]Also at Borough of Manhattan Community College, City University of New York, New York, USA.
[s]Also at Department of Financial and Management Engineering, University of the Aegean, Chios, Greece.
[t]Also at Centre for High Performance Computing, CSIR Campus, Rosebank, Cape Town, South Africa.
[u]Also at Louisiana Tech University, Ruston, Louisiana, USA.
[v]Also at Institucio Catalana de Recerca i Estudis Avancats, ICREA, Barcelona, Spain.
[w]Also at Department of Physics, University of Michigan, Ann Arbor, Michigan, USA.
[x]Also at Graduate School of Science, Osaka University, Osaka, Japan.
[y]Also at Physikalisches Institut, Albert-Ludwigs-Universität Freiburg, Freiburg, Germany.
[z]Also at Institute for Mathematics, Astrophysics and Particle Physics, Radboud University Nijmegen/Nikhef, Nijmegen, Netherlands.
[aa]Also at Near East University, Nicosia, North Cyprus, Mersin, Turkey.
[bb]Also at Institute of Theoretical Physics, Ilia State University, Tbilisi, Georgia.
[cc]Also at CERN, Geneva, Switzerland.
[dd]Also at Department of Physics, Stanford University, Stanford, California, USA.
[ee]Also at Ochadai Academic Production, Ochanomizu University, Tokyo, Japan.
[ff]Also at Manhattan College, New York, New York, USA.
[gg]Also at Novosibirsk State University, Novosibirsk, Russia.
[hh]Also at LPNHE, Sorbonne Université, Paris Diderot Sorbonne Paris Cité, CNRS/IN2P3, Paris, France.
[ii]Also at The City College of New York, New York, New York, USA.
[jj]Also at Departamento de Física Teorica y del Cosmos, Universidad de Granada, Granada (Spain), Spain.
[kk]Also at Department of Physics, California State University, Sacramento, California, USA.
[ll]Also at Moscow Institute of Physics and Technology State University, Dolgoprudny, Russia.
[mm]Also at Département de Physique Nucléaire et Corpusculaire, Université de Genève, Genève, Switzerland.
[nn]Also at Institut de Física d'Altes Energies (IFAE), Barcelona Institute of Science and Technology, Barcelona, Spain.

[oo]Also at School of Physics, Sun Yat-sen University, Guangzhou, China.
[pp]Also at Department of Applied Physics and Astronomy, University of Sharjah, Sharjah, United Arab Emirates.
[qq]Also at Institut für Experimentalphysik, Universität Hamburg, Hamburg, Germany.
[rr]Also at National Research Nuclear University MEPhI, Moscow, Russia.
[ss]Also at Institute for Particle and Nuclear Physics, Wigner Research Centre for Physics, Budapest, Hungary.
[tt]Also at Giresun University, Faculty of Engineering, Giresun, Turkey.
[uu]Also at Department of Physics, Nanjing University, Nanjing, China.
[vv]Also at Institute of Physics, Academia Sinica, Taipei, Taiwan.
[ww]Also at Department of Physics, University of Malaya, Kuala Lumpur, Malaysia.
[xx]Also at LAL, Université Paris-Sud, CNRS/IN2P3, Université Paris-Saclay, Orsay, France.